CHITOSAN FIBROUS SCAFFOLDS FOR CARTILAGE TISSUE ENGINEERING

BY

GUILLAUME RENE RAGETLY

DISSERTATION

Submitted in partial fulfillment of the requirements
for the degree of Doctor of Philosophy in VMS - Veterinary Clinical Medicine
in the Graduate College of the
University of Illinois at Urbana-Champaign, 2010

Urbana, Illinois

Doctoral Committee:

Associate Professor Dominique J Griffon, Chair
Associate Professor David Bunick
Associate Professor Brian T Cunningham
Assistant Professor Wanda J Gordon-Evans
Associate Professor David J Schaeffer

ABSTRACT

The biocompatibility of chitosan and its similarity with glycosaminoglycans make it attractive for cartilage engineering despite its limited cell adhesion properties. Structural and chemical characteristics of chitosan scaffolds may be improved for cartilage engineering application. We planned to evaluate chitosan meshes produced by a novel replica molding technique and the effect of chitosan structure on mesenchymal stem cells chondrogenesis. Another objective was to improve cell adhesion and chondrogenesis on chitosan by modifying the chemical composition of the scaffold (reacetylation, collagen II or hyaluronic acid coating).

A replica molding technique was developed to produce chitosan meshes of different fiber-width. A polyglycolic acid mesh served as a reference. Constructs were analyzed at two and 21 days after seeding chondrocytes with confocal microscopy, scanning electron microscopy, histology and quantitative analysis (weights, DNA, glycosaminoglycans and collagen II). Chondrocytes maintained their phenotypic appearance and a high viability but attached preferentially to polyglycolic acid. Matrix production per chondrocyte was superior on chitosan.

Chitosan meshes and sponges were analyzed after seeding and culture of mesenchymal stem cells under chondrogenic condition for 21 days. The cellularity was similar between groups but matrix production was greater in fibrous constructs.

Chitosan and reacetylated-chitosan scaffolds were coated with collagen II or hyaluronic acid. Scaffolds were characterized prior to seeding mesenchymal stem cells. Chitosan meshes were then coated with collagen at two densities. Polyglycolic acid served as a reference. Constructs were evaluated after seeding or culture of mesenchymal stem cells for 21 days in chondrogenic medium. Mesenchymal stem cells adhered less to reacetylated-chitosan despite collagen coating. Hyaluronic acid did not

affect cell adhesion. The cell attachment on chitosan correlated with collagen density. The cell number and matrix production were improved after culture in collagen coated meshes.

The differences between polyglycolic acid and chitosan are likely to result from the chemical composition. Chondrogenesis is superior on chitosan meshes compared to sponges. Collagen II coating is an efficient way to overcome the poor cell adhesion properties of chitosan. These findings encourage the use of chitosan meshes coated with collagen II and confirm the importance of biomimetic scaffolds for tissue engineering. The decreased cell adhesion on reacetylated chitosan and the poor mechanical stability of polyglycolic acid limit their use for tissue engineering.

To Chantal, Florence, Paul…

This thesis is dedicated to my parents who have raised me to be the person I am today. You have been with me every step of the way. Thank you for all the unconditional love, guidance, and support that you have always given me, helping me to succeed. Thank you for everything. I love you!

This thesis is dedicated to Chantal who has helped me so much over the last few years, already by being on my side. I have no doubt that I will not have been able to be here without you. Thanks for being here. I love you.

ACKNOWLEDGMENTS

This project would not have been possible without the support of many people.

I would like to thank my adviser, Dr Dominique Griffon, who helped me progress during these four years and supported my program.

Thanks to my committee members, Dr David Bunick, Dr Brian Cunningham, Dr Wanda Gordon-Evans, and Dr David Schaeffer, who offered guidance and support. Thanks to Dr Christopher Byron, Dr Yong Sik Chung, Dr Hae Beom Lee, Dr Page Fredericks and Adrienne Lane for their support and help.

Last but not least, many thanks to my wife who always offered support and help, and spent so much time giving me advice, and reviewing manuscripts, abstracts, or thesis...

TABLE OF CONTENTS

LIST OF FIGURES

LIST OF TABLES

LIST OF ABBREVIATIONS

CF:	Chitosan fibrous scaffold
Chi 4:	Chitosan scaffolds composed of fibers measuring 4 μm in width
Chi 13:	Chitosan scaffolds composed of fibers measuring 13 μm in width
Chi 22:	Chitosan scaffolds composed of fibers measuring 22 μm in width
Chi-Col 2:	Chitosan scaffold coated with 4 $mg.mL^{-1}$ type II collagen
Chi-Col 4:	Chitosan scaffold coated with 2 $mg.mL^{-1}$ type II collagen
CS:	Chitosan sponge
DD:	Degree of deacetylation
DMEM:	Dulbecco's modified Eagle's medium
ECM:	Extracellular matrix
FBS:	Fetal Bovine Serum
FTIR:	Fourier-transform infrared
GAG:	Glycosaminoglycans
HA:	Hyaluronic acid
MSCs:	Mesenchymal stem cells
PBS:	Phosphate buffered saline
PGA:	Polyglycolic acid
qRT-PCR:	Quantitative real time polymerase chain reaction
SEM:	Scanning electron microscopy
TEM:	Transmission electron microscopy
3-D:	Three-dimensional

CHAPTER 1: INTRODUCTION

Cartilage disease is a leading cause of lameness and loss of function in human and animals. Tissue engineering offers new strategies for treating damaged or diseased cartilage, where cells are allowed to proliferate and organize their extracellular matrix in a three-dimensional lattice to form *ex vivo* a clinically functional tissue. Chitosan is a natural aminopolysaccharide with a superior biocompatibility attributed to its structural similarity with glycosaminoglycans naturally present in the extracellular matrix of cartilage. A great deal of research has recently focused on chitosan for its use as a biomaterial in a number of biomedical applications and more specifically in the field of cartilage tissue engineering. In fact, chitosan is mechanically strong, biodegradable, biocompatible, and it can be molded as porous structures of various geometries and forms. However, its chemical composition limits cell adhesion and its structural characteristics have not been evaluated for cartilage tissue engineering applications. Chitosan scaffolds do not fulfill all criteria necessary for cartilage tissue engineering and further modifications are necessary before their clinical application.

The long-term goal of this research is to modify the structural characteristics and the chemical composition of chitosan scaffolds in order to improve cartilage tissue engineering application with chitosan scaffolds. Our first objective is to produce non-woven pure chitosan scaffolds with fibers of different widths using a novel replica molding technique, and to evaluate their use for cartilage tissue engineering. Our second objective is to ameliorate the microstructure of chitosan scaffolds to obtain constructs with better chondrogenic differentiation of mesenchymal stem cells. Our last objective is to improve cell adhesion on chitosan scaffolds by modification of the degree of deacetylation of chitosan and/or type II collagen coating or hyaluronic acid

coating to overcome their decreased cell adhesion and improve the resulting characteristics of the engineered constructs.

CHAPTER 2: LITERATURE REVIEW

2.1. Structure and Physiology of Articular Cartilage

Articular cartilage is the specialized organ covering the ends of diarthrodial joints. It is tough, resilient, and structured to undergo years of cyclic loading without breaking down. Cartilage is only 2 to 3 mm thick in humans or even less in small animals (less than 2 mm in dogs)(Frisbie et al, 2006), but it can support one to 9.36 megapascals of force an average of two million times each year (Silva et al, 2002; Yoshida et al, 2006). Articular cartilage varies in thickness, cell density, and mechanical properties within the same joint, among joints, and among species; however, in all synovial joints, cartilage has the same general structure and components, and performs the same functions (Athanasiou et al, 1991). An understanding of the structure and physiology of articular cartilage is essential for the development of a repair technique. In fact, both restorative techniques and cartilage tissue engineering aim at the restitution of the cartilage physiology by replicating its structure and composition. Articular cartilage consists of cells, water, and an extracellular matrix (ECM) (Ewing et al, 1990). Matrix composition and structural orientation allow articular cartilage to convert shear and compression forces into tensile forces at the bone surface.

Chondrocytes are distinguished from other cells by a spheroid shape and the synthesis of type II collagen, large aggregating proteoglycans, and specific non-collagenous proteins. Uninjured adult articular cartilage has no vascular supply and the cells exchange gas and nutrients by way of diffusion through a double barrier (synovial fluid and cartilage matrix) (Buckwalter et al, 1997). This perfusion of the matrix and

chondrocytes occurs from movement of the synovial fluid that occurs with the loading and unloading that accompanies joint motion. Because of the small pore size in the superficial zone (around 50 angstroms), it may take ten seconds to several hours for molecular diffusion into the cartilage to occur, depending on the structure, size, charge, and weight of the molecule (Wallis et al, 1987). The nature of this system leaves chondrocytes with a low concentration of oxygen relative to most other tissues. The total metabolic activity of the tissue is low because of the low cell density (cells make up only about five percent of the wet weight of cartilage) despite chondrocytes being surprisingly active metabolically. After completion of skeletal growth, most chondrocytes stop dividing but continue to synthesize collagens, proteoglycans, and non-collagenous proteins. This continued synthetic activity suggests that maintenance of articular cartilage requires substantial ongoing internal remodeling of the macromolecular framework of the matrix.

The matrix of the articular cartilage consists of two components that give the tissue its form and stability: the tissue fluid (65 to 80% of the wet weight) and the framework of structural macromolecules (20 to 35% of the wet weight). The interactions between the tissue fluid and the macromolecular framework give the tissue its mechanical properties of stiffness and resilience (Ewing et al, 1990; Maroudas et al, 1987). Three classes of macromolecules are present within the tissue but differ in their concentrations and contributions to the tissue properties. Collagens contribute for more than 60% of the dry weight of cartilage, proteoglycans for 25 to 30% of the dry weight, and non-collagenous proteins and glycoproteins for 10 to 20% of the dry weight. Articular cartilage contains two major classes of proteoglycans: large aggregating proteoglycan monomers or aggrecans and small proteoglycans including decorin, biglycan, and fibromodulin (Poole et al, 1996; Roughley, 2006). The large aggregating

proteoglycans help maintaining the fluid within the matrix. Proteoglycans consist of a protein core with one or more hydrophilic glycosaminoglycans (GAG) chains. The GAG consists of unbranched polysaccharides with negatively charged carboxylate or sulfate groups that attract cations, hence water. GAG found in cartilage include hyaluronic acid (HA), chondroitin sulfate, keratan sulfate, heparan sulfate, and dermatan sulfate. Aggrecans have large numbers of chondroitin-sulfate and keratan-sulfate chains attached to the protein core filament. Most aggrecans associate non-covalently with HA and small non-collagenous proteins to form proteoglycan aggregates. The formation of aggregates helps to anchor proteoglycans within the matrix, preventing their displacement during deformation of the tissue. Proteoglycans retain water within the matrix of cartilage, therefore playing a crucial role in the creep and stress relaxation of cartilage loaded in compression. The pressurization of the fluid phase contributes to more than 90% of the load transmission function of cartilage. The collagen network resists the osmotic pressure caused by the inorganic ions associated with the proteoglycans and provides the tensile stress of the tissue (Moskowitz, 2001). Under stress, fluid moves in and out of tissue and mechanical properties change with fluid movement establishing both the stiffness and the viscoelastic properties of cartilage. Viscoelasticity describes materials that exhibit time dependent strain. Articular cartilage is also anisotropic, which means that the intrinsic material properties depend on the matrix orientation and composition, as well as the direction in which the cartilage is loaded. Collagen fibrils are distributed relatively uniformly throughout the depth of the cartilage, except for the collagen-rich superficial zone. The collagen fibrillar meshwork gives cartilage its form and tensile strength (Moskowitz, 2001). Articular cartilage contains multiple genetically distinct collagen types, specifically types II, VI, IX, X, and XI. Types II, IX, and XI form the cross-banded fibrils seen with

electron microscopy. The organization of these fibrils into a tight meshwork that extends throughout the tissue provides the tensile stiffness and strength of articular cartilage and contributes to the cohesiveness of the tissue by entrapping the large proteoglycans. The principal collagen, type II collagen, makes up more than 90% of the total collagen content of hyaline cartilage (Hollander et al, 1994; Mayne, 1989). Type II collagen is composed of three identical collagen fibers that form a triple helix and is assembled outside the cell in a staggered fashion. Its diameter ranges from 140 to 500 nm (Fertala et al, 1996; Shoulders et al, 2009). The non-collagenous proteins organize and stabilize the macromolecular framework of the matrix, while others help chondrocytes bind to the macromolecules of the matrix. In general, they consist primarily of proteins and have a few attached monosaccharides and oligosaccharides. Anchorin CII, a collagen-binding chondrocyte surface protein, may help anchoring chondrocytes to the collagen fibrils of the matrix. Cartilage oligomeric protein, an acidic protein, is concentrated primarily within the territorial matrix of the chondrocyte and binds to chondrocytes. This molecule may have value as a marker of cartilage turnover and of progression of cartilage degeneration in patients affected by osteoarthritis. The functions of fibronectin and tenascin in articular cartilage remain poorly understood, but they may have roles in matrix organization and cell-matrix interactions.

The concentration of molecules and cells varies among sites within articular cartilage and also with age, injury to the cartilage, and disease. The morphological changes from the articular surface to the subchondral bone make possible to layer adult cartilage into superficial, transitional (or middle), deep (or radial), and calcified zones. The matrix differs with respect to concentrations of water, proteoglycan, and collagen; and with respect to the size of the aggregates (Ewing et al, 1990). Cells in different

zones differ not only in shape, size, and orientation relative to the articular surface, but also in metabolic activity. Each of these zones has a specific physiologic response to force (Cole et al, 2004). The superficial zone has the highest cell density, where chondrocytes are small and flattened with their long axis parallel to the surface. Cells in the transitional zone assume a spheroidal shape and synthesize a matrix that has larger-diameter collagen fibrils, a higher concentration of proteoglycan, and lower concentrations of water and collagen compared to the superficial zone. In the deep zone, the cells are larger and arranged with their long axes perpendicular to the surface. The cellular arrangement throughout the different zone is complementary to the organization of the collagen fibrils. Fibril alignment has a tangential orientation in the superficial layer and an orientation perpendicular to the articular surface in the deeper layers. The superficial layer can therefore withstand tension in the plane of the articular surface. In contrast, the fibrils in the middle and deep zones are organized to provide increased resilience to compressive forces. The collagen fibrils are more concentrated at the surface of the cartilage, whereas the concentration of proteoglycans is increasing with increasing depth from the cartilage surface (Todhunter et al, 2003).

The interdependence of the chondrocytes and the extracellular matrix contributes to the maintenance of articular cartilage throughout life. The main functions of the chondrocytes are the synthesis and degradation of matrix macromolecules. Enzymes produced by chondrocytes are presumably responsible for degradation of the matrix macromolecules, and chondrocytes respond to the presence of fragmented matrix molecules by increasing their synthetic activity to replace the degraded components of the ECM. The mechanisms that control the balance between these activities remain poorly understood, but cytokines with catabolic and anabolic effects appear to have important roles (van der Kraan et al, 2002). For example, interleukin-1

induces the expression of matrix metalloproteases degrading the macromolecules and interferes with the synthesis of matrix proteoglycans at the transcriptional level. Other cytokines, such as insulin-dependent growth factor-I and transforming growth factor-beta, oppose these catabolic activities by stimulating matrix synthesis and cell proliferation. In response to a variety of stimuli, these cytokines are synthesized and released into the matrix, where they bind to receptors on the cell surfaces (autocrine or paracrine mechanisms) or become trapped within the matrix. The degradative response are the result of a complex cascade that includes the activation or inhibition of interleukin-1, stromelysin, aggrecanase, plasmin, and collagenase by factors such as prostaglandins, transforming growth factor-beta, tumor necrosis factor, tissue inhibitors of metalloproteases, tissue plasminogen activator, plasminogen activator inhibitor, and other molecules. The details of how the mechanical loading of joints influences the function of chondrocytes remain unknown, but deformation of the matrix produces mechanical, electrical, and physicochemical signals that may have major roles in stimulating chondrocytes (Gray et al, 1988). Loading may also cause persistent changes in the molecular organization of the matrix, altering the response of the chondrocytes to subsequent loading. The capacity of the cells to respond to stimuli decreases with aging. These age-related changes may limit the ability of the cells to maintain the tissue and thereby contribute to the degeneration of the articular cartilage.

2.2. Pathophysiology and Repair of Cartilage Defects

The relationship between duration, intensity, and frequency of an applied force on articular cartilage is described as an envelope of function (Cole et al, 2004; Dye, 1996). The envelope of function of a joint describes a range of energy absorption that is

compatible with tissue homeostasis of an entire joint system. The upper limit of a given joint's envelope of function represents a threshold between homeostatic loading and excessive loading initiating inflammation and repair. The range of loads sufficient to activate such a physiologic response, but insufficient to cause macrostructural failure, can be termed the zone of supraphysiologic overload (Cole et al, 2004; Dye, 1996). Cartilage defects can be caused by both macrostructural failure and supraphysiologic overload. In the first stages of cartilage damage, the matrix contains a higher percentage of the proteoglycans in a nonaggregated form, unbound to HA. This breakdown of proteoglycan architecture increases the permeability of the matrix. The increase in water content results in a significant diminution of the hydraulic pressure in early osteoarthritic cartilage. This causes a reduction in the compressive stiffness of the tissue, which can be identified clinically as the softening of early chondromalacia. While collagen content is initially maintained, collagen organization is severely perturbed. Three collagenases of the matrix metalloproteinase family can cleave the triple helix of type II collagen. This results in a decrease in the tensile stiffness and strength provided by the normal three dimensional architecture of the collagen interfibrillar network. The water content of cartilage increases further as a result of collagen loss. These events are followed by cell metaplasia and loss. The activity of the chondrocytes is affected by the mechanical loads, hydrostatic pressures, and soluble mediators leading to the fibrillation, fissuring, and erosion of cartilage.

The limited potential for chondrocyte proliferation and the avascular nature of the cartilage tissue all contribute to the poor healing potential of adult cartilage, eventually leading to osteoarthritis (Tew et al, 2001). Initially small focal lesions, not necessarily associated with significant clinical problems, usually progress to partial-thickness chondral injury. The process of destruction advances downward until the

osseous region is reached leading to full-thickness osteochondral defects, more commonly symptomatic (Goldring, 2000). Full-thickness chondral defects fill with blood and quickly organize into a fibrous clot. Undifferentiated bone marrow elements, blood, and platelets organize in the defect. These cells produce a reparative granulation tissue which becomes less vascular and more firm. The fibrous tissue undergoes a progressive hyalinization and chondrification to produce a fibro-cartilaginous tissue. This fibrocartilage has reduced resilience and stiffness, poor wear characteristics, and a predilection for deterioration over time.

Osteoarthritis may develop secondary to the progression of an isolated cartilage defect (Cole et al, 2004; Dye, 1996). Cartilage disease is a leading cause of lameness and loss of function in human and animals (LeCouteur et al, 2005; Piermattei et al, 2006). According to the Center for Disease Control, one of every three adults in the United States is affected by osteoarthritis (Helmick et al, 2008). In 2003, the total cost of arthritis and other rheumatic conditions reached approximately 128 billion dollars in the United States and has since increased due to demographics in western countries and advances in geriatric medicine (Centers for Disease Control and Prevention (CDC), 2007; Hootman et al, 2006). The national economic cost of equine lameness has been estimated between 678 million and one billion dollars in 1998 (Seitzinger et al, 2000). Lameness due to joint injury and disease is the most prevalent cause of diminished athletic function and wastage in racing horses (Goodrich et al, 2006; Jeffcott et al, 1982). Osteoarthritis is also estimated to affect as much as 20% of the canine population over one year of age and 90% of cats over 12 years of age (Hardie et al, 2002; Johnston, 1997). Considerable attention has consequently focused on cartilage resurfacing techniques in both human and veterinary medicine to treat cartilage defects.

Reparative strategies for cartilage defects utilize marrow stimulation techniques to induce formation of fibrocartilage. The premise of bone marrow stimulation techniques is to attract undifferentiated mesenchymal cells from the underlying bone marrow, and rely on them and the physiologic vascular response to injury to heal the full-thickness chondral defect (Cole et al, 2004). Bone marrow stimulation techniques for the treatment of chondral defects include abrasion arthroplasty, débridement and drilling, and microfracture. They typically result in a partial filling of the articular defect with fibrocartilage (primarily type I collagen). This contrasts with the desired hyaline cartilage that is mainly type II collagen produced by the chondrocytes. In terms of articular cartilage repair, this tissue has reduced mechanical properties and deteriorates over time. Varying amounts of fibrous tissue, fibrocartilage tissue, and articular cartilage-like tissue filling the defects have been reported after marrow penetrating techniques. Proponents of these techniques advocate their technical simplicity, low patient morbidity, and cost effectiveness. However, clinical improvement obtained from these procedures is usually short lived since the repair tissue generated is largely fibrous in nature with poor durability (Cole et al, 2004).

Restorative treatments attempt to replace damaged cartilage with hyaline or hyaline-like tissue using osteochondral or chondrocyte transplantation (Lewis et al, 2006). The rationale behind osteochondral transfer is to replace the damaged cartilage-bone unit with healthy tissue obtained from a non weight bearing area. The technique consists in preparation of the chondral lesion, creation of the recipient socket(s) and graft(s) harvest followed by delivery of the graft(s) (Cole et al, 2004). Autologous chondrocyte transplantation involves collection of cartilage from the patient, *in vitro* expansion, and reimplantation in a full-thickness articular surface defect (Grande et al, 1989). Both resurfacing procedures have their limitations. They require the harvest of

normal cartilage or osteochondral graft from a non-weight bearing region with the risk of donor site morbidity (Barnewitz et al, 2006; Bartlett et al, 2005; Lewis et al, 2006). The final tissue obtained with both techniques does not have the exact same properties of the surrounding cartilage. Osteochondral transfer can also lead to graft fracture, graft delamination, and loose bodies. Avascular necrosis must be considered a risk, particularly if multiple deep plugs are harvested or deposited (Hangody et al, 1997). Autologous chondrocyte transplantation requires two surgeries and carries the risk of graft delamination or failure and intra-articular adhesions (Driesang et al, 2000; Lewis et al, 2006; Peterson et al, 2002). The clinical need for improved options in reconstructive surgery has motivated research aimed at creating new cartilage *in vitro* and *in vivo*.

2.3. Cartilage Tissue Engineering

Tissue engineering is a rapidly developing field offering new perspectives in the treatment of damaged cartilage. The basic premise of cartilage tissue engineering relies on the use of a scaffold to encourage cells to proliferate and organize their ECM in order to form *ex vivo* a clinically functional tissue, exhibiting histochemical, biochemical and biomechanical properties identical to native cartilage. Three key constituents form the basis of a tissue engineering approach, namely, cells, a scaffold, and signaling molecules (Athanasiou et al, 2001). Thus, the goal is to encourage cells to adhere to the three-dimensional (3-D) matrix and form a clinically functional tissue. However, the cell source, 3-D matrix and culture conditions matching these goals remain unclear (Chung et al, 2008; Coutts et al, 2001).

Primary chondrocytes and mesenchymal progenitor cells are the main cell types used for cartilage tissue engineering applications. Both primary and passaged chondrocytes have been seeded onto scaffolds and tested for their ability to make cartilaginous material (Freed et al, 1993). The use of chondrocytes is appealing because their differentiated phenotype allows the cells to produce an extracellular matrix of desired properties. However, the use of primary chondrocytes is limited because of the morbidity associated with over-harvesting cartilage. Thus, serial passage of chondrocytes as monolayers is a convenient means to acquire a large number of cells that generally retain the chondrocyte phenotype throughout the first few passages. The dedifferentiation process affecting chondrocytes cultured on protein monolayers is well recognized and has prompted the development of 3-D culture techniques for cartilage engineering and the search of alternative cell sources (Brodkin et al, 2004). The use of mesenchymal stem cells (MSCs) as a cell source is attractive because they can be harvested from bone marrow aspirates, adipose, and other tissues with less morbidity than chondrocytes (Fortier, 2005; Gao et al, 2007; Helder et al, 2007). They have self-renewal abilities, are immuno-privileged, and can differentiate into several cell types including chondrocytes (Caplan, 2005; Gao et al, 2007). MSCs, in constrast to chondrocytes, integrate better into damaged sites according to several studies (Obradovic et al, 2001; Vunjak-Novakovic, 2002), and repairs by MSCs may last longer than those in which chondrocytes are used (Hui et al, 2004). However, in one study, MSCs injected in a fibrin vehicle failed to improve the long-term histologic appearance or biochemical composition of full-thickness cartilage lesions in horses (Wilke et al, 2007). These findings may reflect a deficient retention of MSCs after injection in the lesion or an inability of MSCs to achieve the genetic profile of a fully differentiated chondrocyte. Research efforts currently focus on improving the

chondrogenic potential of MSCs *in vitro*, as well as their delivery *in vivo*. Two approaches are possible: a fully-differentiated construct can be implanted within the defect or only a basic building block can be implanted *in vivo* to ensure that the differentiation and remodeling of repair tissue occur under physiological conditions. Regardless of the approach, delivering cells cultured on biodegradable carriers may improve their retention within the damaged area (Radice et al, 2000). In addition, scaffolds provide a novel strategy to modulate the differentiation of cells (Bosnakovski et al, 2006; Wollenweber et al, 2006).

Cell behavior is affected by the signaling molecules as well as both the structural characteristic and the chemical composition of the scaffold, ultimately impacting the performance of tissue-engineered constructs (Athanasiou et al, 2001; Li et al, 2006; Moroni et al, 2006; Pei et al, 2002). The scaffolds should have several inherent properties including appropriate mechanical strength, biodegradability, biocompatibility, a porous structure, and surface characteristics promoting cell adhesion and proper cell differentiation (Coutts et al, 2001; Freed et al, 1994). The list of biomaterials tested for cartilage repair is extensive but a scaffold fulfilling those criteria has yet to be determined (Coutts et al, 2001). Polyglycolic acid (PGA) mesh has been extensively studied for cartilage tissue engineering but its *in vivo* application has been limited due to its low mechanical properties (Goldstein et al, 1999; Griffon et al, 2005; Griffon et al, 2006; Jeon et al, 2007).

2.4. Chitosan Scaffolds for Cartilage Tissue Engineering

The biocompatibility and similarity of chitosan to GAG naturally present in the ECM of cartilage make it particularly attractive as a candidate for the repair of cartilage

defects (VandeVord et al, 2002). Chitosan is formed by alkaline deacetylation of chitin, the second most abundant natural polysaccharide, primarily obtained as a subproduct of shellfish, such as crabs and shrimps (Chenite et al, 2000). Chitosan is composed of glucosamine and N-acetyl glucosamine linked in a β(1–4) manner; the glucosamine/N-acetyl glucosamine ratio being referred as the degree of deacetylation (DD). Depending on the source and preparation procedure, its molecular weight ranges from 300 to over 1000kD with a degree of deacetylation from 50% to 95%. Chitosan is normally insoluble in aqueous solutions above pH 7; however, the free amino groups of glucosamine are protonated in dilute acids (pH < 6.0) which facilitate solubility of the molecule. Chitosan has been studied for use in a number of biomedical applications including wound dressings, drug delivery systems, and space filling implants and has gained Food and Drug Administration approval for human use in wound dressing (Khor et al, 2003; Madihally et al, 1999). A number of researchers have examined the host tissue response to chitosan-based implants. These materials evoke a minimal foreign body reaction, with little or no fibrous encapsulation (Mao et al, 2004; VandeVord et al, 2002). Considerable attention has recently focused on chitosan-based materials and their applications in the field of cartilage tissue engineering (Chen et al, 2007; Di Martino et al, 2005; Griffon et al, 2005; Griffon et al, 2006; Jeon et al, 2007; Kasahara et al, 2008; Madihally et al, 1999; Nettles et al, 2002; Nettles et al, 2002; Suh et al, 2000; Yamane et al, 2005; Yamane et al, 2006). Chitosan has adequate mechanical properties for this application (Di Martino et al, 2005; Griffon et al, 2005; Griffon et al, 2006; Jeon et al, 2007; Kasahara et al, 2008; Madihally et al, 1999; Nettles et al, 2002; Yamane et al, 2005; Yamane et al, 2006). Lysozyme is the primary enzyme responsible for *in vivo* degradation of chitosan through hydrolysis of acetylated residues. Highly deacetylated forms may last several months *in vivo*; eventual

degradation products being oligosaccharides of variable length. Chitosan is also an attractive biomaterial as it can be molded as porous structures of various geometries and forms. However, the chitosan scaffolds used in previous studies do not fulfill all criteria necessary for cartilage tissue engineering (Coutts et al, 2001). The structural characteristics and the chemical composition of chitosan scaffolds could therefore be further modified for cartilage tissue engineering applications.

2.5. Structure of Chitosan Scaffolds

The physical properties of a 3-D scaffold affect cell behavior, ultimately determining the performance of a tissue-engineered construct (Li et al, 2006; Moroni et al, 2006). The 3-D structures most commonly used for articular cartilage tissue engineering application consist of fiber meshes and sponges (Lee et al, 2008; Raghunath et al, 2007). The scaffold microstructure can guide cellular organization, cell proliferation, cell differentiation, and matrix production (Chen et al, 2007; Griffon et al, 2006; Lee et al, 2008; Li et al, 2006; Malda et al, 2005; Raghunath et al, 2007; Sasmazel et al, 2008; Yamane et al, 2006). However, the principal requirement for the scaffold is to act as an open mesh to permit cells to permeate its entire structure during initial attachment and to ensure that nutrients or waste can diffuse in or out as needed. Previous approaches to produce chitosan scaffolds meeting this requirement for structural openness include freeze-drying, wet spinning, and electrospinning.

Freeze-drying is a widely accepted method to form a sponge-like structure. Porous chitosan structures can be formed by freezing and lyophilizing chitosan-acetic acid solutions in suitable molds. During the freezing process, ice crystals nucleate from the solution and grow along the lines of thermal gradients. Exclusion of the chitosan

acetate salt from the ice crystal phase and subsequent ice removal by lyophilization (water sublimation) generates a porous material whose mean pore size can be controlled by varying the freezing rate and hence the ice crystal size (Suh et al, 2000). Increasing the freezing rate will increase the crystal size and therefore the pore size. However, the growth of crystals along the line of thermal gradient lead to variability in pore size within each scaffold (Nettles et al, 2002). Finally, the pore diameter of the resulting scaffolds can only be controlled in the 1 to 250 μm range (Madihally et al, 1999).

Wet spinning has been used to manufacture polymer fibers and has been adapted to obtain chitosan meshes. The process involves extruding a chitosan solution through a spinneret into a coagulation bath inducing the precipitation of the chitosan followed by post-drawing. Solvents are commonly used to guarantee the spinnability of the chitosan solution. Several interplaying factors, such as coagulation rate, diffusion rate difference between solvent and coagulant, and coagulation temperatures determine the morphology of the resultant fibers (Tuzlakoglu et al, 2004). The post-draw allows to reduce the diameter of the fibers but usually not to less than 10 μm and to diminish the entanglement. Despite recent advances allowing wet spinning without solvents, its use for the fabrication of chitosan scaffolds is limited by the minimal diameter of the fibers obtained and the lack of uniformity of the fibers.

Electrospinning has been adapted to chitosan in an effort to create smaller diameter fibrous networks. The principle consists in using an electric field to draw a polymer solution from a spinneret to a collector. A high voltage electric field (10 – 20 kV) is used to generate a surface charge sufficient to overcome the surface tension in a pendant drop of the polymer fluid (Bhattarai et al, 2005). Several processing parameters (type of solution, viscosity, surface tension, net charge density, flux in the

syringe, and ambient parameters) control the electrospinning process, especially the diameter and morphology of the resulting fibers (Pham et al, 2006). The variability in constitution inherent to natural products, the poor solubility and the high surface tension due to the polycationic nature of chitosan complicate the matter, often requiring various plasticizers and surfactants to be added to the blend. In fact, high electrical forces are required to produce electrospun fibers of chitosan because of its surface tension. Moreover, particles are often formed during the electrospinning process, likely due to the repulsive forces between ionic groups in the chitosan backbone (Lee et al, 2009). The diameters of chitosan fibers produced by electrospinning range from 38 nanometers to few micrometers but most chitosan solution were mixed with trifluoroacetic acid, glutaraldehyde, polyethylene oxide, or triton X-100 (Bhattarai et al, 2005; Geng et al, 2005; Lee et al, 2009; Schiffman et al, 2007). The biocompatibility of these solution modifiers must be considered carefully before application of fibrous product from this process to cell cultures and, further, *in vivo* implantation. As an alternative approach to improve its electrospinnability, chitosan can be mixed with other synthetic or natural polymers such as poly(ethylene oxide), poly(vinyl alcohol), or poly(lactic acid). These approaches are limited by differences in water solubilities of the components and also differing biological effects of the hybrid scaffolds compared to chitosan scaffolds (Bhattarai et al, 2005; Lee et al, 2009). Finally, the high velocities of the product deposition at the target combined with the softness of the chitosan blend compress the scaffold, detracting from its openness to cell diffusion. These limitations justify the search for new methods to produce pure chitosan fibers of a pre-determined diameter.

Despite the growing interest for chitosan as a biomaterial for tissue engineering, most studies evaluating pure chitosan scaffolds have focused on sponges (Griffon et al,

2005; Griffon et al, 2006; Jeon et al, 2007; Nettles et al, 2002; Subramanian et al, 2005; Suzuki et al, 2008). Fibrous scaffolds may be more appealing than sponges and films for cartilage tissue engineering as they simulate more closely the fibrous nature of the native cartilaginous ECM (Moroni et al, 2006). The scaffold microstructure can guide cellular organization, cell proliferation, and matrix production (Chen et al, 2007; Griffon et al, 2006; Lee et al, 2008; Li et al, 2006; Malda et al, 2005; Raghunath et al, 2007; Sasmazel et al, 2008; Yamane et al, 2006). More specifically, fiber diameter and surface topology were found to affect MSCs seeding, proliferation and spreading (Moroni et al, 2006). The differentiation of stem cell is also affected by the scaffold structure (Fromstein et al, 2008). Li et al. showed that polycaprolactone fibrous scaffolds were suitable for supporting chondrogenic induction of human bone marrow-derived MSCs *in vitro* (Li et al, 2005). Culturing MSCs on the scaffolds not only produced comparable quantities of GAGs, but also exhibited similar levels of chondrogenic gene expression as MSCs cultured as in a cell pellet, an established model of chondrogenic induction. Culture on fibrous scaffolds did not necessitate the extremely high cell densities previously shown to be critical for MSC differentiation. A decreased fiber diameter was found to stimulate chondrocyte proliferation and GAG production (Li et al, 2006), and enhance the chondrogenic differentiation of mesenchymal stem cells (Wise et al, 2008). The high surface area–volume ratio and controlled porous architecture of these meshes also ensures abundant area for cell attachment and allows for a higher density of cells to be cultured. However, scaffold evaluation requires the control of the uniformity of fiber diameter and of the chemical composition to facilitate a rigorous comparison between scaffolds. The influence of chitosan fibrous matrices in terms of fiber diameter and arrangement on chondrocyte functions remains poorly characterized. Although chondrogenic differentiation of

MSCs has been documented on a chitosan copolymer gel, the extent to which the structural characteristics of chitosan scaffolds modulate the chondrogenic potential of MSCs remains largely unexplored (Cho et al, 2004).

2.6. Cell Adhesion on Chitosan Scaffolds

Limited adhesion of chondrocytes and MSCs on chitosan compared to other biomaterials such as PGA has been previously reported by our group (Griffon et al, 2010). Others have confirmed these results which limit the application of chitosan for tissue engineering (Amaral et al, 2007; Seda Tigli et al, 2007; Wenling et al, 2005). The initial attachment of cells to a scaffold is a prerequisite for a successful tissue engineering outcome as it is a decisive factor for cell-matrix interactions (Mahmood et al, 2004). Improving cell attachment and cell distribution on chitosan-based scaffolds is therefore essential for cultivation of clinically relevant constructs. The ideal seeding criteria on 3-D scaffolds have been described as: (i) a high yield (or percentage of seeded cells attaching to the matrix) to optimize the use of donor cells, (ii) a high kinetic rate, to minimize the time during which shear-sensitive cells will be suspended freely in the medium, and (iii) a spatially uniform attachment of cells throughout the matrix, to provide a basis for uniform tissue generation (Vunjak-Novakovic et al, 1998).

The influence of the DD of chitosan on cell attachment remains controversial and varies between reports and cell types (Fakhry et al, 2004). In several studies, deacetylation increased the attachment of fibroblasts, Schwann cells, keratinocytes, and neurons to chitosan films or sponges (Amaral et al, 2007; Chatelet et al, 2001; Freier et al, 2005; Seda Tigli et al, 2007; Tigli et al, 2008; Wenling et al, 2005). However, in

others, a lower DD of chitosan improved chondrogenesis without affecting the attachment of chondrocytes, fibroblasts, or osteoblasts (Hamilton et al, 2006; Kuo et al, 2006; Suphasiriroj et al, 2009; Suzuki et al, 2008). The extent to which reacetylation of chitosan could improve MSCs seeding for cartilage tissue engineering remains unclear.

Besides the reduction of nonspecific protein adsorption by molecular modification of the biomaterial itself, the strategy most commonly employed to improve cell adhesion on biomaterials focuses on immobilization of adhesion molecules to ensure controlled interaction between the cells and the scaffold (Carvalho et al, 2008). The effect of specific molecules on cell adhesion is dependent on the chemical modification, the bulk biomaterial, and the type of cells evaluated (Wang et al, 2003). The molecular candidate should ideally not only improve cell attachment but also promote proper cell differentiation.

2.7. Chemical Modifications of Chitosan

Chemical modifications can be useful to improve cell adhesion but also to modulate cell signaling in order to influence cell differentiation. The biomaterial used for cartilage tissue engineering should have several inherent properties including appropriate mechanical strength, biodegradability, biocompatibility, and surface characteristics promoting cell adhesion and proper cell differentiation (Coutts et al, 2001; Freed et al, 1994). Clearly, it is not realistic to expect that any one material will fulfill the entire list of requirements for cartilage tissue engineering. However, it is possible to combine different types of material and adjust the chemical composition and the properties of the scaffold (Ameer et al, 2002). The particular benefits of hybrid scaffolds result from the combined effects of the different polymers on cell seeding,

proliferation, differentiation, and structural support. The combination of chitosan with other biomaterials can have synergetic effects on cell adhesion, the principal drawback of chitosan (Griffon et al, 2010), and on cell differentiation and extracellular matrix formation. Few chitosan-based scaffolds have previously been described.

Iwasaki et al. reported on an alginate-based chitosan hybrid mesh, which increased cell attachment and proliferation in vitro compared to alginate scaffold (Iwasaki et al, 2004). The tensile strength of these hybrid scaffolds was also increased but the overall seeding yield was still low. Chitosan has been combined with poly(l-lactic acid); the modified substrate showed increased cell adhesion, proliferation and biosynthetic activity compared to poly(l-lactic acid) (Cui et al, 2003). Hsu et al. developed chitosan-alginate-hyaluronic acid complexes with or without covalent attachment of arginine-glycine-aspartic acid (RGD) containing protein to increase the cellular attachment on chitosan (Hsu et al, 2004). Scaffolds were seeded with chondrocytes and cartilage was observed one month after in vivo implantation both in presence or absence of RGD indicating potential of this composite material for cartilage regeneration. However, the mechanical stability of those scaffolds was limited. Chitosan-based scaffolds can also be used to deliver growth factors in a controlled fashion to promote the ingrowth and biosynthetic ability of chondrocytes. Lee et al. reported porous type I collagen-chitosan-GAG scaffolds loaded with TGF-β1 (Lee et al, 2004). This scaffold exhibited controlled release of TGF- β 1 and promoted cartilage regeneration. Moreover, addition of chitosan to the type I collagen scaffold was done to improve the mechanical properties and stability of the collagen network by inhibiting the action of collagenases (Lee et al, 2004; Taravel et al, 1996). The functionalization of chitosan by incorporating other proteins is therefore a promising approach to improving its performance in articular cartilage repair (Lee et al, 2002). Different molecules have the

potential to increase cell adhesion on chitosan. The molecule used should not only improve cell attachment but also promote proper cell differentiation.

The peptide RGD is the coating agent most often used to promote the attachment of cells on material surfaces (Hersel et al, 2003; Hubbell, 1995). However, RGD was found to inhibit fibroblast adhesion and proliferation on reacetylated chitosan films (Carvalho et al, 2008). Moreover, it was found to limit chondrogenesis of MSCs (Carvalho et al, 2008; Connelly et al, 2007).

Type II collagen is another candidate which could improve cell attachment via interactions with the integrins, the discoidin-domain receptors, and the annexin V receptors (Durr et al, 1993; Freyria et al, 2009; Gigout et al, 2008; Reid et al, 2000). Type II collagen differs from type I collagen in structure, distribution, and effects on cells (Duan et al, 2007; Kim et al, 2010). Type I collagen can be found in skeletal tissue but also in skin, cornea, arteries, internal organs, and granulation tissues; whereas the natural distribution of type II collagen is more specific to skeletal tissues (hyaline cartilage and bone growth plate). Although type I collagen coating has been found to improve cell adhesion on chitosan, the use of type II collagen is more attractive as a biomimetic strategy to improve both MSCs adhesion and chondrogenic differentiation as it simulates more closely the nature of the native cartilaginous ECM (Lutolf et al, 2005; Moroni et al, 2006; Stevens et al, 2005). Type II collagen has been shown to improve chondrogenesis through integrin interactions which modulate the transforming growth factor (TGF) signaling cascade involving Smad 2 and Smad 3 (Schneiderbauer et al, 2004). Type II collagen has been used as a bulk biomaterial in few tissue engineering applications (Chang et al, 2010; Hsu et al, 2006; Pieper et al, 2002; Tsai et al, 2002; Yen et al, 2009). Scaffolds composed of bulk type II collagen-poly-caprolactone improved chondrocytes adhesion and proliferation compared to poly-

caprolactone scaffolds (Chang et al, 2010). In one study, chondrocyte proliferation and distribution were improved in type II collagen matrices compared to type I collagen matrices (Pieper et al, 2002). Although the mechanical properties and dimensional stability of type II collagen prevent its use as a bulk biomaterial, they do not affect its potential as a coating molecule for scaffolds used in skeletal tissue engineering (Hsu et al, 2006). To our knowledge, the evaluation of type II collagen coating has only been limited to one study on poly-lactide-coglycolide scaffolds (Hsu et al, 2006).

Hyaluronic acid is another candidate which could improve cell attachment via a CD44-mediated recruitment of cells (Herrera et al, 2007). Fast and early cell-HA interactions tether cells to the surface, providing the temporal and spatial framework for slower integrin-mediated interactions to occur (Cohen et al, 2006; Peniche et al, 2007; Tan et al, 2007; Yamane et al, 2005; Zaidel-Bar et al, 2004; Zimmerman et al, 2002). HA seems particularly promising in cartilage tissue engineering applications since it has been an important mainstay of the clinical arsenal against joint disease for decades. The use of intra-articular injection of HA to reduce lameness has been supported by several clinical studies (Asheim et al, 1976; Frisbie et al, 2009; Rose, 1979). Experimentally, intra-articular injection of HA has been shown to improve weight bearing after radiocarpal bone osteochondral fracture as determined by force plate analysis and to preserve articular cartilage integrity as determined by histopathologic analysis (Auer et al, 1980; Frisbie et al, 2009; Gingerich et al, 1981). Results of clinical studies in horses and humans indicate that high molecular weight HA has better clinical efficacy than low molecular weight HA (Atamaz et al, 2006; Philips, 1989). In cartilage tissue engineering, HA was found to improve cell adhesion and proliferation on chitosan fibrous sheets (Yamane et al, 2005). However, the effect of the HA coating on cell distribution was not evaluated.

2.8. Objectives and Hypotheses

The long-term goal of this research is to modify the structural characteristics and the chemical composition of chitosan scaffolds in order to improve their application in cartilage tissue engineering.

We plan to accomplish the overall objective of this application by pursuing the following specific aims:

(1) To produce non-woven chitosan scaffolds composed of fibers of 4, 13, and 22 μm in width using a novel replica molding technique, and to evaluate adhesion, proliferation, and the synthesis of the ECM by chondrocytes cultured on these chitosan fibrous scaffolds compared to PGA mesh with fibers of 13 μm in diameter.

We hypothesized that chitosan and PGA scaffolds of similar fiber diameter would result in constructs of similar properties. We also hypothesized that decreasing the fiber width of chitosan would improve the characteristics of the extracellular matrix.

(2) To compare MSCs chondrogenesis on chitosan sponges and meshes.

We hypothesized that chitosan fibrous scaffolds would stimulate chondrogenesis of MSCs compared to chitosan sponges.

(3) To determine the extent to which reacetylation of chitosan and/or type II collagen coating or HA coating could improve MSCs seeding.

We hypothesized that MSCs adhesion would be greater on chitosan meshes compared to reacetylated chitosan meshes, that type II collagen coating would improve cell seeding efficiency on both chitosan and reacetylated chitosan scaffolds, and that hyaluronic acid would improve cell seeding on chitosan scaffolds.

(4) To produce chitosan fibrous scaffolds coated with different densities of type II collagen and to evaluate the effect of this coating on MSCs seeding and chondrogenesis.

We hypothesized that coating chitosan meshes with type II collagen would improve MSCs adhesion and chondrogenesis.

CHAPTER 3: METHODOLOGY AND RESULTS

Unless otherwise specified, the reagents were obtained from Sigma (Sigma, St. Louis, MO, USA).[1]

3.1. Cartilage Tissue Engineering on Fibrous Chitosan Scaffolds Produced by a Replica Molding Technique

3.1.1. Materials and Methods

3.1.1.1. Scaffolds:

The chitosan ("Chito Clear" fg95, Primex, Iceland) used in this study has a molecular weight of about 500 kDA, a degree of deacetylation greater than 95 % and a viscosity of 500 cP at 1% concentration. Three types of non-woven fibrous scaffolds

[1] The materials of this thesis have been previously published in:
- Ragetly GR, Slavik GJ, Cunningham BT, Schaeffer DJ, Griffon DJ: Cartilage tissue engineering on fibrous chitosan scaffolds produced by a replica molding technique. J. Biomed. Mater. Res. A. 93:46–55, 2010
- Ragetly GR, Griffon DJ, Lee HB, Fredericks LP, Gordon-Evans WG, Chung YS: Effect of chitosan scaffold microstructure on mesenchymal stem cells chondrogenesis. Acta Biomaterialia. 6(4):1430-6, 2010
- Ragetly GR, Griffon DJ, Lee HB, Chung YS. Effect of collagen II coating on mesenchymal stem cell adhesion on chitosan and on reacetylated chitosan fibrous scaffolds. Journal of Material Sciences: Material in Medicine. 2010, May 25. Epub ahead of print.
- Ragetly GR, Griffon DJ, Chung YS. The effect of type II collagen coating of chitosan fibrous scaffolds on mesenchymal stem cell adhesion and chondrogenesis. Acta Biomaterialia. 2010, May 22. Epub ahead of print.

were prepared using a replica molding technique (Slavik et al, 2007). A 3 % chitosan solution in 0.2 M acetic acid was filtered (0.45 μm and 0.2 μm pore nylon membrane syringe filter) and poured into an array of microchannels recessed into a molded surface of polydimethylsiloxane (Figure 1A). The mold was inverted into a pool of coagulant solution consisting of 0.150M NaOH / 0.150M Na2SO4 ([Na+] = 0.450M, pH = 13.0 accounting for ionic activity corrections) in deionized water at 40°C for 45 minutes. Released fibers were allowed to soak in the coagulant bath for 24 hours. The dimensions and shape of the channels in the master template were defined by a standard photolithographic process followed by anisotropic reactive ion etching of the underlying silicon wafer. Replica castings of this silicon wafer surface in elastomeric polydimethylsiloxane served as the mold for chitosan. Three types of scaffolds were produced with fibers varying in width: 1- Chi 22: 22 ± 4 μm (n = 24) 2- Chi 13: 13 ± 3 μm (n = 24), 3- Chi 4: 4.7 ± 1.6 μm (n = 24) (Figure 1 B-D). The fiber size was evaluated by scanning electron microscopy (SEM) by random measurements and confirmed using calibrated optical microscopy while still in the medium.

Our reference group consisted of a PGA mesh previously tested for in-vitro chondrogenesis (n = 24) (Synthecon Inc., Houston, TX) (Griffon et al, 2005; Griffon et al, 2006; Seddighi et al, 2008). This non-woven mesh is made of 13 μm-diameter fibers with a void volume of 97%.

All scaffolds were standardized to a dry weight of 2.0 ± 0.1 mg. They were sterilized with ethylene oxide gas and rehydrated through successive passage in phosphate buffered saline (PBS) and culture medium solutions (Marreco et al, 2004). The culture medium consisted of Dulbecco's modified Eagle's medium (DMEM) containing 4.5 $g.L^{-1}$ glucose, 10 % Fetal Bovine Serum (FBS, ATCC, Manassas, VA, USA), 584 $mg.L^{-1}$ glutamine, 100 $U.mL^{-1}$ penicillin, 100 $\mu g.mL^{-1}$ streptomycin, 10 mM

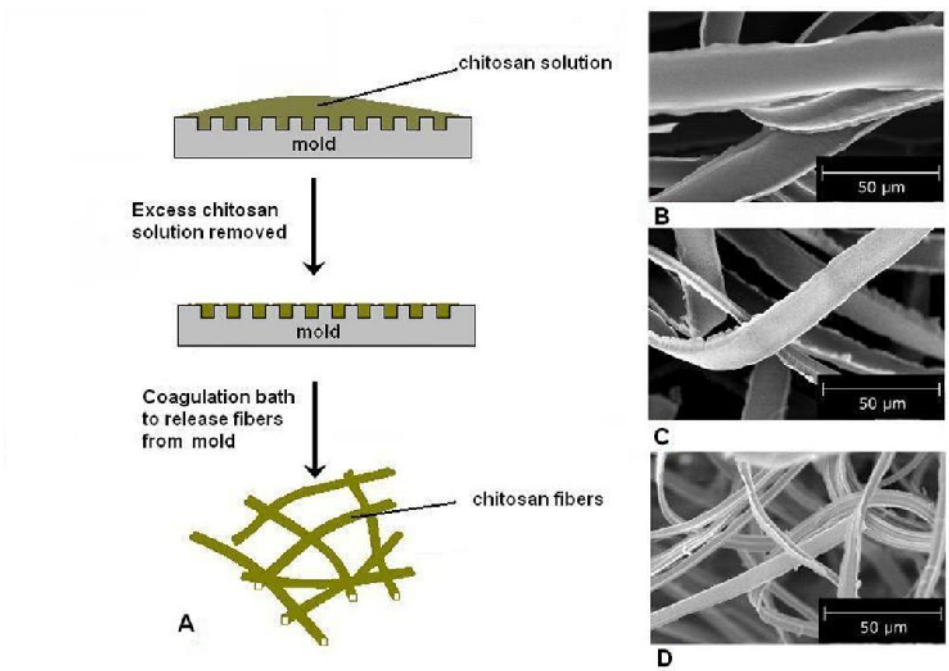

Figure 1: Fabrication of novel random fibrous chitosan scaffolds. A: Schematic illustration of the micromolding process. B-D: SEM micrographs of chitosan scaffolds composed of fibers measuring 22 µm (B), 13 µm (C), and 4 µm (D) in width.

N-2-hydroxyethylpiperazineN'-2-ethanesulfonic acid (HEPES), 0.1 mM nonessential amino acids, 0.4 mM proline, 50 $\mu g.mL^{-1}$ ascorbic acid and 25 $\mu g.mL^{-1}$ amphotericin B (Griffon et al, 2006).

3.1.1.2. Chondrocytes:

Cartilage was aseptically collected from both stifles of four four-week-old pigs. NIH guidelines for the care and use of laboratory animals have been observed and all procedures in this study were approved by the Institutional Animal Care and Use Committee of the University of Illinois. Cartilage was obtained from weight bearing and non-weight bearing surfaces of the femoral condyles and tibial plateau. Cartilage was then minced in 1 mm^3 cubes, rinsed in PBS with 2 % penicillin-streptomycin, prior to overnight digestion in culture medium and 0.15 % collagenase type II (Worthington, Freehold, NJ) (Griffon et al, 2006). Cells from two pigs were pooled together in each experiment to decrease individual variability. Cell number and viability were evaluated via trypan blue exclusion using a haemocytometer. For each experiment, samples of cells were placed in a six-well plate to evaluate cell attachment under monolayer culture. Samples of pooled fresh cells were also used to determine the DNA content per cell. A cell suspension containing $2.5x10^6$ cells in 150 µL of medium was dropped on the surface of each scaffold (12 of each per experiment: PGA, Chi 22, Chi 13 and Chi 4) and allowed to incubate at 37˚C for one hour. After one hour the procedure was repeated and 0.5 ml of medium was added prior to incubation for two hours. Scaffolds seeded with a total of $5x10^6$ chondrocytes were transferred to untreated six-well non-tissue culture plates and placed on a platform shaker oscillating at 100 rpm. The constructs were maintained in culture medium for 48 hours or 21 days. The culture medium was changed three times a week.

3.1.1.3. Evaluation of Constructs:

Seeding was evaluated at 48 hours in 24 constructs via SEM, DNA, water and GAG quantifications. Chondrogenesis was evaluated after 21 days of culture in 72 constructs via SEM, live/dead assay, histology, DNA, water, GAG and type II collagen quantifications.

Live/dead assay

The viability of chondrocytes in the constructs was determined using a live/dead assay kit (Molecular Probes, Carlsbad, CA), where calcein AM labels viable cells (green fluorescence) and ethidium homodimer 1 labels dead cells (red fluorescence) according to the manufacturer's protocol. Briefly, constructs were washed three times in sterile PBS for two minutes, and sectioned perpendicularly into 1.5 mm–thick slices using a parallel razor blade. Slices from the periphery and centre of each construct were placed on a glass slide and immersed in 200 μL of PBS solution containing 2 mM calcein AM and 4 mM ethidium homodimer 1 reagents prior to incubation for 40 min at 37ºC. Constructs were observed via confocal microscopy (Olympus BX50 Confocal Microscope, Center Valley, PA) using Melles Griot Argon and Krypton lasers at excitation wavelengths of 488 nm and 568 nm. The intensities of viable and dead cells were recorded on four slides at a magnification of 40 x and two slides at a magnification of 10 x (Figure 2 A-D). The slides were analyzed using the Fluoview software (Olympus) to determine the ratio between viable and dead cells Figure 2 E).

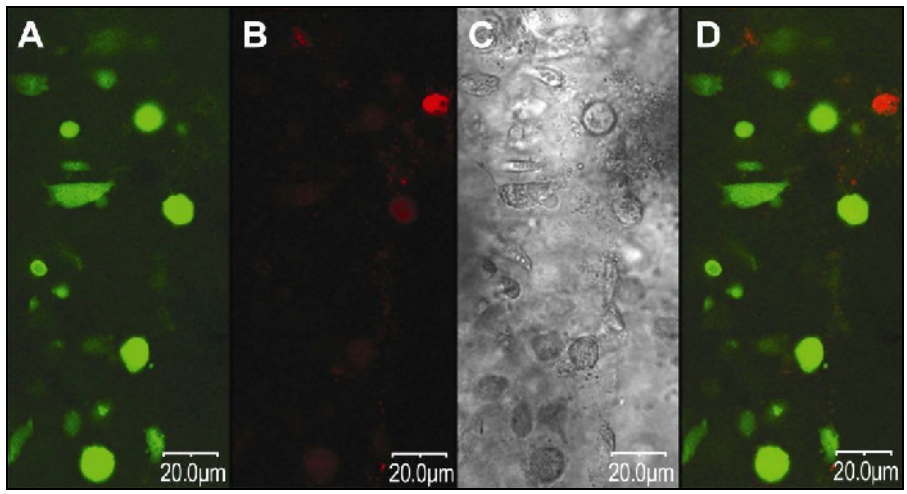

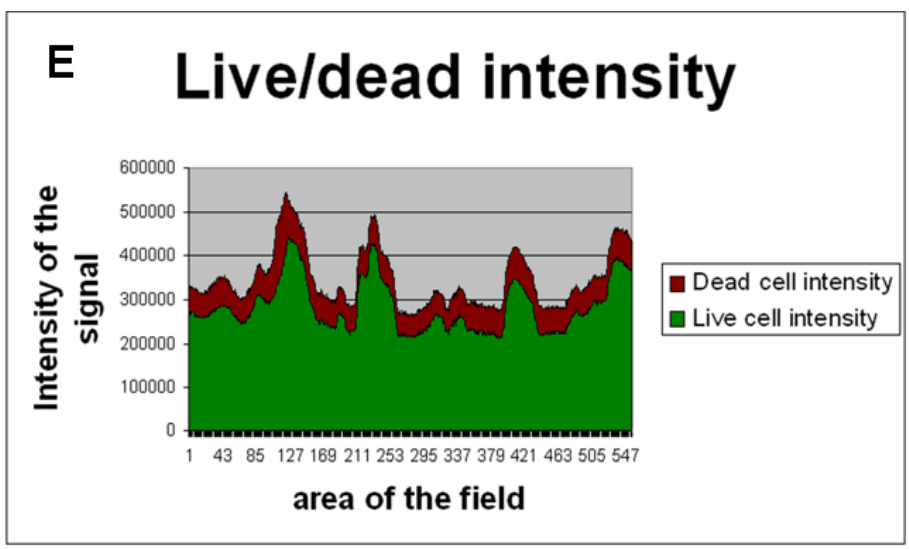

Figure 2: Live/dead assay of a chitosan construct. A: Argon laser allows identification of live cells. B: Same field: Krypton laser allows identification of dead cells. C: Same field without laser. D: Same field with combined Argon and Krypton allowing visualization of both live and dead cells for analysis. E: Intensity ratio from the corresponding field obtained by computer analysis.

Scanning electron microscopy

Constructs were fixed in a 2.5 % gluteraldehyde solution (Electron Microscopy Sciences, Hatfield, PA) with sodium cacodylate buffer for two hours. After rinsing with buffer, they were submerged in 1 % osmium tetroxide (Electron Microscopy Sciences) in 0.1 M sodium cacodylate for 90 minutes. Following a buffer rinse, the constructs were dehydrated through an ethanol series. Finally, constructs were placed in hexamethyldisilazane (Electron Microscopy Sciences) for 45 minutes and left under a fume hood until completely dry. Each construct was bisected in order to evaluate the surfaces as well as the central section of the construct. A total of two samples (superficial and centre) were mounted for each construct and sputter coated with gold – palladium prior to examination with SEM (Hitachi S4700, Schaumburg, IL) at 1.0 kV. Criteria evaluated included cell morphology, size, attachment to the support and presence of cytoplasmic extensions. Cells contained in 115x80 μm fields acquired at five superficial and five central positions within the constructs were counted (Griffon et al, 2005; Griffon et al, 2006).

Histopathology

The constructs were fixed in 10% neutral buffered formalin, embedded in plastic and cut via microtome to produce 1 μm-thick sections (Seddighi et al, 2008). Sections were stained with Safranin O Green or Toluidine Blue O using a technique previously described and were examined to evaluate cell and construct morphology and the presence of matrix and remnants of scaffold (Getzy et al; Grogan et al, 2006).

Water, DNA, and GAG contents

Scaffolds were weighed before and after dehydration to determine their wet and dry weights, respectively. The water content was subsequently calculated as:

Water content (%) = (Weight wet – Weight dry) x 100% / Weight wet

Samples were digested in papain for 16 hours at 60°C and assayed for GAG content via spectrophotometry with 1,9 dimethylmethylene blue chloride (Farndale et al, 1986). Shark chondroitin sulfate (5 to 50 $\mu g.mL^{-1}$) was used as a standard (Griffon et al, 2006). The same papain digestion technique was used for a fluorometric assay of DNA with Hoechst 33258 (Kim et al, 1988). The cell seeding efficiency was calculated 48 hours after seeding as a ratio between the number of cells attached and the number of cells seeded on each scaffold. The number of cells attached was obtained using the average DNA content per chondrocyte estimated previously by our group (5.87 pg per cell) (Griffon et al, 2005). The change in dry weight was calculated and expressed as a percentage.

Type II collagen content

Type II collagen content was determined by enzyme linked immunosorbent assay (Arthrogen-CIA® Native Type II Collagen Detection Kit, Chondrex, Redmond, WA) after digestion of the constructs in pepsin and elastase (Griffon et al, 2006). Collagen fibrils were solubilised with pepsin and further digested with pancreatic elastase. The optical density of the reacted collagen with monoclonal antibody was read at 490 nm (Seddighi et al, 2008).

3.1.1.4. Statistical Analysis

DNA, water contents, GAG, GAG/DNA ratio, Type II collagen/DNA ratio; viability of the chondrocytes (%), cell counts via SEM and increase in dry weight (%) were compared between groups with a risk factor of less than 0.05 considered statistically significant. All data were expressed as mean ± standard deviation. Statistical differences were evaluated with a one-way analysis of variance and Tukey's highly significant differences test using Systat 11.0 statistical software (Wilkinson, Chicago, IL).

3.1.2. Results

The initial viability of chondrocytes isolated in this study and determined by trypan blue was greater than 95 %.

3.1.2.1. Seeding Control:

Scanning Electron Microscopy

Polyglycolic acid constructs contained more cells than any of the chitosan constructs. All cells seeded on chitosan scaffolds had the size and rounded appearance of normal chondrocytes (Figure 3, Figure 4 AC). Most cells seeded on the PGA scaffolds had the phenotypic appearance of normal chondrocytes. However, isolated cells tended to be stellate in shape, with prominent cytoplasmic extensions. The cells tended to be grouped in chondrones rather than being uniformly distributed on the surface of chitosan scaffolds. This heterogeneity resulted in a wide variation in cell number per field on scanning electron microscopy of chitosan constructs.

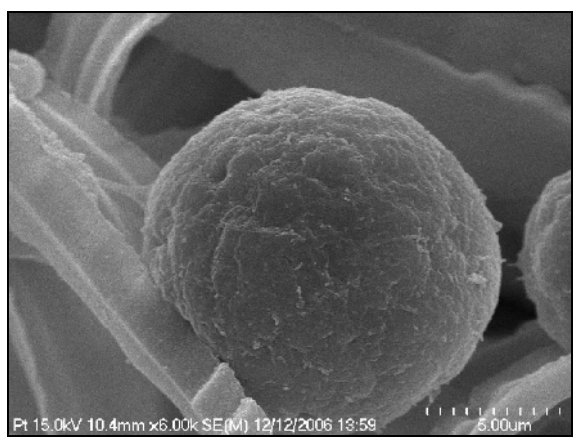

Figure 3: Scanning electron microscopy micrograph of a Chi 4 construct 48 hours after seeding chondrocytes (Magnification 6000x). The chondrocyte attached to the fiber exhibits a rounded shape and has the size of a normal chondrocyte.

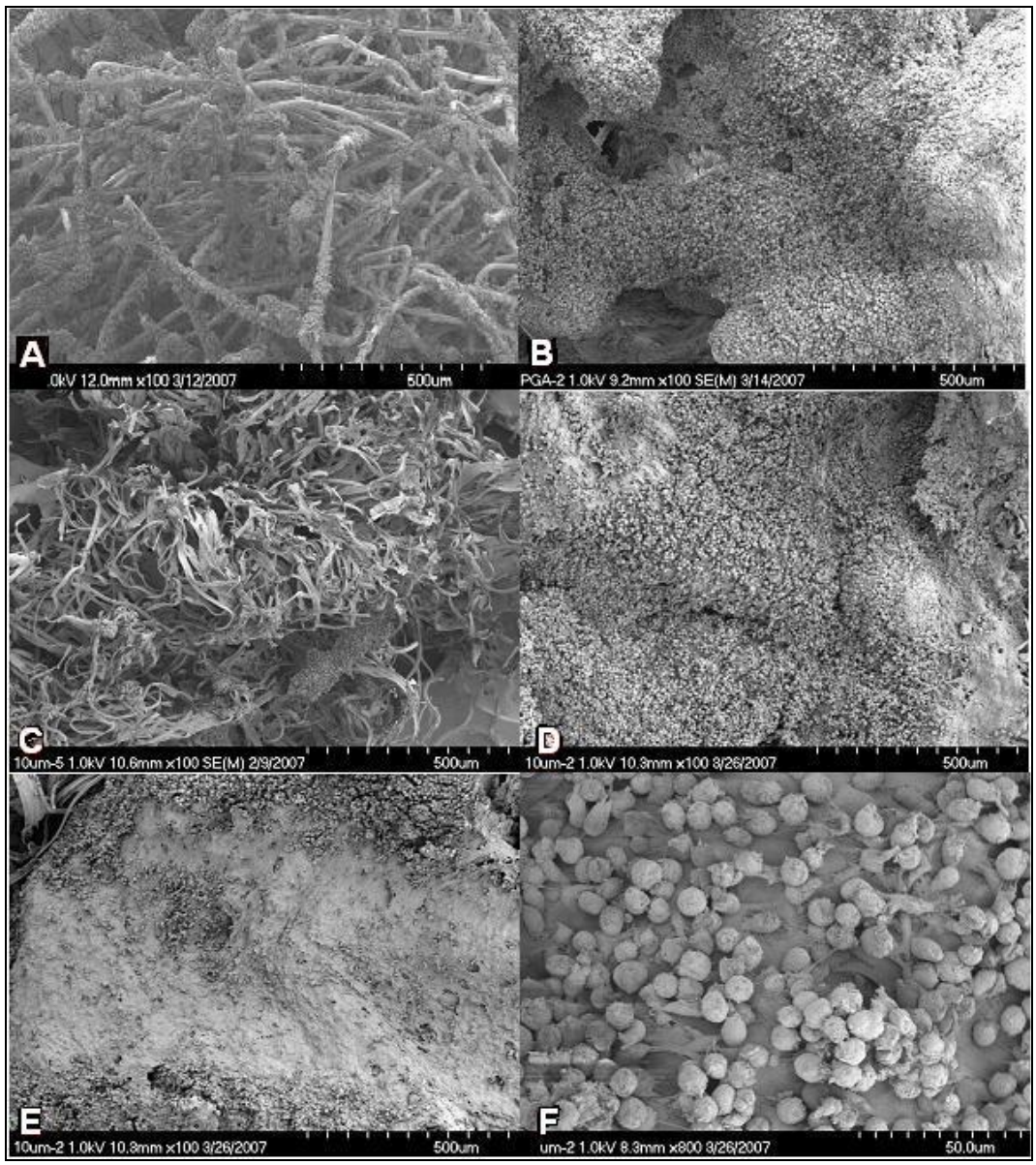

Figure 4: Scanning electron microscopy of constructs seeded with chondrocytes. A: PGA mesh, 48 hours after seeding. B: PGA, 21 days after seeding. C: Chi 4, 48 hours after seeding. D: Chi 4, 21 days after seeding. E: Center of a Chi 4 construct, 21 days after seeding. Cells are embedded in abundant extracellular matrix (100x). F: High magnification SEM of a Chi 13 construct, 21 days after seeding. Note the rounded appearance of cells and their relationship to adjacent ECM (800x).

DNA quantification confirmed SEM findings. At 48 hours after seeding, the quantity of total DNA yield per mg wet weight was 0.10 ± 0.04 $\mu g.mg^{-1}$ for Chi 4, 0.18 ± 0.02 $\mu g.mg^{-1}$ for Chi 13, 0.16 ± 0.01 $\mu g.mg^{-1}$ for Chi 22, 0.47 ± 0.09 $\mu g.mg^{-1}$ for PGA. The PGA mesh contained more DNA than chitosan constructs ($p < 0.001$). Chitosan constructs composed of larger fibers (22 or 13 μm) contained more DNA than those made of 4 μm-width fibers ($p = 0.02$ and $p = 0.05$, respectively). The cell seeding efficiency after 48 hours of culture was 48.8% for Chi 4, 70.2% for Chi 13, 65.7% for Chi 22, and 121.4% for PGA.

3.1.2.2. Evaluation of the Constructs after twenty-one Days:

Cell viability

The viability of the chondrocytes estimated by the live/dead assay did not differ between the four groups and was above 80 % for all scaffold types.

Scanning electron microscopy

Chondrocytes tended to form a film covering the surface of each construct and were embedded in ECM (Figure 4 BDEF). The amount of ECM observed in chitosan constructs appeared to correlate inversely with the width of fibers, more matrix being noted on 4 μm-width fibers. This group consisted essentially of a uniform matrix into which cells were embedded (Figure 4 EF). Cell counts were higher for PGA and Chi 22 than Chi 13 and Chi 4 constructs (Table 1). Whereas the chitosan scaffolds appeared intact, few remnants of PGA fibers were identified.

Composition	Chitosan	Chitosan	Chitosan	PGA
Fiber diameter (µm)	4	13	22	13
DNA (%/ww) (n=10 per group)	0.058 ± 0.01 [a]	0.062 ± 0.02 [a]	0.053 ± 0.01 [a]	0.808 ± 0.15 [b]
Number of cells per field (SEM) (n=4 per group)	53 [a]	59 [a]	95 [b]	99 [b]
Water (%) (n=10 per group)	92.0 ± 0.6	93.0 ± 0.7	93.0 ± 0.3	94.0 ± 0.6
Increase in dw (%) (n=10 per group)	330 ± 129	271 ± 138	328 ± 123	250 ± 159
GAG (%/ww) (n=10 per group)	0.72 ± 0.5 [a]	0.61 ± 0.6 [a]	0.52 ± 0.2 [a]	13.50 ± 3.0 [b]
GAG/DNA (n=10 per group)	31.4 ± 18 [a b]	27.3 ± 11.9 [a b]	35.8 ± 2.9 [a]	19.3 ± 3.1 [b]
Collagen II/DNA (n=6 per group)	101.41 ± 42.5 [a]	109.65 ± 88.3 [a]	110.80 ± 64.3 [a]	7.53 ± 3.5 [b]

Table 1: Water content, SEM and biochemical analysis of PGA and chitosan constructs (Mean ± Standard Deviation) 21 days after seeding. a, b: groups with different letters differ statistically ($p < 0.05$)

Histopathology

No major differences were found between the two histological stains (Figure 5 AB). Positive intensities were consistent with the presence of GAG surrounding cells in all groups (Figure 5 ABDE). In these areas, cell density was low with moderate distance between cells. These cells exhibited the size and rounded appearance characteristic of normal chondrocytes. This appearance may correspond to a more hyaline-like matrix formed in chitosan constructs (Figure 5 AC). As for the SEM evaluation, the chitosan scaffolds appeared intact, whereas few remnants of PGA fibers were identified on histological sections.

Cell number

PGA constructs contained more DNA than any other groups. The only statistical difference between chitosan groups was found between Chi 4 containing more DNA than Chi 22 (Table 1).

Quantitative evaluation of the extracellular matrix

The water content did not differ between groups (Table 1). The percentage of increase in dry weight was lowest in the PGA group and greatest in Chi 4 (Table 1). PGA constructs contained more GAG than chitosan constructs ($p < 0.001$). Within chitosan constructs, GAG content correlated inversely with fiber-width (Table 1). PGA constructs achieved a GAG/DNA ratio (19.4 ± 3.1) generally lower than chitosan constructs (range from 27.3 to 35.8 for the GAG/DNA). This difference was significant between Chi 22 and PGA ($p < 0.001$) (Table 1). The type II collagen/DNA ratio in all chitosan constructs (101.4 to 110.8) was greater than in PGA constructs (7.5 ± 3.5) ($p < 0.001$) (Table 1).

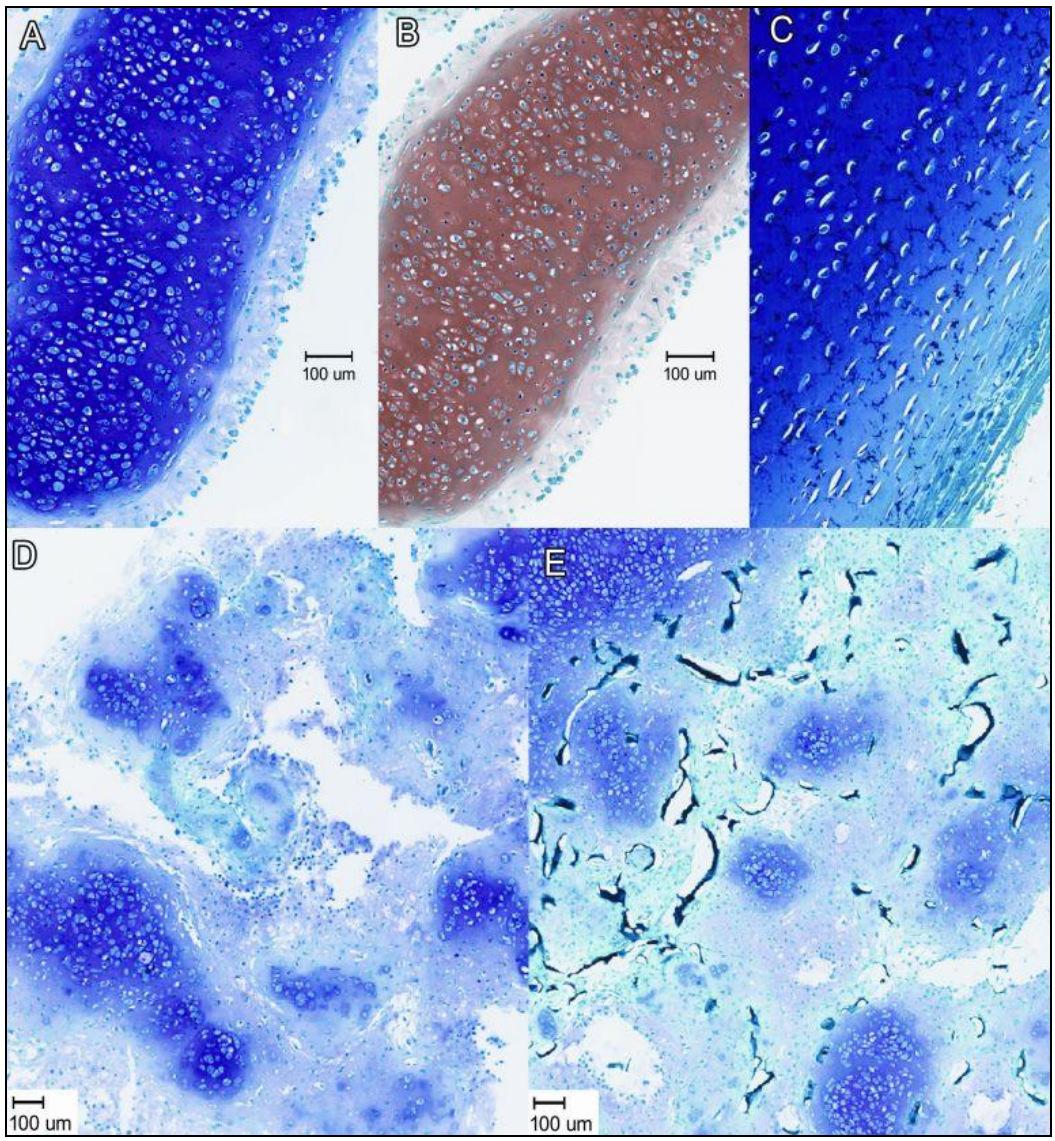

Figure 5: Histological analysis of PGA and chitosan constructs after 21 days of culture. A-B: Histological appearance of the same area of a Chi 13 construct stained with Toluidine Blue O (A) and Safranin O (B). C: Section of native cartilage stained with Toluidine Blue O for comparison. D-E: Histological appearance (Toluidine Blue O) of a PGA construct (D) and a Chi 22 construct (E) (4x).

3.2. Effect of Chitosan Scaffold Microstructure on Mesenchymal Stem Cells Chondrogenesis

3.2.1. Materials and methods

3.2.1.1. Scaffolds

The chitosan (Taehoon bio, Korea) had a molecular weight of about 400 kDA, a degree of deacetylation of 90% and a viscosity of 330 cP at a 0.5% concentration. The same chitosan solution was used to prepare the two types of scaffold. Chitosan flakes were dissolved and stirred at room temperature for 48 hours in a 0.2 M solution of acetic acid to obtain a 2% chitosan solution.

Chitosan fibrous scaffolds (CF, n = 30) were prepared using the wet spinning method (Figure 6). The chitosan solution was pumped into a 0.1 mm×1,500 holes spinneret using the geared metering pump. To coagulate the chitosan solution, the spinneret was immersed in an aqueous spin bath containing 10% sodium hydroxide. After exiting the coagulation bath, fibers were washed in alternative hot and cold water baths. Fibers (measuring 13 µm in diameter) were cut and dispersed in water, prior to filtration with 100 stainless steel mesh and drying. Chitosan fibrous scaffolds were cut to measure 5 mm in diameter and 3 mm in height.

Chitosan sponge scaffolds (CS, n = 30) were prepared using a freeze-drying technique (Griffon et al, 2005). The chitosan solution was poured into a 96-well mold, and cooled at a controlled rate of - 0.3°C.min^{-1} to – 80°C for 72 hours to obtain a mean pore size of 120 µm. The resulting solid product was then lyophilized for 48 hours. Scaffolds had a diameter of 5 mm, and a height of 3 mm.

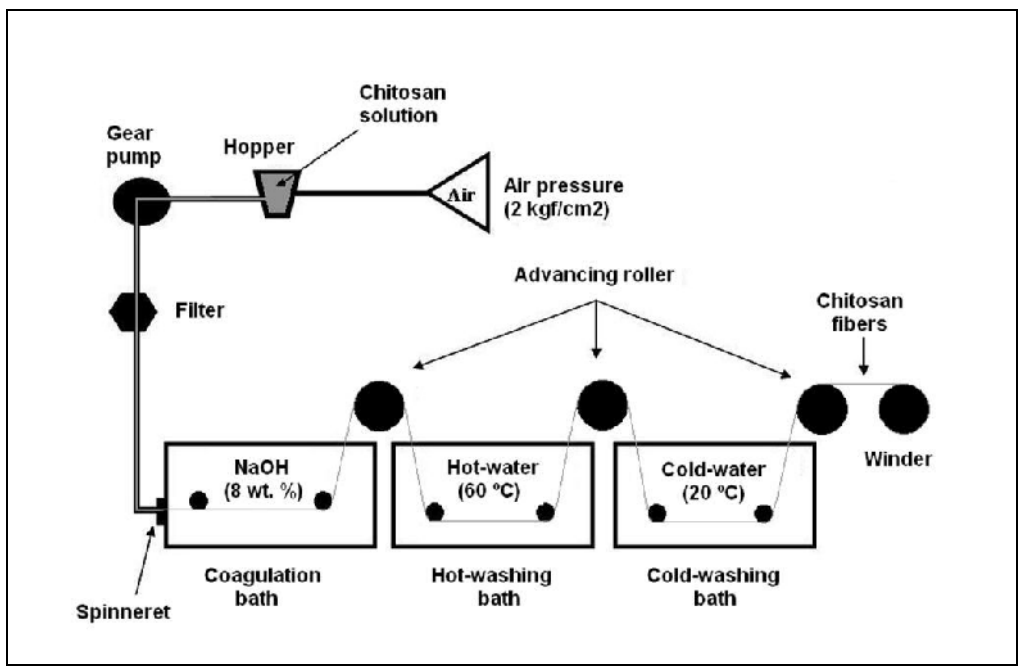

Figure 6: Diagram representing the wet spinning apparatus used to produce chitosan microfibers.

All scaffolds were standardized to a dry weight of 3.3 ± 0.3 mg. They were sterilized with ethylene oxide gas and rehydrated through a series of ethanol/PBS solutions (100, 95, 75, 50, 0% ethanol) (Marreco et al, 2004). Scaffolds were subsequently incubated at 37°C on a shaker incubator in DMEM (ATCC) for 24 hours before cell seeding (Griffon et al, 2006).

3.2.1.2. Mesenchymal Stem Cells:

A mesenchymal cell line (D1 ORL UVA, ATCC) derived from a multipotent mouse bone marrow stromal precursor was used for this study. Complete culture medium consisted of DMEM containing 4.5g.L^{-1} glucose, supplemented with 10% fetal bovine serum (ATCC), 100 U.mL^{-1} penicillin, and 100 μg.mL^{-1} streptomycin. Cells were harvested at their fourth passage and resuspended in chondrogenic medium prior to seeding. Chondrogenic medium consisted of DMEM containing 4.5g.L^{-1} glucose, supplemented with 1% Insulin-Transferrin-Selenous acid (Collaborative biomedical products, Bedford, MA), 10 ng.mL^{-1} TGF-β1 (R&D system, Minneapolis, MN), 5.33 μg.mL^{-1} linoleic acid, 1.25 μg.mL^{-1} bovine serum albumin, 1 mM sodium pyruvate, 100 U.mL^{-1} penicillin, 100 μg.mL^{-1} streptomycin and 100 nM dexamethasone. A cell suspension containing $2.0x10^6$ cells in 100 μL of medium was dropped on the surface of each scaffold (30 CF and 30 CS scaffolds) placed in untreated six-well non-tissue culture plates. Each construct was allowed to incubate at 37˚C for one hour. After one hour, 4.5 ml of chondrogenic medium was added to each well and the plates were placed on a platform shaker oscillating at 60 rpm. The constructs were maintained at 37°C and 5% CO2 in chondrogenic medium for 72 hours, 10 days, or 21 days. The medium was changed three times a week.

3.2.1.3. Evaluation of the Scaffolds:

The microstructure of the scaffolds (n = 3 per group) was evaluated by SEM. Each scaffold was bisected in order to evaluate the surface as well as the central section of the scaffold. Two sections per scaffold (superficial and centre) were mounted and sputter coated with gold-palladium prior to examination with SEM (Hitachi S4700) at 1.0 kV.

Scaffolds (n = 5 per group) were weighed before and after dehydration to determine water content.

Total surface area was determined with Brunauer, Emmett, and Teller calculations in a surface area analyzer (ASAP2010 Gemini 2360, Micromeritics, Norcross, GA) (Park et al, 2005). Briefly, a glass cell containing the scaffold was placed into liquid nitrogen for gas adsorption onto each scaffold. Once the adsorption of nitrogen gas was completed, the glass cell containing the scaffold was placed in a water bath at ambient temperature and desorption of gas was calculated. Surface area was measured on at least three samples for each type of scaffold.

3.2.1.4. Evaluation of Constructs:

Seeding was evaluated at 72 hours via SEM (n = 3 per group), dry (n = 5) and wet (n = 8) weight measurements, and DNA quantification (n = 5). Chondrogenesis was evaluated after 10 days of culture via SEM (n = 2 per group), dry (n = 5) and wet (n = 9) weight measurements, and DNA and GAG quantifications (n = 5). Chondrogenesis was evaluated after 21 days of culture via SEM (n = 2 per group), live/dead assay (n = 2), histology (n = 2), dry (n = 6) and wet (n = 10) weights measurements, DNA and GAG quantifications (n = 3), and quantitative real time polymerase chain reaction (qRT-PCR) (n = 4).

Scanning electron microscopy

The same construct fixation protocol as described above was used. Following fixation, each construct was bisected in order to evaluate the surface as well as the central section of the construct. A total of two sections per construct (superficial and centre) were mounted for each construct and sputter coated with gold-palladium prior to examination with SEM (Hitachi S4700) at 1.0 kV. Criteria evaluated included cell morphology, cell attachment to the support, cell density, matrix production, and chitosan integrity.

Histopathology

The constructs were fixed in 10% neutral buffered formalin, embedded in plastic and cut via microtome to produce 1 μm-thick sections (Seddighi et al, 2008). Sections were stained with Safranin-O Green. Slides were examined to evaluate cell morphology, presence of ECM and integrity of the chitosan. The area containing extracellular matrix was measured using the ImageJ program (National Institutes of Health, Bethesda, MD) and expressed as a percent of the total area covered by the construct in each image. Two images from each of the two samples per group were included in the analysis.

Live/dead assay

The viability of cells in the constructs was determined using the live/dead viability/cytotoxicity kit (Invitrogen) according to the manufacturer's protocol. Confocal microscopy (Olympus BX50 Confocal Microscope, Olympus) allowed the visualization of calcein AM and ethidium homodimer-1. The intensities of viable and dead cells were recorded on four slides per construct at a magnification of 40x and two

slides at a magnification of 10x. The slides were analyzed using "Fluoview" software (Olympus) to determine the percentage of viable cells.

Weights, water content, DNA and glycosaminoglycans

Specimens were weighed before and after dehydration to determine water content.

The fluorometric assay described above was used to evaluate DNA content (Kim et al, 1988). The cell seeding efficiency was calculated using the number of cells contained in constructs after 72 hours of culture compared to the number of cells initially seeded on each scaffold. The number of cells contained in the constructs was calculated using the average DNA content per cell (11.4 pg per cell) evaluated by fluorometric assay at the time of cell seeding on cell suspensions containing 10^6 and $5x10^6$ cells.

The GAG content was evaluated via spectrophotometry as described above (Farndale et al, 1986).

Quantitative real time PCR

Snap frozen constructs were pulverized in liquid nitrogen using a dismembranator (Braun Biotech Int., Germany) (Reno et al, 1997). Total RNA was isolated from the powdered tissue using the RNeasy mini kit (Qiagen, Valencia, CA) according to the manufacturer's instructions. The isolated RNA was treated on a column with a DNase digestion kit (Qiagen) to eliminate genomic DNA contamination. Subsequently, first-strand cDNA was synthesized using the High-Capacity cDNA reverse Transcription Kits (Applied Byosystem, Foster City, CA). Quantitative real time PCR (qRT-PCR) was performed using TaqMan® Universal PCR Master Mix

(Applied Biosystems) with Mus musculus type I collagen (EMm00468761), type II collagen (Mm00491889) and type X collagen (Mm00487041) Taqman® Gene Expression Assays primer and probes (Applied Biosystems) and Eukaryotic 18s rRNA Endogenous Control (Applied Biosystems). An ABI Prism 7000 Sequence Detection System (Applied Biosystems) and its associated ABI 2.0 software were used to obtain the data. The qRT-PCR reactions were carried out in 50 µL final volumes. Each sample was run in triplicate. Thermal cycling was carried out for 40 cycles. The mRNA expression levels of target genes were normalized by dividing their value by the value of the 18s mRNA level. The gene expression levels in the chitosan fibrous scaffold (CF) group relative to the chitosan sponge (CS) group were analyzed by the $2^{-\Delta\Delta CT}$ method using the CS group as the calibrator (Livak et al, 2001).

3.2.1.5. Statistical Analysis

Cell viability, dry and wet weights, DNA content, GAG content, GAG/DNA ratio, and mRNA expression levels were compared between the sponge and fibrous chitosan scaffolds with a risk factor of less than 0.05 considered statistically significant. All data were expressed as mean ± standard deviation. Statistical differences were evaluated between the CF and the CS constructs with a t-test using Systat 11.0 statistical software.

3.2.2. Results

3.2.2.1. Evaluation of the Scaffolds

The fiber diameter in the meshes and the pore size in the sponges were homogeneous and respectively 13 µm in diameter and 120 µm in diameter (Figure 7).

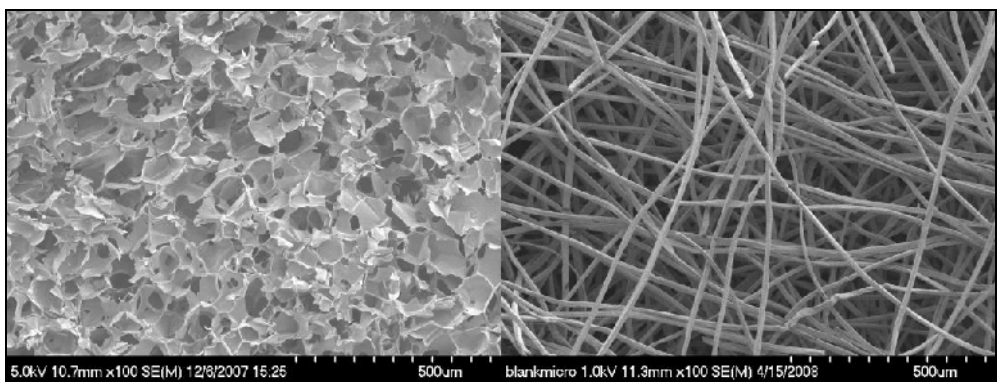

Figure 7: Scanning electron micrographs of the scaffolds. Left: Chitosan sponge scaffold. Right: Chitosan fibrous scaffold. (100x)

The water content of the CS scaffolds (97.7 ± 0.3%) was greater than that of the CF scaffolds (95.4 ± 0.6%) ($p = 0.042$).

The total surface area of the CS scaffolds (9.2 $m^2.g^{-1}$) was greater than that of the CF scaffolds (0.51 $m^2.g^{-1}$).

3.2.2.2. Seeding Phase:

Most MSCs exhibited a spindle-shape with prominent cytoplasmic extensions. The cells tended to be grouped rather than uniformly distributed on the surface of both types of scaffolds (Figure 8 A-B). Cell attachments in the center of the scaffolds did not seem as abundant as at the periphery. No major difference in cell morphology, cell attachment, and cell density between the different scaffold types was observed.

The wet weight of the CS constructs (143 ± 26 mg) was greater than that of the CF constructs (78 ± 29 mg) 72 hours after seeding ($p < 0.001$). At 72 hours no difference in dry weight was found between the two groups (6.0 ± 1.0 mg for CS and 4.5 ± 1.2 mg for CF, $p = 0.112$). The DNA content was also similar between CS constructs (36.6 ± 6.3 $\mu g.mg^{-1}$) and CF constructs (33.0 ± 8.8 $\mu g.mg^{-1}$)($p = 0.475$). The cell seeding efficiency after 72 hours of culture averaged 85.04 ± 10.15% in all scaffolds.

3.2.2.3. Evaluation of Chondrogenesis at ten and twenty-one Days:

Scanning electron microscopy

At 10 and 21 days, cells were embedded in ECM but did not appear to form aggregates. All constructs appeared to contain more ECM after 21 days than after 10 days of culture. Fibrous scaffolds seemed to contain more ECM. The morphology of cells changed from the spindle-shape after seeding to a rounder morphology at 21 days

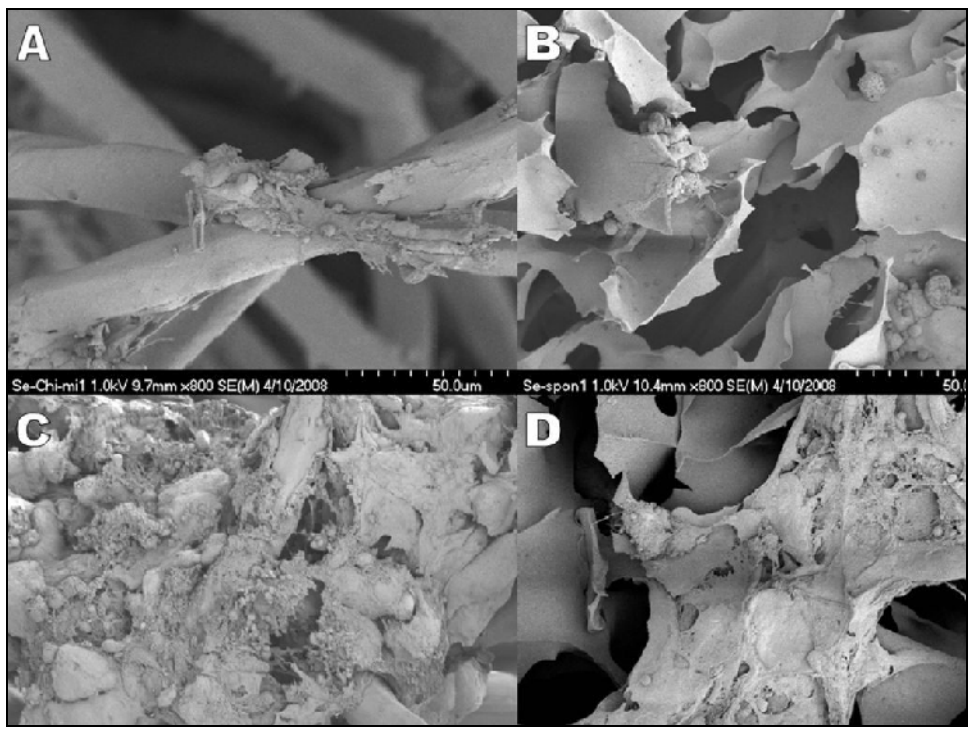

Figure 8: Scanning electron micrographs of constructs seeded with mesenchymal stem cells. A: Chitosan fibrous scaffolds 72 hours after seeding. B: Chitosan sponges 72 hours after seeding. C: Chitosan fibrous scaffolds 21 days after seeding. D: Chitosan sponges 21 days after seeding. (800x)

(Figure 8). However, only cells not embedded in matrix could be observed. The structural appearance of chitosan appeared intact after 21 days of culture in both groups (Figure 8 CD).

Histopathology

Cell and ECM distribution were not homogeneous: more cells and ECM were present in the periphery of the constructs. More ECM was subjectively observed in the fibrous constructs (Figure 9). The chitosan structure appeared intact in all constructs. The surface area covered by extracellular matrix on histology was 26.3 ± 19.2 % for the CF constructs and 6.2 ± 2.5 % for the CS constructs. Despite the important variability, a trend for increased extracellular matrix in the CF constructs was present ($p = 0.083$).

Weights, water content, live/dead assay, DNA and glycosaminoglycans

The dry weights did not differ between the two groups at all evaluation times (6.5 ± 0.6 mg for CS and 6.0 ± 0.6 mg for CF at 10 days ($p = 0.227$) and 6.3 ± 0.9 mg for CS and 5.8 ± 1.1 mg for CF at 21 days ($p = 0.331$)). The wet weight of the CS constructs was greater than the CF constructs at 10 (131.3 ± 18.4 mg for CS and 93.5 ± 15.8 mg for CF, $p < 0.001$) and 21 days (135.6 ± 17.6 mg for CS and 95.7 ± 36.6 mg for CF, $p = 0.006$). The water content of the CS constructs at 10 days (95.0 ± 0.7%) was greater than that of the CF constructs (94.1 ± 0.3%)($p = 0.033$). A similar trend was present at 21 days, with a water content equal to 95.3 ± 0.6% for CS and 94.5 ± 0.77% for CF ($p = 0.07$).

The viability of the chondrocytes estimated by a live/dead fluorescent assay at 21 days did not differ between the two groups and was above 90% for all scaffolds (96.2 ± 9% for CS and 95.6 ± 10% for CF, $p = 0.538$). The DNA content was not

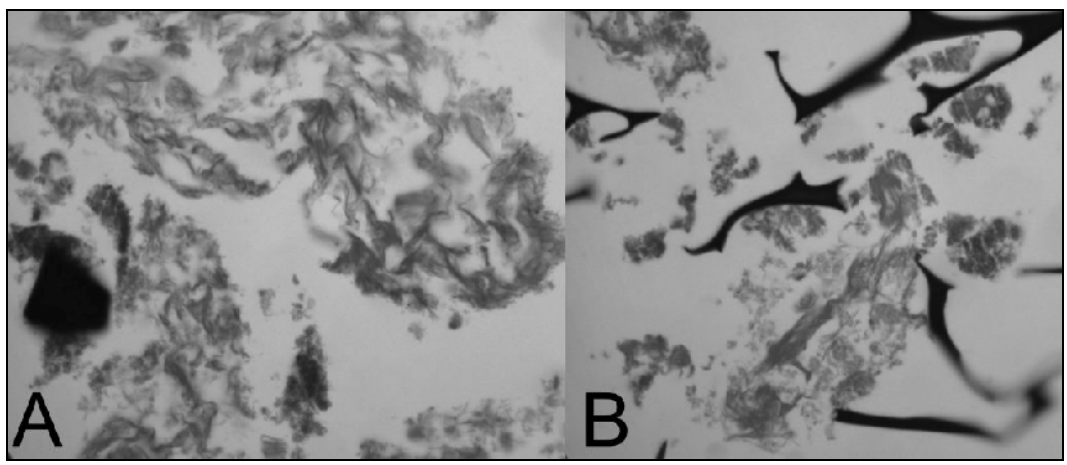

Figure 9: Histological Safranin-O Green stained sections. A: Chitosan fibrous scaffolds 21 days after seeding. B: Chitosan sponges 21 days after seeding. The scaffold is stained in black.

significantly different at 10 or 21 days after seeding between the two scaffold types (35.8 ± 11.9 $\mu g.mg^{-1}$ for CS and 44.7 ± 8.5 $\mu g.mg^{-1}$ for CF at 10 days ($p = 0.58$) and 38.7 ± 8.8 $\mu g.mg^{-1}$ for CS and 43.4 ± 3.9 $\mu g.mg^{-1}$ for CF at 21 days ($p = 0.15$)).

The GAG content and the GAG/DNA ratios did not differ between the CF and the CS groups at 10 days. At 21 days, CF constructs contained more GAG than CS constructs (2.64 ± 0.32 $\mu g.mg^{-1}$ dry weight and 0.93 ± 0.29 $\mu g.mg^{-1}$ dry weight, respectively; $p < 0.01$) (Figure 10). There was also a trend toward an increased GAG/DNA ratio for the CF group (0.058 ± 0.004 for CF and 0.026 ± 0.015 for CS; $p = 0.07$).

Quantitative real time PCR

The level of mRNA expression for the type II collagen gene was three times greater for the CF group compared to the CS group at 21 days ($p = 0.04$) (Figure 11). No difference in type I collagen and type X collagen mRNA expression was found between the two groups.

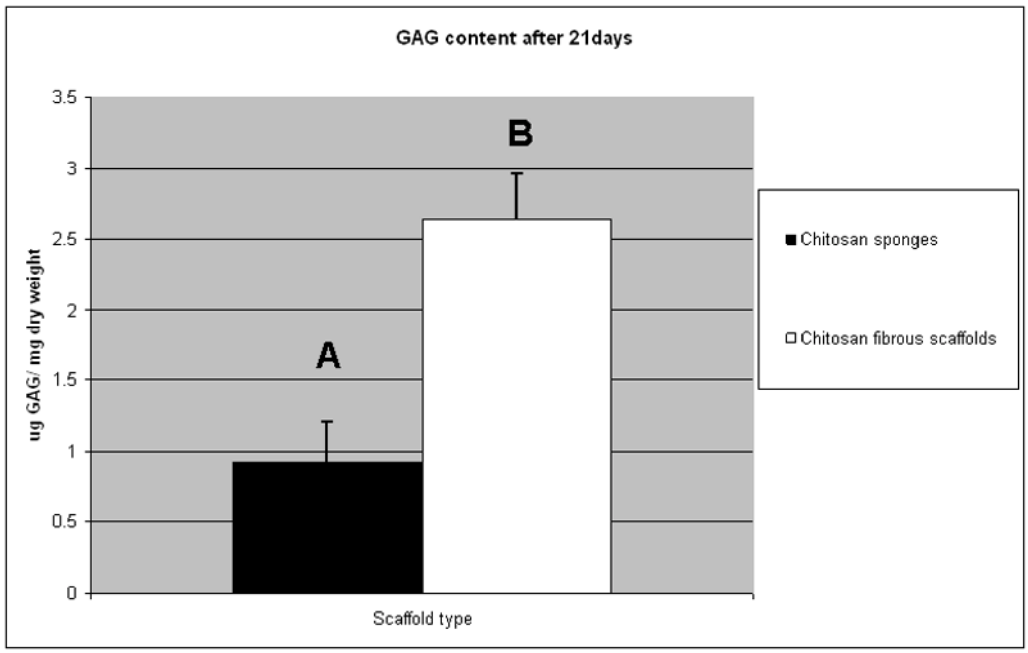

Figure 10: GAG content 21 days after seeding. A, B: groups with different letters differ statistically ($p < 0.05$).

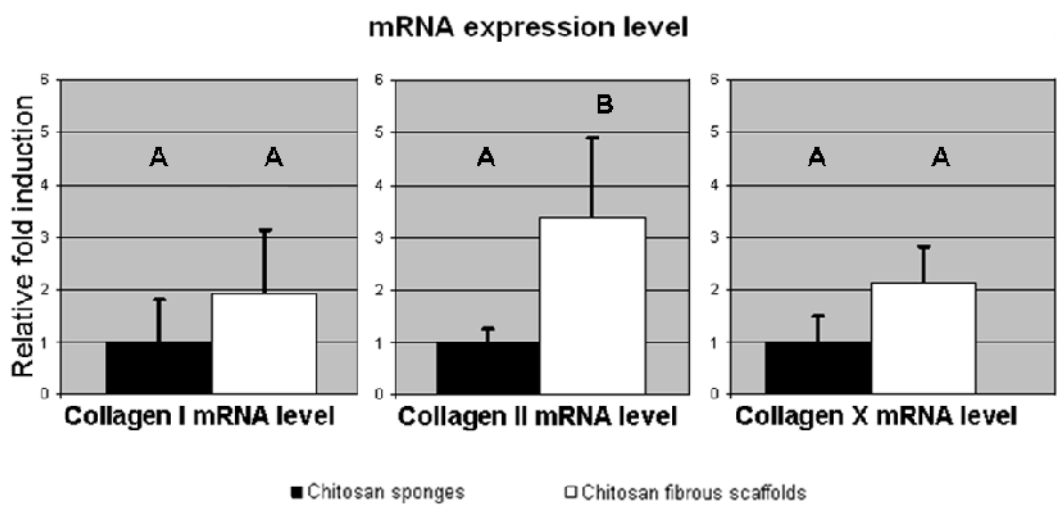

Figure 11: mRNA expression level of type I collagen, type II collagen and type X collagen, 21 days after seeding. A, B: groups with different letters differ statistically ($p < 0.05$).

3.3. Modification of the Chemical Composition of Chitosan Scaffolds to Improve Mesenchymal Stem Cells Adhesion

3.3.1. Preliminary Study on Hyaluronic acid Coating

A preliminary study was performed to test the effects of HA coating on cell adhesion, cell proliferation and extracellular matrix production of MSCs seeded on fibrous scaffolds obtained with the wet spinning technique with (n = 22) or without HA coating (n = 22). The scaffolds were prepared following the same protocol as described in paragraph 3.2.1.1. The hyaluronic acid coating was obtained by placing the chitosan scaffolds in a 0.5% sodium hyaluronate solution (Hylartin® V, Pfizer Animal Health products, NY) for 12 hours prior to drying. MSCs were harvested at their fourth passage and resuspended in chondrogenic medium as described in paragraph 3.2.1.2. A cell suspension containing $2.0x10^6$ cells in 100 μL of medium was dropped on the surface of each scaffold. Each construct was allowed to incubate at 37˚C for one hour. After one hour, 4.5 ml of chondrogenic medium was added to each well and the plates were placed on a platform shaker oscillating at 60 rpm. The constructs were maintained at 37°C and 5% CO2 in chondrogenic medium for 72 hours, 10 days, or 21 days. The medium was changed three times a week.

Following the same protocols as described in paragraph 3.2.1.4., seeding was evaluated at 72 hours via SEM (n = 3 per group), dry (n = 5) and wet (n = 8) weight measurements, and DNA quantification (n = 5). Chondrogenesis was evaluated after 10 days of culture via SEM (n = 2 per group), DNA and GAG quantifications (n = 5). Chondrogenesis was evaluated after 21 days of culture via SEM (n = 2 per group), live/dead assay (n = 2), DNA and GAG quantifications (n = 3). All data were expressed

as mean ± standard deviation. Statistical differences were evaluated between the two groups of constructs with a t-test using Systat 11.0 statistical software.

After seeding, most MSCs exhibited a spindle shape with prominent cytoplasmic extensions. No major difference in cell focal adhesions and cell density was observed between the different types of scaffolds. Cell attachment did not seem as abundant in the center of the scaffolds as in the periphery. No difference in wet weight (79.4 ± 16.0 mg), dry weight (4.7 ± 1.0 mg), and water content (93.67 ± 1.55%) was found between groups after seeding. Uncoated chitosan fibrous constructs contained the same amount of DNA (32.8 ± 9.7 $\mu g.mg^{-1}$) compared to the HA-coated fibrous constructs (31.7 ± 12.1 $\mu g.mg^{-1}$).

All constructs appeared to contain more ECM after 21 days than after 10 days of culture based on SEM evaluation. The morphology of cells changed from the spindle-shape after seeding to a rounder morphology at 21 days. No difference was observed between the two groups. The viability of cells at 21 days did not differ between the two groups and was above 85% for all scaffolds. The DNA content was not significantly different at 10 or 21 days after seeding between the two scaffold types (43.5 ± 7.38 $\mu g.mg^{-1}$ for the non-coated and 37.4 ± 6.9 $\mu g.mg^{-1}$ for the coated at 10 days and 41.4 ± 3.9 $\mu g.mg^{-1}$ for the non-coated and 42.8 ± 6.9 $\mu g.mg^{-1}$ for the coated at 21 days).

The GAG content ratios did not differ between the two groups at 10 and 21 days (2.11 ± 1.50 $\mu g.mg^{-1}$ for the non-coated and 1.30 ± 0.41 $\mu g.mg^{-1}$ for the coated at 10 days and 2.34 ± 0.20 $\mu g.mg^{-1}$ for the non-coated and 2.01 ± 0.43 $\mu g.mg^{-1}$ for the coated at 21 days).

3.3.2. Evaluation of the Degree of Deacetylation and type II Collagen Coating: Materials and Methods

3.3.2.1. Scaffolds:

The chitosan (Texanmedtecho, Korea) used in this study has a molecular weight of 400 kDA and a degree of deacetylation of 92%. Chitosan powder was dissolved and stirred at room temperature for 48 hours in 2 wt. % aqueous acetic acid solution to obtain a 4 wt. % chitosan solution.

Chitosan fibrous scaffolds were prepared using the wet spinning method described above. Chitosan fibrous scaffolds were cut to measure 4 mm in diameter and 1.5 mm in height (group 1).

A portion of the chitosan fibers was reacetylated by suspension in 150 ml of methanol and acetic anhydride (1 mol per glucosamine unit). The mixture was stirred at 40ºC for 24 hours. The treated fibers were washed several times with 100% ethanol, and air-dried. Fibers were cut to 51 mm and carded to obtain the reacetylated chitosan fibers web. The web was bonded by passing through the water-jet chamber and dried. Reacetylated chitosan fibrous scaffolds were cut to measure 4 mm in diameter and 1.5 mm in height (group 3).

Two types of type II collagen solutions were used to coat the scaffolds. Solution 1 was obtained by dissolving 10 mg of type II collagen (Calf type II collagen, Elastin Products Company) in 10 ml of 0.4 $mg.mL^{-1}$ of acetic acid. The two types of scaffolds (chitosan and reacetylated chitosan) were placed in solution 1 for one hour. The chitosan scaffolds dissolved in the collagen solution. The reacetylated chitosan scaffolds were freeze-dried (group 4). Solution 2 was obtained by adding ethanol to solution 1 at a concentration of 3 $mg.mL^{-1}$ to prevent dissolution of chitosan scaffolds.

The two types of scaffolds (chitosan (group 2) and reacetylated chitosan (group 5)) were kept in solution 2 for one hour and dried at room temperature.

A total of 30 scaffolds were prepared for each of the following groups:

1- Chitosan scaffolds

2- Collagen-coated chitosan scaffolds

3- Reacetylated chitosan scaffolds

4- Collagen-coated reacetylated chitosan scaffolds (without ethanol)

5- Collagen-coated reacetylated chitosan scaffolds (with ethanol).

All scaffolds had a dry weight of 1.98 ± 0.18 mg. They were sterilized with ethylene oxide gas and rehydrated through a series of ethanol/PBS solutions (100, 95, 75, 50, 0% ethanol) (Marreco et al, 2004). The scaffolds were subsequently incubated at 37°C on a shaker incubator in DMEM (ATCC) for 2 hours prior to cell seeding (Griffon et al, 2006).

3.3.2.2. Mesenchymal Stem Cells:

The same mesenchymal cell line (D1 ORL UVA, ATCC) and same culture medium as above were used for this study. Cells were harvested at their fourth passage and suspended in medium prior to seeding. A cell suspension containing $1.0x10^6$ cells in 20 µL of medium was dropped on the surface of each scaffold (15 scaffolds per group, 5 groups) and placed in untreated six-well non-tissue culture plates. Each construct was allowed to incubate at 37˚C for one hour. After one hour, 4 ml of culture medium was added to each well and the plates were placed on a platform shaker oscillating starting at 30 rpm and increased to 60 rpm after 3 hours. The constructs were maintained at 37°C and 5% CO2 in culture medium for 24 hours, 48 hours, or 72 hours.

3.3.2.3. Evaluation of the Scaffolds:

Fourier-transform infrared spectroscopy

Fourier-transform infrared (FTIR) spectra of each scaffold type (n = 3) were analyzed by spectrophotometry (Nicolet Nexus FTIR 670, Thermo Electron, Waltham, MA) of dehydrated specimens ground with potassium bromide powder and compressed into pellets. Element analysis was used to determine the degree of substitution of the N-acyl groups and the presence of collagen.

Scanning electron microscopy

Each scaffold (n = 2 per group) was mounted and sputter coated with gold-palladium prior to examination with SEM at 1.0 kV. Criteria evaluated included fiber size, surface characteristics, and the presence of type II collagen.

Transmission electron microscopy

The scaffolds (n = 2 per group) were fixed in a Karnovsky's fixative in phosphate buffered 2% glutaraldehyde and 2.5 % paraformaldehyde. The scaffolds were then washed in Sorenson's phosphate buffer. Microwave fixation was achieved with 2% osmium tetroxide, followed by the addition of 3% potassium ferricyanide for five minutes. After washing the samples, saturated uranyl acetate was added for one hour. The specimens were dehydrated in a series of increasing concentrations of ethanol. Acetonitrile was used as the transition fluid between ethanol and the epoxy. An infiltration series was done with an epoxy mixture using the epon substitute Lx112. The resulting blocks were polymerized at 90ºC overnight, trimmed and ultra-thin sectioned with diamond knives. Transverse (n = 3) and longitudinal (n = 3) sections of 0.35 μm were cut with diamond knives in each specimen. Light microscopy slides were made

with one transverse and one longitudinal section and stained with Toluidine Blue O and Basic Fucshine. Transmission electron microscopy (TEM) sections (two transverse and two longitudinal sections) were stained with uranyl acetate and lead citrate, and examined with a transmission electron microscope (Hitachi H600, Schaumburg, IL, USA). Criteria evaluated included homogeneity of the fiber size, presence of a coating at their surface and homogeneity of the coating.

Type II collagen content

Type II collagen content per scaffold (n = 3 per group) was determined by the same enzyme linked immunosorbent assay (Arthrogen-CIA® Native Type II Collagen Detection Kit, Chondrex) described above (Griffon et al, 2006).

Water content and porosity

Scaffolds (n = 5 per group) were weighed before and after dehydration to determine their wet and dry weights, and water content.

The porosity was calculated using the equation (Chang et al, 2010):

Porosity (%) = [(Weight wet – Weight dry)/Water density] / Sample volume

The sample volume was 0.03 cm^3 for all scaffolds. The water density was considered 1 $g.cm^{-3}$.

Mechanical property of the chitosan and reacetylated chitosan scaffolds

The tensile properties of the scaffolds were evaluated according to ASTM D-5035 using universal instron tester (Model LR5kPlus, Lloyd instrument Co). The chitosan and reacetylated chitosan scaffolds were cut to 100 × 25 mm. Five specimens were tested for each groups. A 5 Newton load cell was used at a constant rate of 100

$mm.min^{-1}$. The same tests were repeated after the scaffolds were placed in PBS buffer solution at 37ºC for 1, 2, and 3 weeks. The breaking strength was measured to evaluate the change of bulk properties and mechanical stability.

3.3.2.4. Evaluation of Constructs:

Evaluation of cell binding kinetics and cell viability

Cell binding kinetics and viability were evaluated after the initial incubation phase, once fresh media was added to each well. The number of cells suspended in medium and their viability were evaluated at one, two, four, six, 18 and 22 hours after the initial seeding via trypan blue exclusion. Measurements were taken separately for each scaffold type among two wells. The cell concentration in the medium was compared for each time point (Vunjak-Novakovic et al, 1998).

Live/dead assay

The viability of cells in the constructs 48 hours after seeding was determined using the live/dead viability/cytotoxicity kit (Molecular Probes) as described above. Constructs (n = 2 per group) were washed three times in sterile PBS for two minutes, placed on a glass slide, and immersed in 200 μL of PBS solution containing 2 mM calcein AM and 4 mM ethidium homodimer 1 prior to incubation for 40 min at room temperature. The intensities of viable and dead cells were recorded on four field of view at a magnification of 40x.

Weights, water, and DNA content

Constructs were weighed 24 (n = 5 per group) and 72 (n = 5 per group) hours after seeding before and after dehydration to determine their wet and dry weights,

respectively. The water content was subsequently calculated. After dehydration, the constructs were assayed for their DNA contents using the same fluorometric assay as described above (Kim et al, 1988). The number of cells contained in the constructs was calculated using the average DNA content per cell (5.34 pg per cell) as evaluated by fluorometric assay at the time of cell seeding on cell suspensions containing $1x10^6$ and $2x10^6$ cells (Griffon et al, 2006).

The number of cells present in the well unattached to a scaffold was evaluated by DNA quantification 24 (n=2 per group) and 72 (n=2 per group) hours after seeding. The cell-media solutions were collected and centrifuged at 250 $rpm.rcf^{-1}$ for ten minutes and the pellet was assayed for DNA content using the above protocol.

Transmission electron microscopy

The evaluation protocol used for the constructs was similar to that described above for the scaffolds. One construct per group was evaluated at 24, 48, and 72 hours after seeding. The light microscopy slides were evaluated to assess the cell distribution. Criteria evaluated via TEM included cell morphology, cell size, cell attachment to the support, and presence of cytoplasmic extensions.

Histology

Light microscopy slides were made following the same protocol as described above for TEM evaluation of the scaffolds. Histological sections were stained with Toluidine Blue O and Basic Fucshine and evaluated to assess the cell distribution.

The constructs (n = 2 per group at 72 hours) were fixed in 10% neutral buffered formalin, embedded in plastic and cut via microtome to produce three 8 μm-thick sections (one superficial, one in the middle, and one at the bottom) (Seddighi et al,

2008). Sections were stained with a trichrome stain. Slides were examined for cell morphology, cell distribution within slides and between slides of the same construct, and integrity of the scaffold.

Scanning electron microscopy

The same construct fixation protocol as above was used. A total of two sections per construct (surface and bottom, n = 2 per group at 72 hours) were mounted for each construct and sputter coated with gold-palladium prior to examination with SEM at 1.0 kV. Criteria evaluated included cell attachment to the support, presence of cytoplasmic extensions, cell density, and integrity of the scaffold.

3.3.2.5. Statistical Analysis

Dry and wet weights, increase in dry weight, water contents, cell counts in medium, cell viability, DNA content, and increase in DNA content between 24 and 72 hours were compared between the five groups with a risk factor of less than 0.05 considered statistically significant. All data were expressed as mean ± standard deviation. Statistical differences were evaluated between the groups with an ANOVA using Systat 11.0 statistical software. Post-hoc analyses were performed with the LSD test.

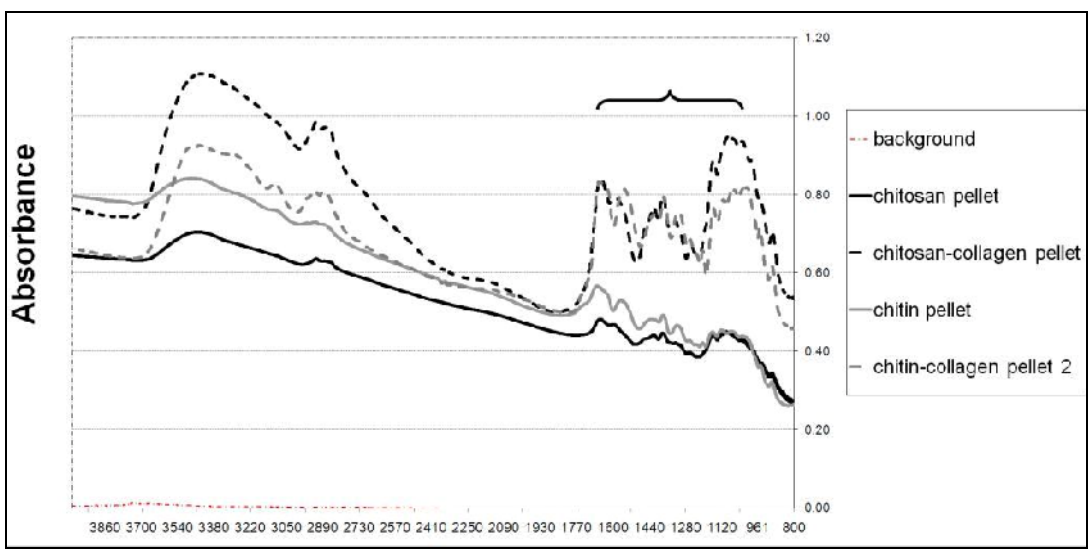

Figure 12: FTIR spectroscopy results. The Element analysis was used to determine the degree of substitution of the N-acyl groups. The presence of collagen was confirmed in the coated scaffolds by the presence of bands typical of amide I, II, and III (brace).

3.3.3. Evaluation of the Degree of Deacetylation and type II Collagen Coating: Results

3.3.3.1. Evaluation of the Scaffolds:

Fourier transform infrared spectroscopy

The degree of deacetylation was 92% for the chitosan scaffolds and 4% for the reacetylated chitosan scaffolds (Figure 12). The presence of collagen was confirmed by the presence of bands typical of amide I (1658 cm^{-1}), amide II (1552 cm^{-1}), and amide III (1240 cm^{-1}) (Figure 12) (Cao et al, 2008).

Scanning electron microscopy

All fibers had a diameter of 13 to 15 µm. They appeared homogeneous within scaffolds and among the different groups. The difference between chitosan and collagen was difficult to distinguish because of similar contrast with SEM evaluation.

Transmission electron microscopy

All fibers appeared of similar size among all TEM samples. A layer of collagen was observed at the surface of the fibers in all collagen-coated scaffolds (Figure 13). No difference in coating was observed between the center and the periphery or between scaffolds. Aggregation of collagen molecules was observed occasionally in the center as well as in the periphery and in all types of collagen-coated scaffolds (Figure 13).

Type II collagen content

Type II collagen was not detected in the non-coated scaffolds. The type II collagen content was 4.11 ± 1.39 $\mu g.mg^{-1}$ for the collagen-coated chitosan scaffolds, 4.98 ± 0.15 $\mu g.mg^{-1}$ for the collagen-coated reacetylated chitosan scaffolds (without

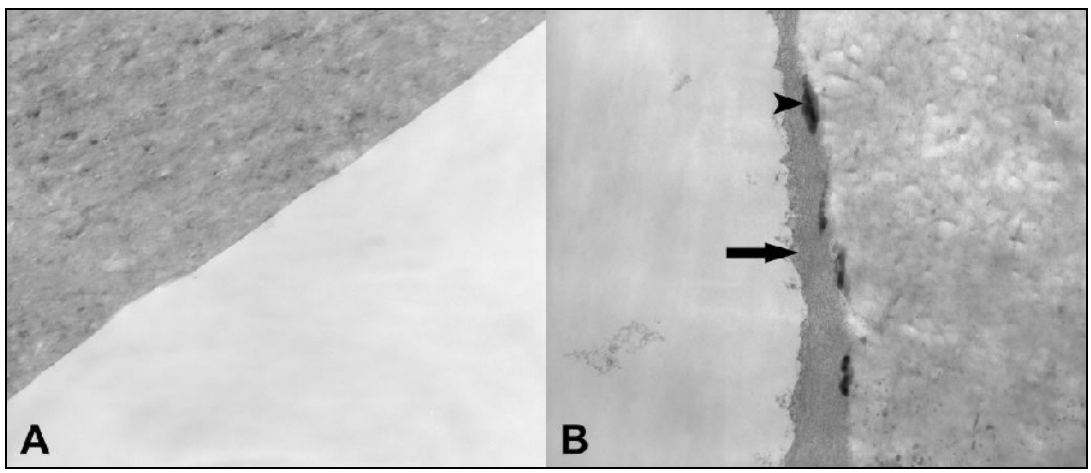

Figure 13: Transmission electron micrographs of the edge of a fiber from a chitosan scaffold (A) and a collagen-coated chitosan scaffold (B). The black arrow indicates the collagen layer seen at the surface of the collagen-coated chitosan fiber; the arrowhead indicates an aggregation of collagen molecules (50,000x).

ethanol), and 8.04 ± 2.00 μg.mg^{-1} for the collagen-coated reacetylated chitosan scaffolds (with ethanol). The collagen-coated reacetylated chitosan scaffolds contained more type II collagen than the collagen-coated chitosan and the collagen-coated reacetylated chitosan (without ethanol) scaffolds ($p = 0.032$ and $p = 0.044$, respectively).

Water content and porosity

No difference was found in water content nor porosity among groups (mean values among the different groups of 92.5 ± 1.8%, $p = 0.653$ and 86.4 ± 20.7%, $p = 0.524$, respectively) (Table 2).

Mechanical property of the chitosan and reacetylated chitosan scaffolds

The stress, strain and maximum load to failure of the chitosan and reacetylated chitosan scaffolds are reported in Table 3.

3.3.3.2. Evaluation of Constructs:

Evaluation of cell binding kinetics and cell viability

Cell death in the medium was negligible (less than 5%) throughout the experiment for all seeding techniques as assessed by trypan blue exclusion. Less than 10% of the cells remained in suspension one hour after the seeding for all scaffold types. No difference in cell concentration was found until six hours after seeding. More cells remained in suspension in the wells of the chitosan scaffolds than in other groups six hours after seeding ($p = 0.014$) but this difference was not found at any later time points ($p > 0.497$).

Composition	Chitosan	Collagen-coated chitosan (ethanol)	Reacetylated chitosan	Collagen-coated reacetylated chitosan	Collagen-coated reacetylated chitosan (ethanol)
Scaffold water content (%) (n = 5 per group)	92.9 ± 1.7 **A**	92.7 ± 1.8 **A**	92.7 ± 1.4 **A**	92.5 ± 1.1 **A**	92.5 ± 1.8 **A**
Scaffold porosity (%) (n = 5 per group)	87.2 ± 19.0 **A**	91.8 ± 22.6 **A**	93.7 ± 20.0 **A**	84.1 ± 19.8 **A**	85.1 ± 20.6 **A**
Construct water content (%) (n = 5 per group)	90.0 ± 2.0 **A**	91.9 ± 3.0 **A**	91.4 ± 2.4 **A**	90.3 ± 1.2 **A**	90.4 ± 3.9 **A**
Cell seeding efficiency at 24 hours (%) (n = 5 per group)	47.2 ± 8.6 **B**	81.8 ± 32.5 **A**	25.5 ± 10.7 **C**	24.6 ± 3.6 **C**	23.5 ± 6.4 **C**

Table 2: Summary statistics of the scaffold water content and porosity, the construct water content, and the cell seeding efficiency of the scaffolds or constructs. A, B, C: groups with different letters differ statistically ($p < 0.05$).

		Week 0	Week 1	Week 2	Week 3
Chitosan scaffold (n = 5 per group)	Maximum load (N)	5.27 ± 0.04	5.24 ± 0.05	5.13 ± 0.03	5.24 ± 0.01
	Stress (N / mm)	0.41 ± 0.01	0.42 ± 0.01	0.39 ± 0.03	0.40 ± 0.04
	Strain (%)	48.6 ± 10.8	50.5 ± 5.33	38.2 ± 1.91	51.6 ± 4.39
Reacetylated chitosan scaffold (n = 5 per group)	Maximum load (N)	5.35 ± 0.04	5.21 ± 0.07	5.12 ± 0.10	5.06 ± 0.04
	Stress (N / mm)	0.41 ± 0.01	0.409 ± 0.01	0.39 ± 0.01	0.395 ± 0.01
	Strain (%)	34.8 ± 9.75	35.6 ± 3.58	35.8 ± 7.27	21.6 ± 5.57

Table 3: Mechanical properties and stability of the chitosan and reacetylated scaffolds (mean ± standard deviation, n=5 per group).

Live/dead assay

The viability of the MSCs estimated by a live/dead fluorescent assay 48 hours after seeding did not differ among the five groups and remained above 83.6% for all constructs (93.9% ± 8.9, $p = 0.447$).

Weights, water, and DNA content

No difference was found between groups in wet weight, dry weight and water content after seeding ($p = 0.249$, $p = 0.403$, and $p = 0.432$, respectively). The water content was 90.8 ± 2.6% (Table 2).

The DNA remained stable within groups from 24 to 72 hours after seeding. ($p > 0.172$ for all scaffold types). The average DNA content was 2.51 ± 0.46 μg for the chitosan constructs, 4.37 ± 1.73 μg for the collagen-coated chitosan constructs, 1.36 ± 0.57 μg for the reacetylated chitosan constructs, 1.32 ± 0.19 μg for the collagen-coated reacetylated chitosan constructs (without ethanol), and 1.25 ± 0.34 μg for the collagen-coated reacetylated chitosan constructs (with ethanol) (Figure 14). The collagen-coated chitosan constructs contained more DNA than any other constructs at 24 and 72 hours ($p < 0.001$ for all comparisons). Chitosan constructs contained more DNA than the collagen coated reacetylated chitosan constructs at 24 hours ($p = 0.030$ and $p = 0.045$) and than all reacetylated chitosan constructs at 72 hours ($p = 0.002$ - 0.004). No difference was found between the reacetylated chitosan constructs at either 24 or 72 hours ($p > 0.696$ and $p > 0.856$, respectively). The cell seeding efficiency after 24 hours of culture was 47.2 ± 8.6% for the chitosan constructs, 81.8 ± 32.5% for the collagen-coated chitosan constructs, 25.5 ± 10.7% for the reacetylated chitosan constructs, 24.6 ± 3.6% for the collagen-coated reacetylated chitosan constructs (without ethanol), and 23.5 ± 6.4% for the collagen-coated reacetylated chitosan constructs (with ethanol)

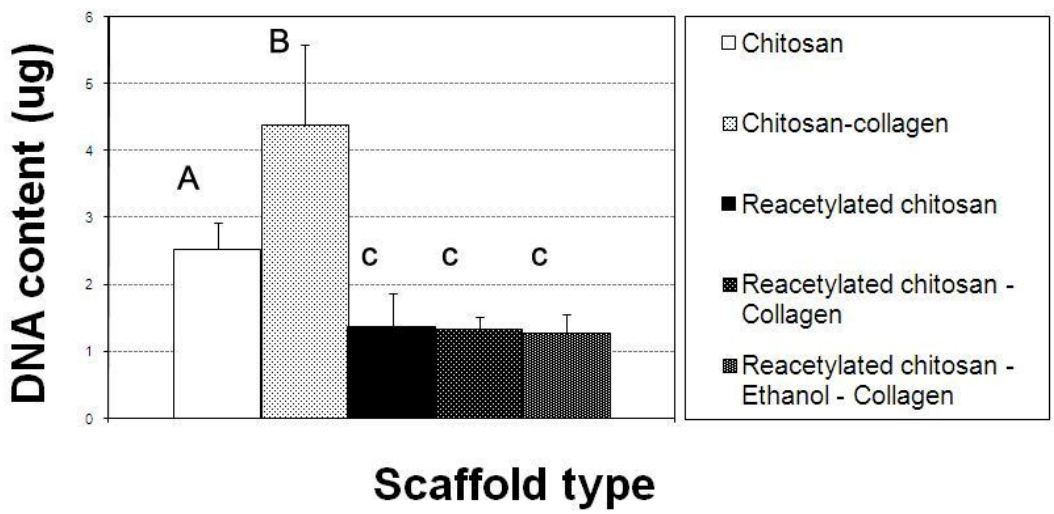

Figure 14: Average DNA content after seeding. A, B, C: groups with different letters differ statistically ($p < 0.05$).

(Table 2). The efficiency of cell seeding was greater on collagen-coated chitosan scaffolds than any other construct ($p < 0.001$ for all comparisons). Seeding was improved on chitosan scaffolds compared to all reacetylated chitosan constructs ($p = 0.016$-0.034). No difference was detected among the different reacetylated chitosan constructs ($p > 0.9$).

No difference in the DNA content of the well was found after 24 hours ($p=0.588$). However, the DNA content of the wells of chitosan constructs was greater than the one of the wells of all other constructs at 72 hours ($p=0.014$).

Transmission electron microscopy

Cells exhibited similar morphological features typical of mesenchymal stem cells including a spindle-shape and elliptical nucleus with usually multiple nucleoli, various mitochondrial profiles, and small vacuoles. No difference in cell morphology was observed between the constructs at 24, 48, and 72 hours after seeding. No difference in cell attachment could be observed between the different groups.

Histology

The cell density and distribution among each construct was assessed with the histological sections stained with Toluidine Blue O and Basic Fucshine. Findings were in agreement with those of DNA content. The cell distribution also appeared to differ among groups (Figure 15). Cells in chitosan constructs tended to be grouped rather than uniformly distributed, whereas cell distribution seemed more uniform in collagen-coated chitosan constructs. Although less obvious, a similar trend was observed in reacetylated chitosan constructs where cells appeared more uniformly distributed along collagen-coated fibers. Examination of the samples stained with trichrome confirmed

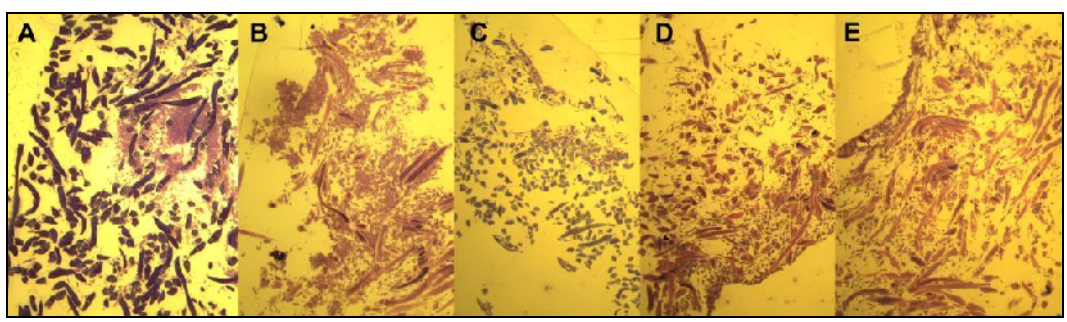

Figure 15: Light microscopy images of the samples prepared for transmission electron microscopy allowing evaluation of cell distribution within each construct. A: Chitosan constructs. B: Collagen-coated chitosan constructs. C: Reacetylated chitosan constructs. D: Collagen-coated reacetylated chitosan constructs (without ethanol). E: Collagen-coated reacetylated chitosan constructs (with ethanol) (10x).

the findings obtained with the light microscopy slides of the TEM in terms of subjective cell numbers and distribution among groups. Cells exhibited the appearance of MSCs in all constructs. The chitosan structure appeared intact in all constructs.

Scanning electron microscopy

Most MSCs exhibited a spindle-shape with prominent cytoplasmic extensions. No major differences in cell morphology were observed among groups. The cells tended to be uniformly distributed within each evaluated surface (surface or bottom). However, marked differences in cell density were observed (Figure 16). The reacetylated chitosan constructs contained fewer cells at the surface and at the bottom than the chitosan-based constructs. More cells were present at the surface and at the bottom of collagen coated chitosan constructs had than in all the other groups. The presence of collagen was associated with a more even distribution of cells, with more cells attached at the bottom of the constructs and cells spreading along the fibers rather than grouped in clumps. It was not possible to count the cells because they exhibited a spindle-shape with prominent cytoplasmic extensions and tended to form sheets. Finally, the structural integrity of fibers seemed intact in all groups.

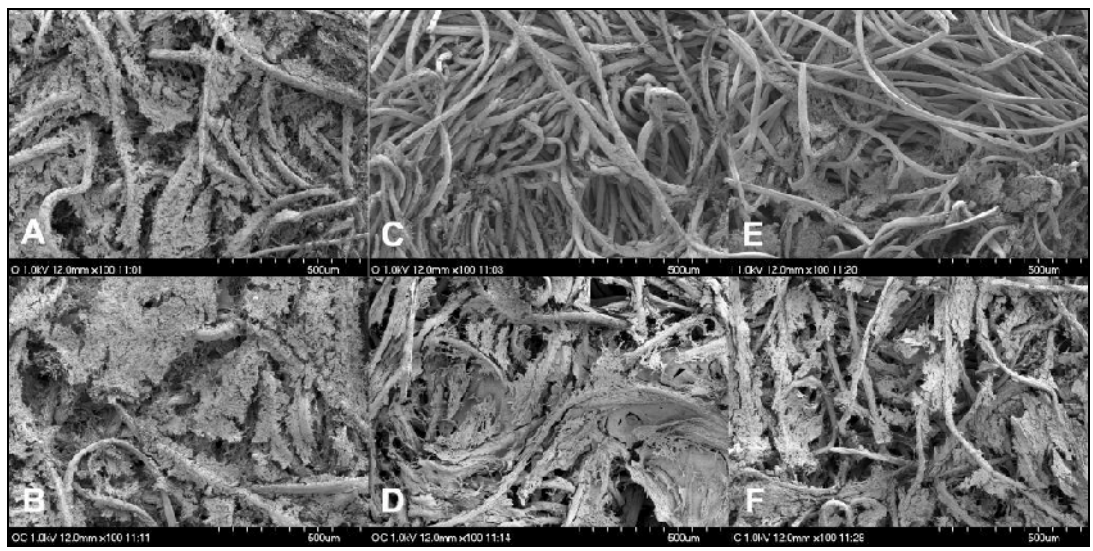

Figure 16: Scanning electron micrographs of the constructs 72 hours after seeding with MSCs. A: Surface of a chitosan construct. B: Surface of a collagen-coated chitosan construct. C: Bottom of a chitosan construct. D: Bottom of a collagen-coated chitosan construct. E: Surface of a reacetylated chitosan construct. F: Surface of a collagen-coated reacetylated chitosan construct (100x).

3.4. Effect of Type II Collagen Coating of Chitosan Fibrous Scaffolds on Mesenchymal Stem Cells Adhesion and Chondrogenesis

3.4.1. Materials and Methods

3.4.1.1. Scaffolds

The chitosan (Texanmedtecho, Korea) used in this study has a molecular weight of 400 kDA and a degree of deacetylation of 92%. Chitosan powder was dissolved and stirred at room temperature for 48 hours in 2 wt. % aqueous acetic acid solution to obtain a 4 wt. % chitosan solution. Chitosan fibrous scaffolds were prepared using a wet spinning method described above. Chitosan fibrous scaffolds were cut to measure 4 mm in diameter and 1.5 mm in height (Chi, n = 30). Two solutions of type II collagen were obtained by dissolving 10 mg and 20 mg of type II collagen (Calf type II collagen, Elastin Products Company, Owensville, MI) in 5 ml of 0.4 $mg.mL^{-1}$ of acetic acid and 3 $mg.mL^{-1}$ of ethanol. Chitosan fibrous scaffolds were dipped for one hour in the 2 $mg.mL^{-1}$ (Chi-Col 2, n = 30) or in the 4 $mg.mL^{-1}$ (Chi-Col 4, n = 30) type II collagen solution and dried at room temperature. The reference group consisted of a polyglycolic acid mesh previously tested for *in vitro* chondrogenesis (PGA, n = 30, Synthecon Inc.) (Griffon et al, 2005; Griffon et al, 2006; Seddighi et al, 2008). The average dry weight of the final scaffolds was 2.92 ± 0.34 mg. All scaffolds were sterilized with ethylene oxide gas and rehydrated through a series of ethanol/PBS solutions (100, 95, 75, 50, 0% ethanol) (Marreco et al, 2004). Scaffolds were subsequently incubated at 37°C on a shaker incubator in DMEM (ATCC) for two hours before cell seeding.

3.4.1.2. Mesenchymal Stem Cells:

The same mesenchymal cell line (D1 ORL UVA, ATCC) was used. Cells were harvested at their fourth passage prior to seeding. A cell suspension containing $1.0x10^6$ cells in 20 μL of medium was dropped on the surface of each scaffold placed in untreated six-well non-tissue culture plates. Each construct was incubated at 37˚C for one hour. After one hour, 4 ml of culture medium was added to each well and the plates were placed on a platform shaker oscillating at 30 rpm and increased to 60 rpm after 3 hours. After 48 hours, the media was changed with chondrogenic medium. The chondrogenic medium was the same as described above. The medium was changed three times a week. The constructs were maintained at 37°C and 5% CO2 under dynamic condition for 48 hours or 21 days.

3.4.1.3. Evaluation of the Scaffolds:

Fourier-transform infrared spectroscopy

Fourier-transform infrared spectra of each scaffold type (n=3) were analyzed by a spectrophotometer (Nicolet Nexus FTIR 670) using dehydrated specimens ground with potassium bromide powder and compressed into pellets. Element analysis was used to determine the presence of collagen.

Scanning electron microscopy

Each scaffold (n = 2 per group) was mounted and sputter coated with gold-palladium prior to examination with SEM (Hitachi S4700) at 1.0 kV. Criteria evaluated included fiber size (based on random measurements on ten fibers per scaffold) and surface characteristics.

Transmission electron microscopy

The scaffolds (n = 2 per group) were fixed using the same fixation protocol was used as described above. For each scaffold, a transverse section and a longitudinal section were evaluated. Light microscopy slides were made at 0.35 μm and stained with toluidine blue O and basic fucshine. TEM sections were stained with uranyl acetate and lead citrate, and examined with a transmission electron microscope (Hitachi H600). Criteria evaluated included presence and homogeneity of the coating at the surface of the fibers.

Type II collagen content

Type II collagen content per scaffold (n = 3 per group) was determined by the same enzyme linked immunosorbent assay (Arthrogen-CIA® Native Type II Collagen Detection Kit, Chondrex) as described above (Griffon et al, 2006).

3.4.1.4. Evaluation of the Constructs:

Seeding was evaluated at 48 hours via live/dead assay (n = 1 per group), dry and wet weight measurements (n = 5), DNA quantification in the constructs (n = 5) and in the medium of the well (n = 3), SEM (n = 2), TEM (n = 1). Chondrogenesis was evaluated after 21 days of culture via dry and wet weight measurements (n = 5), DNA and glycosaminoglycan (GAG) quantification (n = 5), SEM (n = 2), TEM (n = 2), histology (n = 2), and quantitative real time polymerase chain reaction (qRT-PCR) (n = 4).

Live/dead assay

The viability of cells in the constructs 48 hours after seeding was determined using the same method as described above. The intensities of viable and dead cells were recorded on two field views at a magnification of 10x and four field views at a magnification of 40x. The slides were analyzed using a specific software (Fluoview, Olympus) to determine the percentage of viable cells.

Weight, DNA and glycosaminoglycans content

Constructs were weighed after dehydration and digested in papain for 16 hours at 60°C. The same fluorometric and specrtophotometric assays as described above were used to evaluate the DNA and GAG contents, respectively (Kim et al, 1988). The number of cells contained in the constructs was calculated using the average DNA content per cell (6.49 pg per cell) evaluated on cell suspensions containing $1x10^6$ and $2x10^6$ cells at the time of cell seeding (Griffon et al, 2006). The GAG/DNA ratio was obtained by dividing the GAG content (μg) by the DNA content (μg).

After 48 hours, the media and cells left in the wells after the harvest of the constructs were collected and centrifuged (n = 3 per group). Each pellet was assayed for their DNA content.

Scanning electron microscopy

Constructs were fixed using the method described above. A total of two sections per construct (surface and bottom) were mounted and sputter coated with gold-palladium prior to examination with SEM at 1.0 kV. Criteria evaluated included cell morphology, cell attachment to the support, cell density, matrix production, and chitosan integrity. It was not possible to count the cells because they exhibited a

spindle-shape with prominent cytoplasmic extensions and tended to form sheets or were embedded in ECM (Griffon et al, 2005; Griffon et al, 2006).

Transmission electron microscopy

The constructs were fixed following the same protocol as described above. The light microscopy slides were evaluated to assess the cell density and distribution. Criteria evaluated with TEM after seeding included cell morphology and presence of cytoplasmic extensions. Criteria evaluated with TEM after 21 days of culture included cell morphology and the production of ECM.

Histopathology and immunohistochemistry

The constructs were fixed in 10% neutral buffered formalin, embedded in plastic and cut via microtome to produce 6 μm-thick sections (Seddighi et al, 2008). One section from the surface, the middle, and the bottom of each construct were stained with safranin-O fast Green and examined to evaluate cell morphology, presence of ECM, and integrity of the biomaterial. A picture of each section was taken at a magnification of 10x. For each picture, the area containing ECM was measured using the ImageJ program (National Institutes of Health) and expressed as a percent of the total area.

Immunostaining was performed using rabbit polyclonal antibody against aggrecan (Millipore, Billerica, MA, USA) using a 1:100 dilution factor after treatment with chondroitinase (Associates of Cap Code, East Falmouth, MA, USA) in 0.1% bovine serum albumin. One section from the surface, the middle, and the bottom of each construct were stained and evaluated for the density and intensity of the immunostaining.

Quantitative real time PCR

Snap frozen constructs were pulverized in liquid nitrogen using a dismembranator (Braun Biotech Int.) (Reno et al, 1997). Total RNA was isolated from the powdered tissue using the RNeasy mini kit (Qiagen) according to the manufacturer's instructions. The isolated RNA was treated on a column with a DNase digestion kit (Qiagen) to eliminate genomic DNA contamination. The quality of the RNA was evaluated using the ribosomal ratio and the RNA integrity number obtained with a bioanalyzer (Agilent 2100 bioanalyzer, Foster city, CA, USA). Subsequently, first-strand cDNA was synthesized using the high-capacity cDNA reverse transcription kit (Applied Biosystem). qRT-PCR was performed using TaqMan® universal PCR master mix (Applied Biosystems) with Mus musculus type I collagen (Mm468761), type II collagen (Mm491889), type X collagen (Mm487041), and aggrecan (Mm545794) Taqman® primer and probes and eukaryotic 18s rRNA and glyceraldehyde-3-phosphate dehydrogenase (GAPDH) endogenous controls. An ABI Prism 7000 Sequence Detection System (Applied Biosystems) and the ABI 2.0 software were used to obtain the data. The qRT-PCR reactions were carried out in 25 μL final volumes for 45 cycles. Each sample was run in triplicate. The mRNA expression levels of target genes were normalized to the GAPDH mRNA level. The gene expression levels were compared using the 2-ΔΔCT method (Chen et al, 2008; Livak et al, 2001).

3.4.1.5. Statistical Analysis

Cell viability, water content, dry weights, percent increase in dry weight, DNA content, GAG content, GAG/DNA ratio, and mRNA expression levels were compared between the groups with a risk factor of less than 0.05 considered statistically

significant. All data were expressed as mean ± standard deviation. Statistical differences were evaluated between the groups with an ANOVA using Systat 11.0 statistical software. Post-hoc analyses were performed with the least significant difference test. Correlations between collagen content and DNA content after seeding were estimated and tested for significance using the nonparametric Spearman rank correlation coefficient.

3.4.2. Results

3.4.2.1. Evaluation of the Scaffolds:

The presence of collagen was confirmed with the FTIR spectra by the presence of bands typical of amide I (1658 cm^{-1}), amide II (1552 cm^{-1}), and amide III (1240 cm^{-1}) (Cao et al, 2008).

The diameter of the fibers evaluated by SEM was 15.47±2.18 µm and no difference was found between groups (Table 4). The difference between chitosan and collagen within coated scaffolds was difficult to distinguish due to their similar contrasts in SEM.

A layer of collagen was observed by TEM at the surface of the fibers in all collagen-coated scaffolds (Figure 17). No difference in coating was observed between the center and the periphery within each scaffold. The coating appeared thicker for the Chi-Col 4 scaffolds.

Type II collagen was not detected in the non-coated scaffolds. The type II collagen content was 13.10 ± 3.25 $\mu g.mg^{-1}$ for the Chi-Col 2 scaffolds and 22.29 ± 1.53 $\mu g.mg^{-1}$ for the Chi-Col 4 scaffolds (Table 4). The collagen coated scaffolds contained more collagen than the non-coated scaffolds ($p < 0.001$) and the Chi-Col 4 scaffolds contained more type II collagen than the Chi-Col 2 scaffolds ($p = 0.002$).

Composition	Chitosan		Collagen-coated (2 mg/ml) chitosan		Collagen-coated (4 mg/ml) chitosan		Polyglycolic acid	
Fiber diameter (µm) (n = 20 per group)	14.6 ± 2.1	A	17.1 ± 2.5	A	16.0 ± 2.2	A	14.3 ± 1.71	A
Type II collagen content (µg/mg) (n = 3 per group)	0.00 ± 0.00	A	13.10 ± 3.25	B	22.29 ± 1.53	C	0.00 ± 0.00	A
Water content (%) (n = 5 per group)	91.47 ± 1.81	AC	84.97 ± 5.90	B	87.97 ± 2.21	BC	93.25 ± 0.43	A
DNA content after seeding (µg) (n = 5 per group)	7.47 ± 1.99	AB	8.90 ± 1.79	B	10.52 ± 2.82	C	5.18 ± 1.39	A
Cell seeding efficiency (%) (n = 5 per group)	57.5 ± 15.4	AB	68.5 ± 14.7	B	81.0 ± 21.7	C	39.9 ± 10.7	A
Dry weight after culture (mg) (n = 5 per group)	5.42 ± 0.82	A	6.32 ± 0.93	B*	6.02 ± 0.53	B*	2.96 ± 0.23	C
Increase in dry weight (%) (n = 5 per group and time-point)	81.5 ± 25.9	A	113.7 ± 28.7	B	119.2 ± 18.7	B	2.6 ± 8.0	C
DNA content after culture (µg) (n = 5 per group)	9.90 ± 1.47	A	20.76 ± 6.32	B	19.59 ± 3.62	B	5.96 ± 0.85	A
Cell gain (%) (n = 5 per group and time-point)	32.6 ± 19.7	A	133.4 ± 71.1	B	86.3 ± 34.4	B	15.0 ± 16.5	A
GAG content (µg) (n = 5 per group)	13.81±3.33	A	18.38±2.81	B	18.71±4.13	B	13.20±2.28	A
Surface area covered by ECM (%) (n = 6 per group)	38.93±14.24	A	54.60±23.25	B§	56.97±10.51	B	37.60±15.83	A

Table 4: Summary statistics of the characteristics of the scaffolds and constructs after seeding and culture. A, B, C: Groups with different letters differ statistically. *: Denotes a trend with $0.05 < p < 0.1$. §: Denotes a difference with the PGA group and a trend with the Chi group.

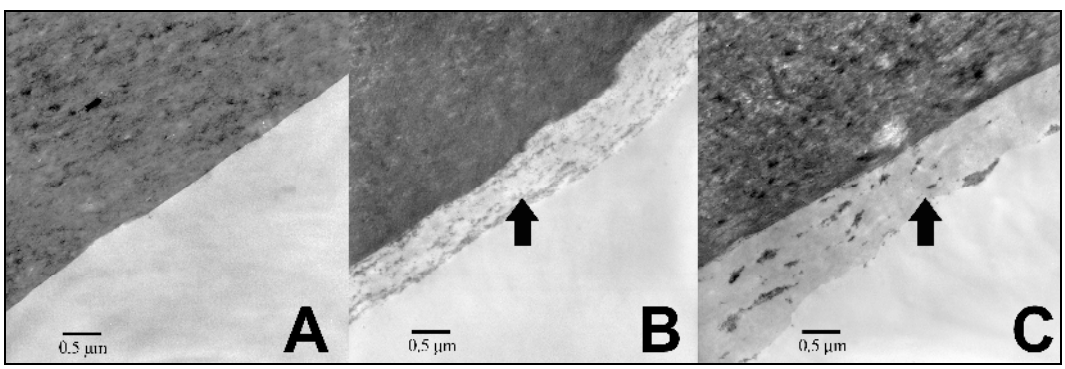

Figure 17: Transmission electron microscopy of the edge of a fiber from a chitosan scaffold (A), a Chi-Col 2 scaffold (B), and a Chi-Col 4 scaffold (C) (50,000x). Black arrow indicates the collagen layer at the surface of the chitosan fiber.

3.4.2.2. Evaluation of Constructs after Seeding

Live/dead assay

The viability of the MSCs estimated with the live/dead assay 48 hours after seeding did not differ between the four groups (82.7% ± 5.9, p = 0.464) (Figure 18).

Weight and DNA content

No difference in dry weight was found between groups of constructs (p=0.731). The water content of the PGA constructs was greater at 48 hours than the water content of the Chi-Col 2 and Chi-Col 4 constructs (Table 4). The water content of the Chi constructs was greater than the water content of the Chi-Col 2 constructs.

Collagen coated constructs contained more DNA than PGA constructs ($p<0.1$, Table 4). The Chi-Col 4 constructs contained more DNA than the Chi constructs (p=0.035). No difference was found between the PGA and Chi constructs (p=0.103). The cell seeding efficiency after 48 hours of culture was 57.5±15.4% for the Chi constructs, 68.5±14.7% for the Chi-Col 2 constructs, 81.0±21.7% for the Chi-Col 4 constructs, and 39.9±10.7% for the PGA constructs (Table 4). A correlation was found between the collagen concentration of the chitosan scaffolds and the DNA content after seeding (Spearman-rho = 0.529, p=0.04). The coefficient of the linear regression corresponded to 20,000 more cells attaching on the scaffold for an increase in type II collagen content of one microgram per milligram. No difference in the DNA content of the media was found after 48 hours (p=0.680).

Scanning electron microscopy

Most MSCs exhibited a spindle-shape with prominent cytoplasmic extensions. No major difference in cell morphology was observed between the different groups.

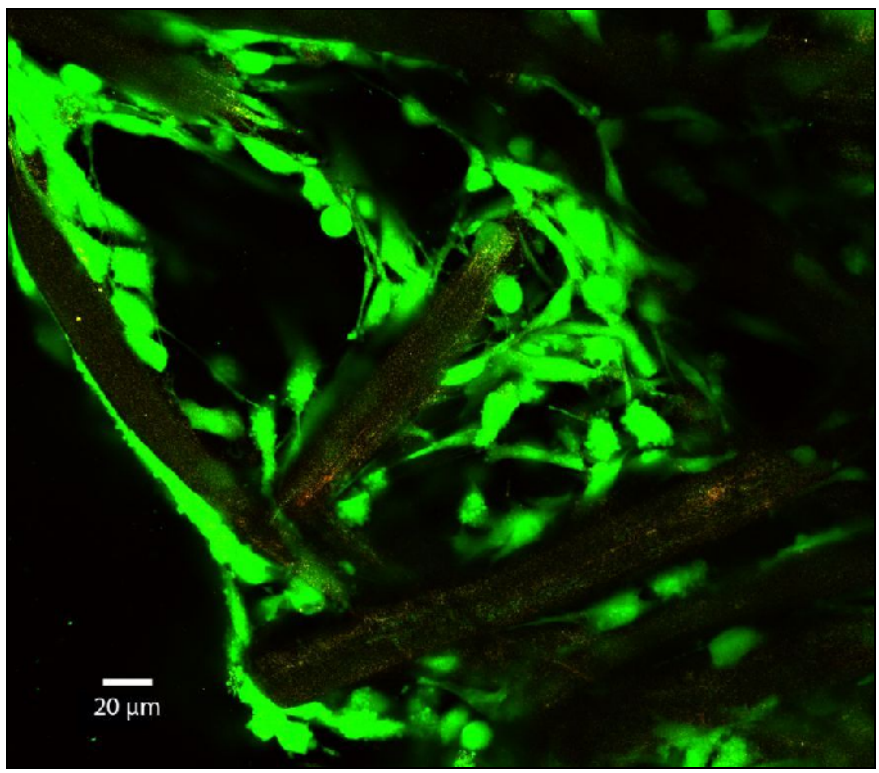

Figure 18: Confocal microscopy view of a Chi-Col 4 construct 48 hours after seeding (40x). The cells are spreading along the fibers and display the green intensity of live cells.

The cells tended to be uniformly distributed within each evaluated surface but more cells were observed at the surface. Marked differences in cell density were observed between constructs (Figure 19). The PGA and Chi constructs had fewer cells than the collagen-coated constructs. This difference was more important for the bottom section. The Chi-Col 4 constructs contained more cells than all the other groups.

Transmission electron microscopy

The cell density and distribution among each construct was assessed with light microscopy. The collagen-coated chitosan constructs contained more cells than the other constructs. The cells in the chitosan constructs tended to be grouped rather than uniformly distributed. This finding differed from the collagen-coated chitosan constructs and the PGA constructs in which cells tended to be more uniformly distributed along the fibers. With TEM, cells exhibited similar morphological features typical of mesenchymal stem cells including a spindle-shape and elliptical nucleus with usually multiple nucleoli, various mitochondrial profiles, and small vacuoles (Figure 20).

3.4.2.3. Evaluation of Constructs after twenty-one Days of Culture:

Weight, DNA and glycosaminoglycans content

The percent increase in dry weight and the final dry weight were greater for all chitosan constructs compared to PGA ($p < 0.001$) and for the Chi-Col 2 and Chi-Col 4 constructs compared to the Chi constructs ($p = 0.033$ and $p = 0.015$, respectively; Table 4). The collagen-coated chitosan constructs contained more DNA and had improved cell proliferation compared to the Chi and PGA constructs ($p < 0.001$ and $p < 0.04$, respectively; Table 4). The collagen-coated chitosan constructs contained more GAG

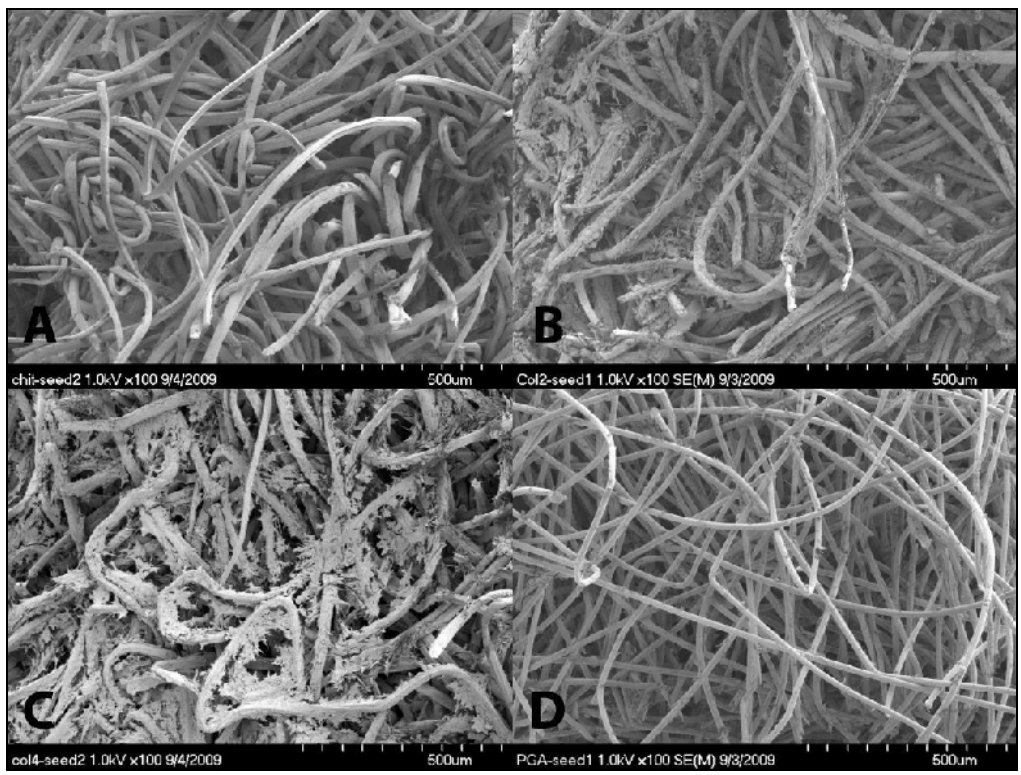

Figure 19: Scanning electron microscopy of the bottom of the constructs 48 hours after seeding with MSCs (100x). A: Chi construct. B: Chi-Col 2 construct. C: Chi-Col 4 construct. D: PGA construct.

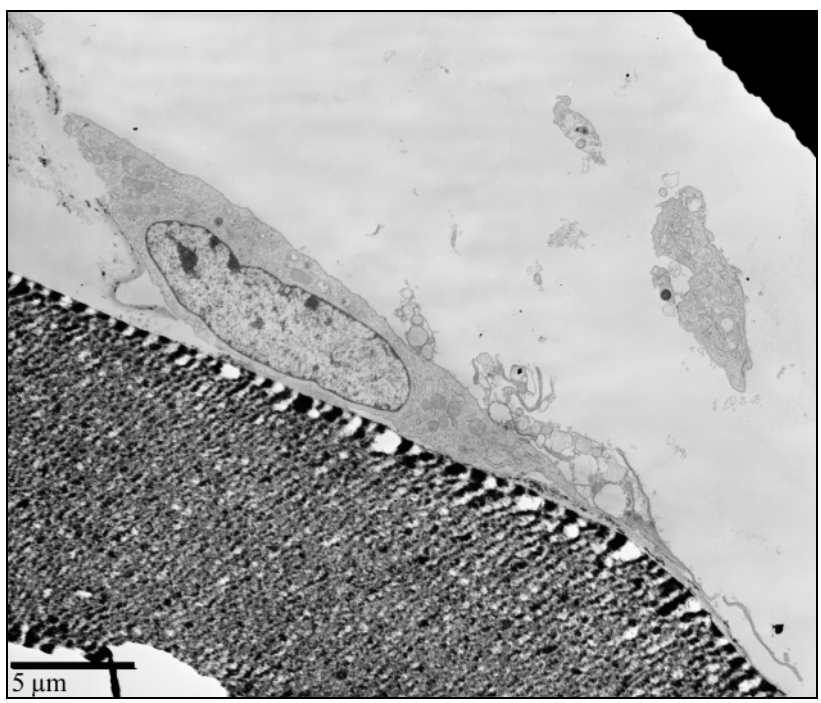

Figure 20: Transmission electron microscopy illustrating the typical appearance of the cells 48 hours after seeding on a Chi-Col 4 scaffold (2,500x). Cells exhibited similar morphological features typical of mesenchymal stem cells including a spindle-shape and elliptical nucleus with usually multiple nucleoli, various mitochondrial profiles, and small vacuoles.

than the Chi and PGA constructs ($p < 0.03$ for all comparison, Table 4). The GAG/DNA ratio was greater for the chitosan constructs (1.38 ± 0.20) compared to the Chi-Col 2 and Chi-Col 4 constructs (0.96 ± 0.33 and 0.99 ± 0.34, $p<0.04$).

Scanning electron microscopy

For all groups, more cells were present at the surface of the constructs. Marked differences in cell density and morphology were observed between the different groups. The collagen coated chitosan constructs contained more cells than the PGA and Chi constructs. Most cells seeded on the Chi-Col 2 and Chi-Col 4 scaffolds had the phenotypic appearance of normal chondrocytes. However, isolated cells tended to be stellate in shape, with prominent cytoplasmic extensions. Conversely, a greater proportion of cells in the Chi constructs and most cells in the PGA constructs had the phenotypic appearance of MSCs (Figure 21 A-D). The cells were embedded in ECM (Figure 21 A-D). More matrix was seen in the collagen coated constructs. The amount of ECM observed within the constructs appeared to correlate with the phenotypic appearance of the cells, more matrix being noted around cells that had the phenotypic appearance of normal chondrocytes. Finally, the structural appearance of the scaffolds appeared intact in all chitosan groups whereas the fibers of the PGA mesh seem to have broken in shorter fragments.

Transmission electron microscopy

The cells were embedded within ECM throughout most evaluated constructs (Figure 22). In the collagen coated constructs, the majority of cells had the appearance of chondrocytes with prominent nuclei and containing the different cytoplasmic organelles such as endoplasmic reticulum, Golgi apparatus and vacuoles (Figure 22 C). An

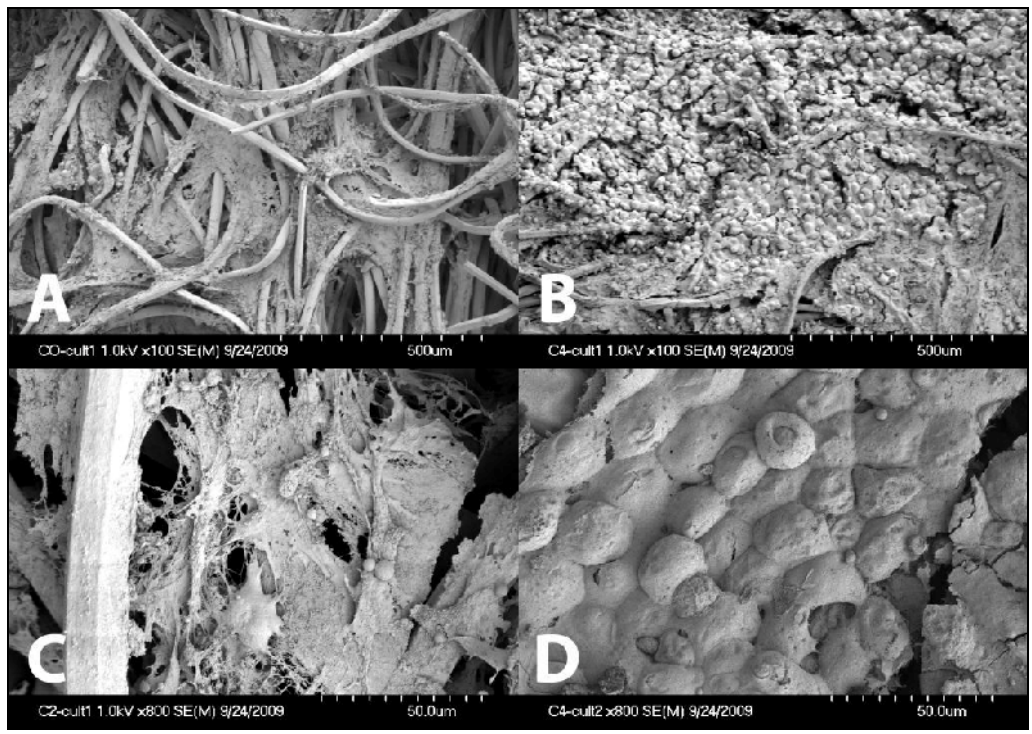

Figure 21: Scanning electron micrographs of the constructs 21 days after seeding with MSCs. A: Surface of a Chi construct. The cells are spreading between the fibers and most cells have the phenotypic appearance of MSCs (100x). B: Surface of a Chi-Col 4 construct. Most cells have the phenotypic appearance of normal chondrocytes (100x). C: Cells having the phenotypic appearance of MSCs in a Chi construct (800x). D: Cells having the phenotypic appearance of normal chondrocytes in a Chi-Col 4 construct (800x).

abundant ECM was observed in the pericellular, inter- and intra-territorial zones containing fibrillar collagens which were faintly cross-banded and randomly oriented (Figure 22 B). In the chitosan and PGA constructs, the ECM was less important in the intra-territorial zone. In the PGA constructs, enlarged individual cisternae of rough endoplasmic reticulum and cells colonizing cracks within broken fibers were observed (Figure 22 A) (Leighton et al, 2007).

Histopathology and immunohistochemistry

For all constructs, more cells and ECM were observed in the periphery of the constructs. The surface area covered by ECM was greater for the collagen coated constructs compared to the Chi and PGA constructs (Table 4). The chitosan structure appeared intact in all constructs whereas some PGA fibers were fragmented. Aggrecan levels were increased in the collagen-coated chitosan constructs compared to the PGA and Chi constructs as evaluated by immunohistochemistry (Figure 23). The matrix of the Chi-Col 4 constructs had strong immunoreactivity for aggrecan, predominantly within the pericellular matrix of the cells.

Quantitative real time PCR

At 21 days, more type II collagen mRNA was expressed in the collagen coated chitosan constructs compared to the PGA constructs (383% increase, $p = 0.016$) and a trend was present for a greater expression of aggrecan mRNA in the collagen coated chitosan constructs compared to the PGA constructs (216% increase, $p = 0.089$). There was a trend for a greater expression of type II collagen mRNA in the collagen coated chitosan constructs compared to the chitosan constructs (231% increase, $p = 0.057$). The level of mRNA expression for type X collagen was greater in all chitosan-based

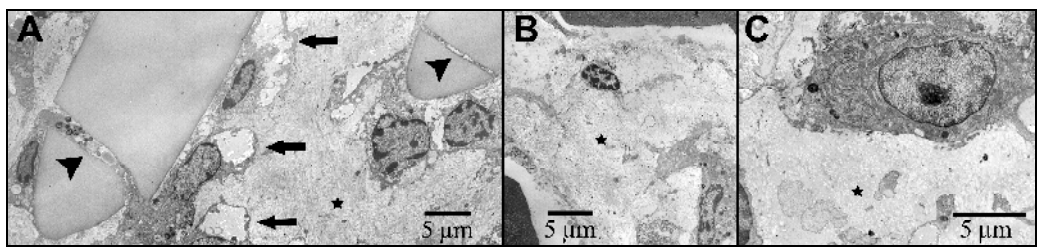

Figure 22: Transmission electron micrographs of the constructs 21 days after seeding with MSCs. A: PGA construct (1,500x). B: Chi-Col 4 construct (1,500x). C: Chi-Col 4 construct (5,000x). An abundant ECM is observed in the pericellular and interterritorial zones (★). In the PGA constructs, enlarged individual cisternae of rough endoplasmic reticulum were observed (arrow) and cells were colonizing the cracks of the broken fibers (arrowhead).

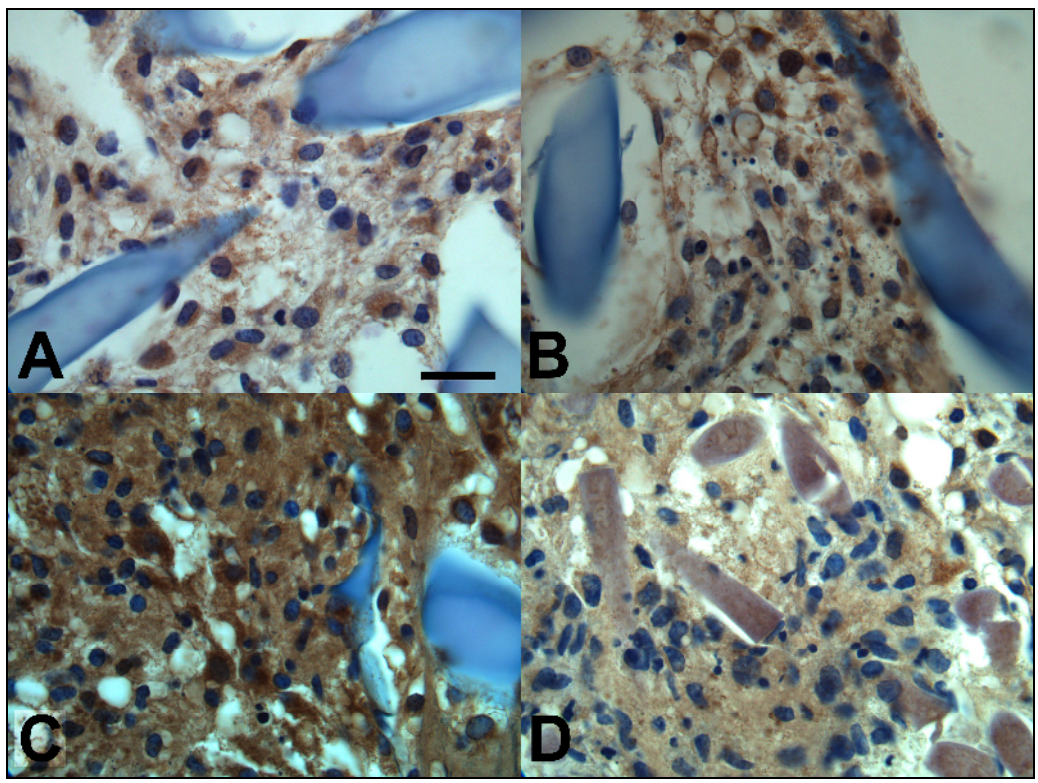

Figure 23: Aggrecan immunohistochemical staining of the constructs 21 days after seeding with MSCs (100x). A: Chi construct, B: Chi-Col 2 construct, C: Chi-Col 4 construct, D: PGA construct. Aggrecan staining was increased with the collagen coating (B,C). The Chi-Col 4 constructs resulted in the highest immunoreactivity for aggrecan in the pericellular matrix.

constructs compared to the PGA (288 to 308% increase, $p < 0.002$). The level of mRNA expression for the type I collagen gene was not different between the chitosan, collagen coated chitosan, and PGA constructs ($p = 0.39$).

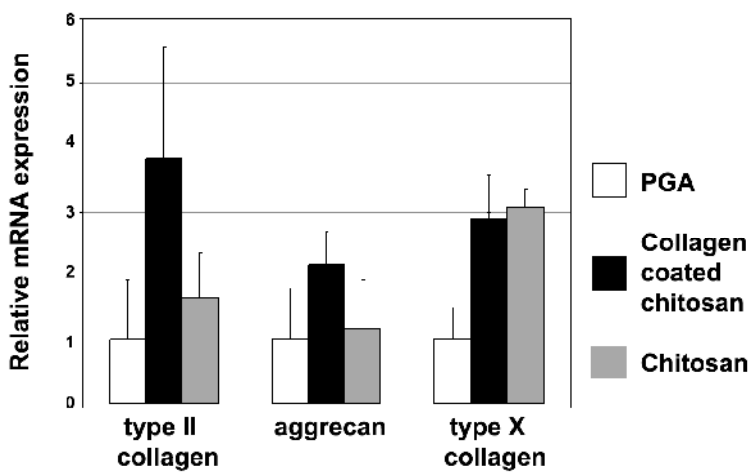

Figure 24: Relative matrix gene expression in the engineered constructs analyzed by real-time quantitative RT-PCR after 21 days (relative to PGA).

CHAPTER 4: DISCUSSION

Chitosan scaffolds previously tested for cartilage tissue engineering do not fulfill all the criteria necessary for clinical application because of their decreased properties for cell adhesion. The effects of their structural characteristics have not been evaluated for cartilage engineering applications. Their chemical composition can be modified to improve cell adhesion for tissue engineering. The main findings of this project are the following:

(1) Fibrous chitosan scaffolds produced by the replica molding technique are effective matrices for cartilage tissue engineering.

(2) Chitosan constructs contained less chondrocytes than the PGA constructs of similar structure but the amount of matrix produced by individual chondrocytes was greater in chitosan than in PGA constructs. The early breakdown of PGA fibers may limit their use for cartilage tissue engineering.

(3) Chondrogenesis on chitosan was improved in fibrous scaffolds compared to sponges.

(4) Decreasing the DD of chitosan scaffolds limits cell adhesion and cannot be effectively overcome by type II collagen coating.

(5) Type II collagen coating improves cell adhesion, cell distribution, and chondrogenesis on chitosan fibrous scaffolds.

4.1. Chitosan Scaffolds for Cartilage Tissue Engineering

Individual cells produced more ECM on chitosan compared to PGA. This difference in matrix production per individual cells is more likely due to the chemical

composition than the structural characteristics of the scaffolds, since one of our chitosan groups was composed of fibers of similar width to those of the PGA mesh (13 μm). The chemical nature of chitosan initially prompted the interest for this biomaterial as a candidate for cartilage engineering and was later offered as an explanation for the chondrogenesis observed on chitosan sponges (Di Martino et al, 2005; Madihally et al, 1999; Mao et al, 2004; Nettles et al, 2002; Suh et al, 2000). This natural polysaccharide degrades to GAGs such as chondroitin, chondroitin-sulfate, dermatane-sulfate, keratin-sulfate and hyaluronic acid. These physiological components of the extracellular matrix of native cartilage contribute to the synthesis of proteins by chondrocytes (Bostman et al, 1990; Lu et al, 1999; VandeVord et al, 2002). Another mechanism that may have contributed to our results relates to the type of adhesion formed between chondrocytes and PGA fibers. Some chondrocytes were found to display a stellate appearance on SEM examination of PGA constructs, a potential sign of dedifferentiation. Although we did not investigate gene expression of these cells, dedifferentiated chondrocytes would be expected to produce less GAG and type II collagen.

Chondrocytes also exhibited a different behavior in terms of attachment to PGA versus chitosan scaffolds. The seeding yield was three times lower on chitosan compared to PGA. The decreased yield on chitosan scaffolds accounts for their lower cell content compared to PGA constructs after three weeks of culture. Cell attachment to 3-D matrices depends on the initial number and viability of cells, the seeding technique and the characteristics of the scaffold (Vunjak-Novakovic et al, 1998). Chondrocytes were harvested from young, healthy animals. The use of healthy cells allows us to eliminate poor viability as a potential cause for the lack of cell attachment to the chitosan scaffolds, although our results may not be extrapolated to chondrocytes collected on a patient requiring joint resurfacing. Similar differences in yield rate were

previously reported when chondrocytes were seeded on chitosan sponges and the PGA mesh included in our study (Griffon et al, 2005; Griffon et al, 2006). The difference in DNA content and cell counts is more likely due to a difference in chemical composition rather than structural properties of the scaffolds. The mechanisms proposed to explain the influence of chemical composition of the biomaterial on direct cell adhesion relate to the presence of adhesion peptides along the surface of the matrix and the surface hydrophobicity (Evans et al, 1998; Jeschke et al, 2002). The PGA mesh used in our study lacks functional groups for cell recognition but dissolved within 21 days of incubation in acellular media (Cui et al, 2003; Tsai et al, 2006; Zhu et al, 2002). On the other hand, cell attachment on chitosan should be enhanced by the surface energy of this polysaccharide resulting from its hydrophilic nature (Moroni et al, 2006). The chitosan used in our study was specifically selected for its high DD and low molecular weight, two characteristics expected to encourage cell adhesion (Hamilton et al, 2006; Mao et al, 2004). The discrepancy between our results and expected yield at 48 hours may be explained by a two-step process recently proposed to contribute to cell attachment, whereby proteins contained in the media are absorbed by the scaffold and provide sites of attachment for cells (Mahmood et al, 2004). Under these premises, the cell adhesion characteristics of a biomaterial may not be directly related to direct cell-matrix interactions but to the differential adsorption of proteins present in the culture medium to the biomaterial (Chastain et al, 2006).

4.2. Fibrous Scaffolds for Cartilage Tissue Engineering

Individual cells recognize structures with dimensions comparable to them (10-100 μm) (Mooney et al, 2003). Therefore, micro-scale characteristics should be

considered when designing scaffolds for tissue engineering. These microstructural characteristics can selectively activate genes and modulate cellular behavior with regards to proliferation and differentiation (Chen et al, 2007; Griffon et al, 2006; Li et al, 2006; Moroni et al, 2006; Sasmazel et al, 2008; Yamane et al, 2006). However, the influence of the microstructure of 3-D scaffolds on chondrocytes and on MSCs chondrogenesis remains poorly understood (Lee et al, 2008).

Our findings using fibrous scaffolds obtained by the replica molding technique confirm the chondrogenesis previously reported on fibrous scaffolds composed of microfibers ranging from 13 to 30 μm in diameter (Freed et al, 1994; Seddighi et al, 2008). The lower DNA content and cell seeding efficiency of the 4 μm-width fibrous chitosan constructs after 48 hours of culture in our study suggests that decreasing the diameter of chitosan fibers may affect cell adhesion. Moroni et al. reported similar results, with mesenchymal stem cells attaching preferentially to 10 μm-diameter fibers compared to fibers of smaller diameter (Moroni et al, 2006). Larger fibers provide spacious surface for the cells to attach, facilitating the formation of secure focal adhesions and thereby improving yield rates. The dimensions of fibers affect other microstructural characteristics such as porosity, permeability, pore size distribution, and surface area, which may also influence cell behavior. For example, cell seeding yield and cell proliferation are affected by the porosity and the pore characteristics of 3-D matrices (Griffon et al, 2006; Lee et al, 2008; Mukherjee et al, 2009; Sasmazel et al, 2008; Yamane et al, 2006). Although all chitosan fibers had similar water content, we cannot eliminate the potential influence of porosity, pore size, geometry and interconnectivity on the characteristics of the final constructs. The results obtained with fibrous scaffolds of different width suggest that the structural characteristics of a scaffold may have more impact on cell proliferation and ECM production than initial

cell adhesion and cell-cell interaction. Indeed, DNA, GAG and collagen contents did not differ between the different chitosan constructs cultured for 21 days, in spite of a decreased cell density on smaller fibers. Higher chondrocyte density was previously correlated with increased amount of GAG and collagen and cartilaginous histomorphologies, presumably due to enhanced cell-cell interactions (Vunjak-Novakovic et al, 1998). Also, the number of cell attached to the scaffold was found to exert a strong influence on the biochemical composition of the constructs and the amount of ECM components accumulated in the tissues on a per-cell basis (Mahmoudifar et al, 2006). Our findings would be consistent with enhanced chondrocyte proliferation and matrix production on scaffolds composed of smaller fibers. This concept is supported by Li et al., who previously described increased cell proliferation and GAG content when chondrocytes were cultured on nanofibrous synthetic scaffolds compared to microfibrous scaffolds (Li et al, 2006). These effects may be mediated by changes in 3-D cytoskeleton occurring when a greater number of secure adhesions form between cells and larger fibers. This cytoskeletal network is composed of actin microfilaments, microtubules, and intermediate filaments known to play key roles in cell signaling, intracellular transport, cell-matrix interactions and cell differentiation (Mooney et al, 1995; Woods et al, 2007). Scaffolds composed of smaller fibers may therefore prompt cells to express proper proteins and signals via cytoskeletal networks (Moroni et al, 2006). In that respect, non-woven fibrous scaffolds approach the random arrangement of fibers in native ECM more closely than a woven mesh of perpendicular fibers stacked in multiple layers (Yamane et al, 2005).

We found that the GAG content and the type II collagen expression by MSCs are enhanced at 21 days in fibrous chitosan constructs compared to sponges. These findings support the concept that altering structural characteristics of a scaffold may be

a viable strategy to promote chondrogenesis by MSCs. Indeed, all scaffolds in this study were produced with the same batch of chitosan, thereby eliminating chemical composition as a possible confounder for our results. We can also eliminate variation in cell numbers as a potential explanation for the differences between our groups, since the DNA content did not differ between constructs at any time during our study. The increased expression of type II collagen mRNA with no difference in expression of type X collagen mRNA in meshes is consistent with improved MSCs chondrogenesis without hypertrophic changes (Pelttari et al, 2006). The absence of difference for type I collagen and type X collagen could however be due to a type II error. Fibrous scaffolds simulate more closely than sponges the structure of native cartilaginous ECM, comprised of collagen fibrils (Moroni et al, 2006). Our results strengthen the argument for developing biomimetic scaffolds to control cellular functions and direct cell-cell interactions toward the formation of a specific tissue (Hubbell, 1995). The effect of microstructure in cartilage tissue engineering has been previously evaluated with chondrocytes on sponges of different pore sizes (Chen et al, 2007; Griffon et al, 2006; Li et al, 2006; Moroni et al, 2006; Sasmazel et al, 2008; Yamane et al, 2006). However, the difference in extracellular matrix production could have been related to difference in cell numbers between the groups. Improved cartilage tissue formation on fibrous scaffolds has been suggested when chondrocytes were cultured *in vivo* on poly(ethylene glycol)-terephthalate/poly-butylene terephthalate (Malda et al, 2005). Although these results were promising, we could not find any previous report of a similar influence of the environmental microstructure on MSCs chondrogenesis. Instead, the development of biomimetic scaffolds to enhance chondrogenic differentiation of MSCs has largely focused on altering the chemical composition rather than the structural characteristics of scaffolds. For example, glucosamine, a precursor of cartilage components, was

shown to direct cell differentiation and cartilage tissue formation when incorporated in hydrogels (Hwang et al, 2006). Following the same rationale, chitosan has been combined with other biomaterials because of its similarity with proteoglycans normally present in native cartilage. The resulting hybrid scaffolds were found to enhance cartilage tissue formation (Chen et al, 2007; Cui et al, 2003). This evidence provided the rationale behind our efforts to produce a scaffold that would provide both chemical (aminopolysaccharide) as well as biophysical (fibrous) lineage-specific cues similar to those of native cartilage matrix. The mechanisms by which chitosan fibers improve chondrogenesis over sponges remain speculative but could rely on enhanced cell-cell and/or cell-matrix interactions. The chondrogenic differentiation of MSCs typically proceeds through condensation, conventionally achieved by adapting pellet and micromass cultures. The formation of cell clusters promotes cadherin-mediated cell-cell interactions. Among these, the N-cadherin and cadherin 11 molecules have been proposed to play a determinant role in MSCs condensation and subsequent chondrogenesis (Luo et al, 2005). Although we did not observe a difference in cell aggregation between groups on SEM and histology, fibrous scaffolds may facilitate cell-cell interactions over sponges. Indeed, cell-cell interactions depend on cell density as well as scaffold structure. Scaffold structure can influence cell contacts by its effects on cell proliferation and migration throughout the matrix. The smaller surface area of the fibrous scaffolds likely increases the chance for cell-cell interactions by decreasing the available biomaterial surface per cell. An open structure consisting of loosely arranged fibers or leached pores can enhance cell diffusion throughout the matrix, thereby promoting cell-cell interaction. However, this last mechanism is unlikely to have contributed alone to our results since cell seeding was similar between groups.

The structure also affects nutrient diffusion within the scaffold (Karande et al, 2004). Fluid flow through the structure is a combination of five important scaffold parameters: porosity, pore size and distribution, interconnectivity, fenestration size and distribution, and pore orientation (Lee et al, 2008; Li et al, 2003). Differences in those characteristics could therefore affect cell-nutrient interaction, possibly resulting in better chondrogenesis for one scaffold type compared to the other (Lee et al, 2008; Sasmazel et al, 2008; Yamane et al, 2006). However, improved mass transport within 3-D matrix has been found to impact cell proliferation (Griffon et al, 2006; Mukherjee et al, 2009). This mechanism is unlikely to have contributed to our results since cell proliferation was similar between groups. The biophysical cues provided by the local microstructural environment rely primarily on interactions between the matrix and cell surface receptors, initiating intracellular signals mediated via cytoskeletal networks (Mooney et al, 1995; Woods et al, 2007). Interestingly, chondrogenesis was improved in scaffolds with the smaller available surface area. However, other scaffold characteristics affect the TGF-β and Hedgehog pathways, known to profoundly influence chondrogenesis (Chen et al, 2008). A fibrous microstructure simulates more closely the relative size relationship between cells and the extracellular matrix proteins contained in cartilage, thereby affecting the interaction with transmembrane integrin receptors (Moroni et al, 2006). These receptors are known to activate actin-filament polymerization and promote focal adhesion formation (Discher et al, 2005). Cell attachment modifies the cytoskeletal network and influences cell signaling and cell function (Mooney et al, 1995; Woods et al, 2007), but can also be affected by differences in mechanical properties between fibrous scaffolds and sponges (Engler et al, 2006; Kong et al, 2005). However, mechanical testing of the scaffolds was not performed as, under the culture conditions used, the meso- or microenvironments are

sensed by individual cells, not the representative volume element (or scaffold) (Gibson et al, 1999). The importance of the cytoskeletal network in chondrogenesis was recently highlighted in a study where decreased chondrogenesis of MSCs on RGD-modified hydrogels was reversed by disrupting the F-actin cytoskeleton (Connelly et al, 2008). Integrin stimulation was found to modulate the TGF signaling cascade involving Smad2 and Smad3 leading to an increase in type II collagen transcription (Schneiderbauer et al, 2004). We cannot conclude as to the contribution of this mechanism to our results because cells were embedded in extracellular matrix preventing our ability to evaluate differences in cytoskeletal organization. Future studies should be conducted to evaluate the expression of chondrogenic differentiation promoters in relation to cytoskeletal organization and cytoplasmic extension.

4.3. Effect of the Degree of Deacetylation on Cell Adhesion on Chitosan Scaffolds

The influence of the DD of chitosan on cell attachment remains controversial and varies between reports and cell types (Fakhry et al, 2004). In several studies, deacetylation improved the attachment of fibroblasts, Schwann cells, keratinocytes, and neurons to chitosan films or sponges (Amaral et al, 2007; Chatelet et al, 2001; Freier et al, 2005; Seda Tigli et al, 2007; Tigli et al, 2008; Wenling et al, 2005). However, in others, a lower DD of chitosan did not affect the attachment of chondrocytes, fibroblasts, or osteoblasts (Hamilton et al, 2006; Kuo et al, 2006; Suphasiriroj et al, 2009; Suzuki et al, 2008). These conflicting results may be due to differences in origin, molecular weight, and/or viscosity of the agents tested (chitosan, chitin, re-acetylated chitosan) as well as differences in experimental design such as cell population and serum supplementation (Hamilton et al, 2006; Suphasiriroj et al, 2009). We describe for

the first time a decreased cell attachment of MSCs on reacetylated chitosan scaffolds (DD: 4%) compared to chitosan (DD: 92%). The scaffolds were produced from the same source of chitosan to avoid variation due to characteristics other than DD. Cells were seeded in medium containing serum, routinely recommended for culture of MSCs. The positive relationship between adhesion of MSCs and the DD of chitosan scaffolds could be explained by several possible mechanisms. It was first suspected that the amine groups of the deacetylated form of chitosan would remain protonated to $-NH_3^+$ in media, resulting in a cationic nature primarily responsible for electrostatic interactions between protonated amine groups and negatively charged cell surfaces (Chatelet et al, 2001; Suphasiriroj et al, 2009). However, the majority of the ammonium groups become dissociated and subsequently uncharged when the medium reaches a pH close to the pKA of chitosan (6.46 to 6.8) (Amaral et al, 2007). This explains why the zeta potentials of chitosan films were null or slightly positive in neutral medium and not affected by the DD (Tomihata et al, 1997). The cell adhesion characteristics of the chitosan may therefore not be directly related to direct cell-matrix interactions but instead, correlate with the differential adsorption of proteins present in the culture medium to the biomaterial (Chastain et al, 2006). Although no correlation has yet been established between the adsorption of type II collagen and the DD of scaffolds, the mechanism of protein adsorption in media containing serum most likely differs from that of single protein adsorption in acidic conditions. Chitosan with a high DD may accelerate cell adhesion after forming polyelectrolyte complexes with serum components such as heparin, platelet-derived growth factor, laminin, or fibronectin (Inui et al, 1995; Mori et al, 1997). Chitosan with a higher DD can bind more growth factors in the serum and protect them from degradation and/or present them to the cells in an active form (Howling et al, 2001; Mori et al, 1997). This could potentially explain

the absence of effect of the DD on fibroblast attachment and proliferation found by Hamilton et al. in serum free media (Hamilton et al, 2006). The DD of chitosan scaffolds has been shown to impact the final constructs in skeletal tissue engineering applications. Several studies have reported improved characteristics of the extracellular matrix produced by chondrocytes (Kuo et al, 2006; Suzuki et al, 2008), or osteoblasts (Amaral et al, 2007; Suphasiriroj et al, 2009) when these cells were cultured on chitosan scaffolds of lower DD. These publications justify our attempts to overcome the poor cell adhesion on chitin and reacetylated chitosan (Chatelet et al, 2001; Freier et al, 2005; Hamilton et al, 2006). Type II collagen did not improve the overall cell seeding efficiency of reacetylated chitosan constructs. Even if the cell distribution appeared more homogeneous in the collagen-coated constructs, the poor adhesion properties of reacetylated chitosan seem difficult to overcome.

4.4. Effect of the Hyaluronic Acid Coating on Chitosan Scaffolds

HA has been used for clinical management of joint disease. Results of clinical studies have shown the efficacy of HA (Atamaz et al, 2006). HA interacts with cells and plays a pivotal role in stimulating chondrocyte metabolism as well as maintaining cell shape and behavior (Akmal et al, 2005; Kuroki et al, 2002; Lee et al, 2000; Takeuchi et al, 2006). HA has also been found to induce a 22-fold increase in proteoglycan synthesis by chondrocytes cultured in a gelatin sponge, presumably via interactions with CD44 receptors (Goodstone et al, 2004). This evidence provided the rationale behind our efforts to use HA to coat chitosan scaffold in order to improve both cell adhesion and cell differentiation. The effects of HA coating have not been studied on MSCs chondrogenesis, even if chondrogenesis has been described on HA-

chitosan hybrid scaffolds (Yamane et al, 2005; Yamane et al, 2006). We did not find evidence that the addition of HA improve MSCs chondrogenesis. It is possible that HA does not have the same effects on MSCs chondrogenesis than on extracellular matrix production by chondrocytes; this lack of effect being or not related to CD44 expression by MSCs. HA may also have eluted from the scaffolds and was therefore removed from the media during the first change of media limiting its effect on cell differentiation. Future studies are required to clarify the stability of HA coating on chitosan scaffolds and the effect of HA on MSCs chondrogenesis.

The addition of HA to the chitosan did not improve MSC attachment to the scaffolds. CD44 expression by the MSCs may be limited, impeding efficient HA interaction (Herrera et al, 2007). It is also possible that the coating technique did not allow strong bonding between the chitosan and the HA leading to rapid elution of the HA from the scaffolds. The elution of HA from the chitosan is possible because of its high water solubility, rapid resorption, and short residence time and despite the anionic behavior of HA complementary to the cationic chitosan (Funakoshi et al, 2005). Fast and early cell-HA interactions tether cells to the surface and provide the temporal and spatial framework for slower integrin-mediated interactions to occur (Cohen et al, 2006; Peniche et al, 2007; Tan et al, 2007; Zaidel-Bar et al, 2004; Zimmerman et al, 2002). Slow integrin-mediated adhesion will not have the time to occur if HA elutes from the scaffold before or during its interaction with the cells. Limiting the elution of HA from chitosan scaffolds may therefore require modifications of the carboxyl and hydroxyl groups of HA and/or crosslinking using divinyl sulfone, glycidyl ether, or dialdehyde (Hahn et al, 2005). The biocompatibility of these modifications must be considered carefully before clinical application of the resulting scaffolds. Polyelectrolyte complex multilayer is an alternative process to increase HA stability on

chitosan without affecting the biocompatibility but it is not feasible for 3-D scaffolds (Hahn et al, 2005).

4.5. Effect of Type II Collagen Coating on Cell Adhesion on Chitosan Scaffolds

The initial attachment of cells during seeding is a prerequisite for a successful tissue engineering outcome as it is a decisive factor for cell-matrix and cell-cell interactions (Mahmood et al, 2004). Considerable attention has recently focused on chitosan scaffolds but their use has been limited because of their deficient properties for cell adhesion (Amaral et al, 2007; Griffon et al, 2010; Seda Tigli et al, 2007; Wenling et al, 2005). Modifying chitosan scaffolds to optimize cell adhesion within the 3-D matrices is crucial to improve seeding yield and uniformity of cell distribution. Our results confirm the low seeding efficiency of chitosan scaffolds (48 to 70% with chondrocytes, 47 to 57% with MSCs) seeded with MSCs. Cells seem to display a greater affinity for each other than for the surface of chitosan, forming clusters that contributed to the uneven cell distribution within constructs. Coating chitosan fibers with type II collagen did not affect the structural properties of the scaffolds but improved cell adhesion. The structure, wettability and porosity of coated scaffolds were consistent with previous reports (Griffon et al, 2010; Nettles et al, 2002). This structural similarity between scaffolds allows direct evaluation of the effect of chemical composition (collagen coating) on cell seeding (Karande et al, 2004; Malda et al, 2005). The coating did not impact cell viability but increased the cell seeding efficiency by 41 to 73% in a dose-dependent manner. The seeding efficiency of the collagen coated scaffold meets the criteria for application in tissue engineering (Vunjak-Novakovic et al, 1998). Type II collagen coating also improved cell distribution in

collagen-coated constructs improving attachment to fibers rather than formation of clusters compared to chitosan constructs. This may help overcome the concern of poor tissue ingrowth in the center of the scaffolds commonly encountered in tissue engineering applications (Griffon et al, 2006; Karande et al, 2004). These effects may be attributed to the presence of binding sites in type II collagen, such as the amino acid sequences GFOGER and RGD. These binding sites have been found to promote cell attachment by the integrins α1, α2, α10, and/or α11β1, the discoidin-domain receptors, and the annexin V receptor (Durr et al, 1993; Freyria et al, 2009; Gigout et al, 2008; Reid et al, 2000).

In the last study, no difference in cell content was found between PGA and chitosan constructs. The seeding efficiency for the PGA scaffolds was 40% after two days of culture. Based on previous studies, we expected that the seeding efficiency of chitosan would be lower than PGA based on previous studies (Griffon et al, 2005; Griffon et al, 2006). However, Vunjak-Novakovic et al. obtained a seeding efficiency of 55% using a similar seeding technique for PGA scaffolds. This percentage actually represented the combined effects of initial attachment and three days of cell proliferation (Vunjak-Novakovic et al, 1998). The similar seeding efficiency obtained on chitosan and PGA is therefore more likely related to a difference in chitosan properties between studies. The DD correlates with attachment of cells such as fibroblasts, Schwann cells, keratinocytes, and neurons to chitosan films or sponges (Amaral et al, 2007; Chatelet et al, 2001; Freier et al, 2005; Seda Tigli et al, 2007; Tigli et al, 2008; Wenling et al, 2005). A lower molecular weight of the chitosan may also improve seeding efficiency (Hamilton et al, 2006). The chitosan used in this study had either a greater DD (92%) compared to the chitosan used in previous studies (85%) (Griffon et al, 2005; Griffon et al, 2006), or a lower molecular weight (480kDa

compared to 500 kDa). Difference in media composition between those studies could also affect cell adhesion due to the differential adsorption of proteins present in the culture medium to the chitosan (Chastain et al, 2006).

4.6. Effect of Type II Collagen Coating on Chondrogenesis on Chitosan Scaffolds

The adhesion of the cells to the matrix is believed to be a decisive factor for intracellular signals, influencing subsequent cell-matrix interaction and cell differentiation (Aydelotte et al, 1988; Mahmood et al, 2004; Reid et al, 2000). The ability of type II collagen to improve chondrogenic differentiation of MSCs was therefore tested and we found that type II collagen coating improved the amount and quality of the ECM present at 21 days in the constructs. The increase in ECM content likely reflects the greater cell content of the collagen coated constructs since the GAG/DNA content was greater in the PGA and chitosan constructs. However, for the collagen coated constructs, the morphological features evaluated by SEM and TEM were more consistent with normal chondrocytes, the ECM quality assessed by GAG quantification and immunohistochemistry was improved, and the type II collagen and aggrecan mRNA expression was increased. These findings suggest an improved differentiation of MSCs in the type II collagen coated scaffolds. The difference in chondrogenesis between coated and non-coated constructs is likely due to the synergistic effect of TFG-β1 and extracellular type II collagen on Smad 2 phosphorylation which has been shown to increase the level of type II collagen mRNA expression (Schneiderbauer et al, 2004), as well as aggrecan mRNA expression (Qi et al, 1997; Qi et al, 1998). The MSCs differentiation was affected by the presence, but not the density, of type II collagen. Integrin stimulation through type II collagen

interactions may improve chondrogenesis once above a threshold level, as for BMP signaling (Bandyopadhyay et al, 2006). However, the two collagen densities studied may also not be different enough to result in distinct cell signaling. Further studies are required to evaluate if a concentration of type II collagen greater than 22µg/mg can further improve the chondrogenic properties of chitosan-based scaffolds. Also, we cannot eliminate the potential influence of improved cell-cell interactions on the chondrogenic differentiation. In fact, the chondrogenic differentiation of MSCs typically proceeds through condensation, conventionally achieved by adapting pellet and micromass cultures. The formation of cell clusters due to increased cell density promotes cadherin-mediated cell-cell interactions. Among these, the N-cadherin and cadherin 11 molecules have been proposed to play a determinant role in MSCs condensation and subsequent chondrogenesis (Luo et al, 2005).

Type X collagen mRNA expression was increased in the chitosan constructs compared to the PGA. Type X collagen has been associated with chondrocyte hypertrophy (Harrington et al, 2004; Steinert et al, 2009). Hypertrophy is usually characterized by an increased cell volume and vacuolization, a production of type X collagen and alkaline phosphatase, and a concomitant decrease in the synthesis of type II collagen and aggrecan (Harrington et al, 2004; Steinert et al, 2009). The only change consistent with hypertrophy for all chitosan constructs is the increased expression of type X collagen mRNA but quantifications of type X collagen and ALP in the ECM were not performed. However, the relation between this finding and an increase in chondrogenic hypertrophy in those constructs seems difficult to establish since marked vacuolization was observed in the PGA constructs. Furthermore, the use of type X collagen mRNA as a marker of chondrogenic hypertrophy for MSCs has recently been questioned (Harrington et al, 2004; Mwale et al, 2006). Further studies should focus on

the significance of the increase in type X collagen mRNA expression in the chitosan constructs.

No difference in cell number or quantitative ECM evaluation was found between the two groups of collagen-coated constructs at 21 days. The cell population in both coated groups increased by 109% compared with the 48 hour assessment; whereas the cell number increased by 32% and 15% in the chitosan and PGA constructs, respectively. The presence of type II collagen seems responsible for an initial stimulation of the cell proliferation. However, the cell number in the collagen coated constructs seems to have reached a plateau at 21 days, possibly because of the scaffold size limitation.

CHAPTER 5: CONCLUSIONS AND FUTURE DIRECTIONS

The chemical structure of chitosan had a positive effect on the production of extracellular matrix by chondrocytes. The replica molding technique was proven to be a good alternative to fabricate chitosan fibrous scaffolds since the resulting fibers had a low variability in their cross-sectional widths and the viability and morphologic appearance of the chondrocytes were comparable or superior to other reports after three weeks of culture. No major difference was found between chitosan meshes of different fiber widths (4 to 22 μm range). The fibrous structure of chitosan scaffolds improved the differentiation of mesenchymal stem cells into chondrocytes, resulting in an extracellular matrix of better quality compared to sponges.

Cell adhesion on chitosan scaffolds was not improved with the degree of acetylation of chitosan or by hyaluronic acid coating but was increased by type II collagen coating. Type II collagen coating also enhanced the chondrogenesis of the MSCs on chitosan-based scaffolds. These findings encourage the use of fibrous chitosan scaffolds coated with type II collagen for cartilage tissue engineering applications and confirm the importance of biomimetic scaffolds for tissue engineering.

The polyglycolic acid mesh tested as a reference in this work did not perform as well as the chitosan scaffolds. The fragmentation of the polyglycolic acid fibers will likely further limit the use of polyglycolic acid for *in vivo* cartilage tissue engineering studies. Similarly, the decreased properties of reacetylated chitosan for cell adhesion will also limit its use for tissue engineering.

Limitations remain before direct clinical application of the chitosan fibrous scaffolds coated with type II collagen to improve treatment of articular cartilage defects. Firstly, MSCs chondrogenesis should be improved to obtain a construct with

similar structural and mechanical properties than native cartilage. The limited knowledge available regarding optimal chondrogenic differentiation impedes the development of novel strategies for the clinical use of MSCs. To improve MSCs chondrogenesis, it is important to start be controlling most culture variables and examining the effects of a specific modification of the culture condition. We used a standard chondrogenic protocol and the only variable evaluated was the scaffold. Many unknowns remain concerning proper chondrogenic differentiation and those should be addressed in future studies, where the scaffold variable should be controlled and other culture variables such as cell source and growth factor provided should be evaluated. Secondly, the construct obtained *in vitro* should integrate with the surrounding tissue once replaced *in vivo*. One solution to improve the integration will be the generation of a biphasic scaffold to mimic the cellular profile of native osteochondral tissue after culture with multi-potent MSCs. The scaffolds designed in this study should be used to develop the chondral portion of the construct while a scaffold with an osteogenic profile should be used to obtain the osteogenic base of the construct. This base may allow a better integration with the adjacent tissue since articular cartilage does not integrate well. Finally, *in vivo* studies will then have to be performed to test the effectiveness of those constructs in handling biomechanical forces and their ability to integrate with the adjacent tissue.

REFERENCES

Akmal M, Singh A, Anand A, Kesani A, Aslam N, et al: The effects of hyaluronic acid on articular chondrocytes. J Bone Joint Surg Br 87:1143-1149, 2005.

Amaral IF, Cordeiro AL, Sampaio P, Barbosa MA: Attachment, spreading and short-term proliferation of human osteoblastic cells cultured on chitosan films with different degrees of acetylation. J Biomater Sci Polym Ed 18:469-485, 2007.

Ameer GA, Mahmood TA, Langer R: A biodegradable composite scaffold for cell transplantation. J Orthop Res 20:16-19, 2002.

Asheim A, Lindblad G: Intra-articular treatment of arthritis in race-horses with sodium hyaluronate. Acta Vet Scand 17:379-394, 1976.

Atamaz F, Kirazli Y, Akkoc Y: A comparison of two different intra-articular hyaluronan drugs and physical therapy in the management of knee osteoarthritis. Rheumatol Int 26:873-878, 2006.

Athanasiou KA, Shah AR, Hernandez RJ, LeBaron RG: Basic science of articular cartilage repair. Clin Sports Med 20:223-247, 2001.

Athanasiou KA, Rosenwasser MP, Buckwalter JA, Malinin TI, Mow VC: Interspecies comparisons of in situ intrinsic mechanical properties of distal femoral cartilage. J Orthop Res 9:330-340, 1991.

Auer JA, Fackelman GE, Gingerich DA, Fetter AW: Effect of hyaluronic acid in naturally occurring and experimentally induced osteoarthritis. Am J Vet Res 41:568-574, 1980.

Aydelotte MB, Kuettner KE: Differences between sub-populations of cultured bovine articular chondrocytes. I. Morphology and cartilage matrix production. Connect Tissue Res 18:205-222, 1988.

Bandyopadhyay A, Tsuji K, Cox K, Harfe BD, Rosen V, et al: Genetic analysis of the roles of BMP2, BMP4, and BMP7 in limb patterning and skeletogenesis. PLoS Genet 2:e216, 2006.

Barnewitz D, Endres M, Kruger I, Becker A, Zimmermann J, et al: Treatment of articular cartilage defects in horses with polymer-based cartilage tissue engineering grafts. Biomaterials 27:2882-2889, 2006.

Bartlett W, Skinner JA, Gooding CR, Carrington RW, Flanagan AM, et al: Autologous chondrocyte implantation versus matrix-induced autologous chondrocyte implantation for osteochondral defects of the knee: a prospective, randomised study. J Bone Joint Surg Br 87:640-645, 2005.

Bhattarai N, Edmondson D, Veiseh O, Matsen FA, Zhang M: Electrospun chitosan-based nanofibers and their cellular compatibility. Biomaterials 26:6176-6184, 2005.

Bosnakovski D, Mizuno M, Kim G, Takagi S, Okumura M, et al: Chondrogenic differentiation of bovine bone marrow mesenchymal stem cells (MSCs) in different hydrogels: influence of collagen type II extracellular matrix on MSC chondrogenesis. Biotechnol Bioeng 93:1152-1163, 2006.

Bostman O, Hirvensalo E, Makinen J, Rokkanen P: Foreign-body reactions to fracture fixation implants of biodegradable synthetic polymers. J Bone Joint Surg Br 72:592-596, 1990.

Brodkin KR, Garcia AJ, Levenston ME: Chondrocyte phenotypes on different extracellular matrix monolayers. Biomaterials 25:5929-5938, 2004.

Buckwalter JA, Mankin HJ: Articular Cartilage: Part I: Tissue Design and Chondrocyte-Matrix Interactions. J Bone Joint Surg 79-A:600-611, 1997.

Cao H, Xu SY: Purification and characterization of type II collagen from chick sternal cartilage. Food Chemistry 108:439-445, 2008.

Caplan AI: Review: mesenchymal stem cells: cell-based reconstructive therapy in orthopedics. Tissue Eng 11:1198-1211, 2005.

Carvalho V, Domingues L, Gama M: The inhibitory effect of an RGD-human chitin-binding domain fusion protein on the adhesion of fibroblasts to reacetylated chitosan films. Mol Biotechnol 40:269-279, 2008.

Centers for Disease Control and Prevention (CDC): National and state medical expenditures and lost earnings attributable to arthritis and other rheumatic conditions-United States, 2003. MMWR Morb Mortal Wkly Rep 56:4-7, 2007.

Chang KY, Hung LH, Chu IM, Ko CS, Lee YD: The application of type II collagen and chondroitin sulfate grafted PCL porous scaffold in cartilage tissue engineering. J Biomed Mater Res A 92:712-723, 2010.

Chastain SR, Kundu AK, Dhar S, Calvert JW, Putnam AJ: Adhesion of mesenchymal stem cells to polymer scaffolds occurs via distinct ECM ligands and controls their osteogenic differentiation. J Biomed Mater Res A 78:73-85, 2006.

Chatelet C, Damour O, Domard A: Influence of the degree of acetylation on some biological properties of chitosan films. Biomaterials 22:261-268, 2001.

Chen M, Patra PK, Warner SB, Bhowmick S: Role of fiber diameter in adhesion and proliferation of NIH 3T3 fibroblast on electrospun polycaprolactone scaffolds. Tissue Eng 13:579-587, 2007.

Chen YL, Chen HC, Chan HY, Chuang CK, Chang YH, et al: Co-conjugating chondroitin-6-sulfate/dermatan sulfate to chitosan scaffold alters chondrocyte gene expression and signaling profiles. Biotechnol Bioeng 101:821-830, 2008.

Chen YL, Lee HP, Chan HY, Sung LY, Chen HC, et al: Composite chondroitin-6-sulfate/dermatan sulfate/chitosan scaffolds for cartilage tissue engineering. Biomaterials 28:2294-2305, 2007.

Chenite A, Chaput C, Wang D, Combes C, Buschmann MD, et al: Novel injectable neutral solutions of chitosan form biodegradable gels in situ. Biomaterials 21:2155-2161, 2000.

Cho JH, Kim SH, Park KD, Jung MC, Yang WI, et al: Chondrogenic differentiation of human mesenchymal stem cells using a thermosensitive poly(N-isopropylacrylamide) and water-soluble chitosan copolymer. Biomaterials 25:5743-5751, 2004.

Chung C, Burdick JA: Engineering cartilage tissue. Adv Drug Deliv Rev 60:243-262, 2008.

Cohen M, Kam Z, Addadi L, Geiger B: Dynamic study of the transition from hyaluronan- to integrin-mediated adhesion in chondrocytes. EMBO J 25:302-311, 2006.

Cole BJ, Malek MM. Articular cartilage lesions : A practical guide to assessment and treatment. New York: Springer, 2004.

Connelly JT, Garcia AJ, Levenston ME: Interactions between integrin ligand density and cytoskeletal integrity regulate BMSC chondrogenesis. J Cell Physiol 217:145-154, 2008.

Connelly JT, Garcia AJ, Levenston ME: Inhibition of in vitro chondrogenesis in RGD-modified three-dimensional alginate gels. Biomaterials 28:1071-1083, 2007.

Coutts RD, Healey RM, Ostrander R, Sah RL, Goomer R, et al: Matrices for cartilage repair. Clin Orthop Relat Res (391 Suppl):S271-9, 2001.

Cui YL, Qi AD, Liu WG, Wang XH, Wang H, et al: Biomimetic surface modification of poly(L-lactic acid) with chitosan and its effects on articular chondrocytes in vitro. Biomaterials 24:3859-3868, 2003.

Di Martino A, Sittinger M, Risbud MV: Chitosan: a versatile biopolymer for orthopaedic tissue-engineering. Biomaterials 26:5983-5990, 2005.

Discher DE, Janmey P, Wang YL: Tissue cells feel and respond to the stiffness of their substrate. Science 310:1139-1143, 2005.

Driesang IM, Hunziker EB: Delamination rates of tissue flaps used in articular cartilage repair. J Orthop Res 18:909-911, 2000.

Duan Y, Wang Z, Yan W, Wang S, Zhang S, et al: Preparation of collagen-coated electrospun nanofibers by remote plasma treatment and their biological properties. J Biomater Sci Polym Ed 18:1153-1164, 2007.

Durr J, Goodman S, Potocnik A, von der Mark H, von der Mark K: Localization of beta 1-integrins in human cartilage and their role in chondrocyte adhesion to collagen and fibronectin. Exp Cell Res 207:235-244, 1993.

Dye SF: The knee as a biologic transmission with an envelope of function: a theory. Clin Orthop Relat Res (325):10-18, 1996.

Engler AJ, Sen S, Sweeney HL, Discher DE: Matrix elasticity directs stem cell lineage specification. Cell 126:677-689, 2006.

Evans MD, Steele JG: Polymer surface chemistry and a novel attachment mechanism in corneal epithelial cells. J Biomed Mater Res 40:621-630, 1998.

Ewing JW, Arthroscopy Association of North America, Bristol-Myers/Zimmer. Articular cartilage and knee joint function: Basic science and arthroscopy. New York: Raven Press, 1990.

Fakhry A, Schneider GB, Zaharias R, Senel S: Chitosan supports the initial attachment and spreading of osteoblasts preferentially over fibroblasts. Biomaterials 25:2075-2079, 2004.

Farndale RW, Buttle DJ, Barrett AJ: Improved quantitation and discrimination of sulphated glycosaminoglycans by use of dimethylmethylene blue. Biochim Biophys Acta 883:173-177, 1986.

Fertala A, Holmes DF, Kadler KE, Sieron AL, Prockop DJ: Assembly in vitro of thin and thick fibrils of collagen II from recombinant procollagen II. The monomers in the tips of thick fibrils have the opposite orientation from monomers in the growing tips of collagen I fibrils. J Biol Chem 271:14864-14869, 1996.

Fortier LA: Stem cells: classifications, controversies, and clinical applications. Vet Surg 34:415-423, 2005.

Freed LE, Vunjak-Novakovic G, Biron RJ, Eagles DB, Lesnoy DC, et al: Biodegradable polymer scaffolds for tissue engineering. Biotechnology (N Y) 12:689-693, 1994.

Freed LE, Marquis JC, Nohria A, Emmanual J, Mikos AG, et al: Neocartilage formation in vitro and in vivo using cells cultured on synthetic biodegradable polymers. J Biomed Mater Res 27:11-23, 1993.

Freier T, Koh HS, Kazazian K, Shoichet MS: Controlling cell adhesion and degradation of chitosan films by N-acetylation. Biomaterials 26:5872-5878, 2005.

Freyria AM, Ronziere MC, Cortial D, Galois L, Hartmann D, et al: Comparative Phenotypic Analysis of Articular Chondrocytes Cultured within Type I or Type II Collagen Scaffolds. Tissue Eng Part A 15:1233-1245, 2009.

Frisbie DD, Kawcak CE, McIlwraith CW, Werpy NM: Evaluation of polysulfated glycosaminoglycan or sodium hyaluronan administered intra-articularly for treatment of horses with experimentally induced osteoarthritis. Am J Vet Res 70:203-209, 2009.

Frisbie DD, Cross MW, McIlwraith CW: A comparative study of articular cartilage thickness in the stifle of animal species used in human pre-clinical studies compared to articular cartilage thickness in the human knee. Vet Comp Orthop Traumatol 19:142-146, 2006.

Fromstein JD, Zandstra PW, Alperin C, Rockwood D, Rabolt JF, et al: Seeding bioreactor-produced embryonic stem cell-derived cardiomyocytes on different porous, degradable, polyurethane scaffolds reveals the effect of scaffold architecture on cell morphology. Tissue Eng Part A 14:369-378, 2008.

Funakoshi T, Majima T, Iwasaki N, Yamane S, Masuko T, et al: Novel chitosan-based hyaluronan hybrid polymer fibers as a scaffold in ligament tissue engineering. J Biomed Mater Res A 74:338-346, 2005.

Gao J, Yao JQ, Caplan AI: Stem cells for tissue engineering of articular cartilage. Proc Inst Mech Eng [H] 221:441-450, 2007.

Geng X, Kwon OH, Jang J: Electrospinning of chitosan dissolved in concentrated acetic acid solution. Biomaterials 26:5427-5432, 2005.

Getzy LL, Malemud CJ, Goldberg VM, Moskowitz RW: Factors influencing metachromatic staining in Paraffin-Embedded Sections of Rabbit and Human Articluar Cartilage: A comparison of the Safranin O and Toluidine Blue O techniques. J Histotech 5:111-116, 1982.

Gibson LJ, Ashby MF: The structure of cellular solids, in Gibson LJ AM (ed): Cellular solids: Structure and Properties.UK, Cambridge University Press, 1999, pp15-51.

Gigout A, Jolicoeur M, Nelea M, Raynal N, Farndale R, et al: Chondrocyte aggregation in suspension culture is GFOGER-GPP- and beta1 integrin-dependent. J Biol Chem 283:31522-31530, 2008.

Gingerich DA, Auer JA, Fackelman GE: Effect of exogenous hyaluronic acid on joint function in experimentally induced equine osteoarthritis: dosage titration studies. Res Vet Sci 30:192-197, 1981.

Goldring MB: The role of the chondrocyte in osteoarthritis. Arthritis Rheum 43:1916-1926, 2000.

Goldstein AS, Zhu G, Morris GE, Meszlenyi RK, Mikos AG: Effect of osteoblastic culture conditions on the structure of poly(DL-lactic-co-glycolic acid) foam scaffolds. Tissue Eng 5:421-434, 1999.

Goodrich LR, Nixon AJ: Medical treatment of osteoarthritis in the horse - a review. Vet J 171:51-69, 2006.

Goodstone NJ, Cartwright A, Ashton B: Effects of high molecular weight hyaluronan on chondrocytes cultured within a resorbable gelatin sponge. Tissue Eng 10:621-631, 2004.

Grande DA, Pitman MI, Peterson L, Menche D, Klein M: The repair of experimentally produced defects in rabbit articular cartilage by autologous chondrocyte transplantation. J Orthop Res 7:208-218, 1989.

Gray ML, Pizzanelli AM, Grodzinsky AJ, Lee RC: Mechanical and physiochemical determinants of the chondrocyte biosynthetic response. J Orthop Res 6:777-792, 1988.

Griffon DJ, Abulencia J, Ragetly GR, Fredericks LP, Chaieb S: A comparative study of seeding techniques and three-dimensional matrices for mesenchymal cells attachment. J Tissue Eng Regen Med in press, 2010.

Griffon DJ, Sedighi MR, Schaeffer DV, Eurell JA, Johnson AL: Chitosan scaffolds: interconnective pore size and cartilage engineering. Acta Biomater 2:313-320, 2006.

Griffon DJ, Sedighi MR, Sendemir-Urkmez A, Stewart AA, Jamison R: Evaluation of vacuum and dynamic cell seeding of polyglycolic acid and chitosan scaffolds for cartilage engineering. Am J Vet Res 66:599-605, 2005.

Grogan SP, Barbero A, Winkelmann V, Rieser F, Fitzsimmons JS, et al: Visual histological grading system for the evaluation of in vitro-generated neocartilage. Tissue Eng 12:2141-2149, 2006.

Hahn SK, Hoffman AS: Preparation and characterization of biocompatible polyelectrolyte complex multilayer of hyaluronic acid and poly-L-lysine. Int J Biol Macromol 37:227-231, 2005.

Hamilton V, Yuan Y, Rigney DA, Puckett AD, Ong JL, et al: Characterization of chitosan films and effects on fibroblast cell attachment and proliferation. J Mater Sci Mater Med 17:1373-1381, 2006.

Hangody L, Kish G, Karpati Z, Szerb I, Udvarhelyi I: Arthroscopic autogenous osteochondral mosaicplasty for the treatment of femoral condylar articular defects. A preliminary report. Knee Surg Sports Traumatol Arthrosc 5:262-267, 1997.

Hardie EM, Roe SC, Martin FR: Radiographic evidence of degenerative joint disease in geriatric cats: 100 cases (1994-1997). J Am Vet Med Assoc 220:628-632, 2002.

Harrington EK, Lunsford LE, Svoboda KK: Chondrocyte terminal differentiation, apoptosis, and type X collagen expression are downregulated by parathyroid hormone. Anat Rec A Discov Mol Cell Evol Biol 281:1286-1295, 2004.

Helder MN, Knippenberg M, Klein-Nulend J, Wuisman PI: Stem cells from adipose tissue allow challenging new concepts for regenerative medicine. Tissue Eng 13:1799-1808, 2007.

Helmick CG, Felson DT, Lawrence RC, Gabriel S, Hirsch R, et al: Estimates of the prevalence of arthritis and other rheumatic conditions in the United States: Part I. Arthritis Rheum 58:15-25, 2008.

Herrera MB, Bussolati B, Bruno S, Morando L, Mauriello-Romanazzi G, et al: Exogenous mesenchymal stem cells localize to the kidney by means of CD44 following acute tubular injury. Kidney Int 72:430-441, 2007.

Hersel U, Dahmen C, Kessler H: RGD modified polymers: biomaterials for stimulated cell adhesion and beyond. Biomaterials 24:4385-4415, 2003.

Hollander AP, Heathfield TF, Webber C, Iwata Y, Bourne R, et al: Increased damage to type II collagen in osteoarthritic articular cartilage detected by a new immunoassay. J Clin Invest 93:1722-1732, 1994.

Hootman JM, Helmick CG: Projections of US prevalence of arthritis and associated activity limitations. Arthritis Rheum 54:226-229, 2006.

Howling GI, Dettmar PW, Goddard PA, Hampson FC, Dornish M, et al: The effect of chitin and chitosan on the proliferation of human skin fibroblasts and keratinocytes in vitro. Biomaterials 22:2959-2966, 2001.

Hsu SH, Chang SH, Yen HJ, Whu SW, Tsai CL, et al: Evaluation of biodegradable polyesters modified by type II collagen and Arg-Gly-Asp as tissue engineering scaffolding materials for cartilage regeneration. Artif Organs 30:42-55, 2006.

Hsu SH, Whu SW, Hsieh SC, Tsai CL, Chen DC, et al: Evaluation of chitosan-alginate-hyaluronate complexes modified by an RGD-containing protein as tissue-engineering scaffolds for cartilage regeneration. Artif Organs 28:693-703, 2004.

Hubbell JA: Biomaterials in tissue engineering. Biotechnology (N Y) 13:565-576, 1995.

Hui JH, Chen F, Thambyah A, Lee EH: Treatment of chondral lesions in advanced osteochondritis dissecans: a comparative study of the efficacy of chondrocytes, mesenchymal stem cells, periosteal graft, and mosaicplasty (osteochondral autograft) in animal models. J Pediatr Orthop 24:427-433, 2004.

Hwang NS, Varghese S, Theprungsirikul P, Canver A, Elisseeff J: Enhanced chondrogenic differentiation of murine embryonic stem cells in hydrogels with glucosamine. Biomaterials 27:6015-6023, 2006.

Inui H, Tsujikubo M, Hirano S: Low molecular weight chitosan stimulation of mitogenic response to platelet-derived growth factor in vascular smooth muscle cells. Biosci Biotechnol Biochem 59:2111-2114, 1995.

Iwasaki N, Yamane ST, Majima T, Kasahara Y, Minami A, et al: Feasibility of polysaccharide hybrid materials for scaffolds in cartilage tissue engineering: evaluation of chondrocyte adhesion to polyion complex fibers prepared from alginate and chitosan. Biomacromolecules 5:828-833, 2004.

Jeffcott LB, Rossdale PD, Freestone J, Frank CJ, Towers-Clark PF: An assessment of wastage in thoroughbred racing from conception to 4 years of age. Equine Vet J 14:185-198, 1982.

Jeon YH, Choi JH, Sung JK, Kim TK, Cho BC, et al: Different Effects of PLGA and Chitosan Scaffolds on Human Cartilage Tissue Engineering. J Craniofac Surg 18:1249-1258, 2007.

Jeschke B, Meyer J, Jonczyk A, Kessler H, Adamietz P, et al: RGD-peptides for tissue engineering of articular cartilage. Biomaterials 23:3455-3463, 2002.

Johnston SA: Osteoarthritis. Joint anatomy, physiology, and pathobiology. Vet Clin North Am Small Anim Pract 27:699-723, 1997.

Karande TS, Ong JL, Agrawal CM: Diffusion in musculoskeletal tissue engineering scaffolds: design issues related to porosity, permeability, architecture, and nutrient mixing. Ann Biomed Eng 32:1728-1743, 2004.

Kasahara Y, Iwasaki N, Yamane S, Igarashi T, Majima T, et al: Development of mature cartilage constructs using novel three-dimensional porous scaffolds for enhanced repair of osteochondral defects. J Biomed Mater Res A 86:127-136, 2008.

Khor E, Lim LY: Implantable applications of chitin and chitosan. Biomaterials 24:2339-2349, 2003.

Kim HJ, Lee JH, Im GI: Chondrogenesis using mesenchymal stem cells and PCL scaffolds. J Biomed Mater Res A 92:659-666, 2010.

Kim YJ, Sah RL, Doong JY, Grodzinsky AJ: Fluorometric assay of DNA in cartilage explants using Hoechst 33258. Anal Biochem 174:168-176, 1988.

Kong HJ, Polte TR, Alsberg E, Mooney DJ: FRET measurements of cell-traction forces and nano-scale clustering of adhesion ligands varied by substrate stiffness. Proc Natl Acad Sci U S A 102:4300-4305, 2005.

Kuo YC, Lin CY: Effect of genipin-crosslinked chitin-chitosan scaffolds with hydroxyapatite modifications on the cultivation of bovine knee chondrocytes. Biotechnol Bioeng 95:132-144, 2006.

Kuroki K, Cook JL, Kreeger JM: Mechanisms of action and potential uses of hyaluronan in dogs with osteoarthritis. J Am Vet Med Assoc 221:944-950, 2002.

LeCouteur RA, Grandy JL: Diseases of the spinal cord, in Ettinger SJ, Feldman EC (eds): Textbook of veterinary internal medicine: diseases of the dog and cat(ed 6th). St. Louis, Mo., Elsevier Saunders, 2005, pp842-865.

Lee J, Cuddihy MJ, Kotov NA: Three-dimensional cell culture matrices: state of the art. Tissue Eng Part B Rev 14:61-86, 2008.

Lee JE, Kim KE, Kwon IC, Ahn HJ, Lee SH, et al: Effects of the controlled-released TGF-beta 1 from chitosan microspheres on chondrocytes cultured in a collagen/chitosan/glycosaminoglycan scaffold. Biomaterials 25:4163-4173, 2004.

Lee JW, Qi WN, Scully SP: The involvement of beta1 integrin in the modulation by collagen of chondrocyte-response to transforming growth factor-beta1. J Orthop Res 20:66-75, 2002.

Lee KY, Jeong L, Kang YO, Lee SJ, Park WH: Electrospinning of polysaccharides for regenerative medicine. Adv Drug Deliv Rev 61:1020-1032, 2009.

Lee V, Cao L, Zhang Y, Kiani C, Adams ME, et al: The roles of matrix molecules in mediating chondrocyte aggregation, attachment, and spreading. J Cell Biochem 79:322-333, 2000.

Leighton MP, Nundlall S, Starborg T, Meadows RS, Suleman F, et al: Decreased chondrocyte proliferation and dysregulated apoptosis in the cartilage growth plate are key features of a murine model of epiphyseal dysplasia caused by a matn3 mutation. Hum Mol Genet 16:1728-1741, 2007.

Lewis PB, McCarty LP, Kang RW, Cole BJ: Basic science and treatment options for articular cartilage injuries. J Orthop Sports Phys Ther 36:717-727, 2006.

Li S, De Wijn JR, Li J, Layrolle P, De Groot K: Macroporous biphasic calcium phosphate scaffold with high permeability/porosity ratio. Tissue Eng 9:535-548, 2003.

Li WJ, Jiang YJ, Tuan RS: Chondrocyte phenotype in engineered fibrous matrix is regulated by fiber size. Tissue Eng 12:1775-1785, 2006.

Li WJ, Tuli R, Okafor C, Derfoul A, Danielson KG, et al: A three-dimensional nanofibrous scaffold for cartilage tissue engineering using human mesenchymal stem cells. Biomaterials 26:599-609, 2005.

Livak KJ, Schmittgen TD: Analysis of relative gene expression data using real-time quantitative PCR and the 2(-Delta Delta C(T)) Method. Methods 25:402-408, 2001.

Lu JX, Prudhommeaux F, Meunier A, Sedel L, Guillemin G: Effects of chitosan on rat knee cartilages. Biomaterials 20:1937-1944, 1999.

Luo Y, Kostetskii I, Radice GL: N-cadherin is not essential for limb mesenchymal chondrogenesis. Dev Dyn 232:336-344, 2005.

Lutolf MP, Hubbell JA: Synthetic biomaterials as instructive extracellular microenvironments for morphogenesis in tissue engineering. Nat Biotechnol 23:47-55, 2005.

Madihally SV, Matthew HW: Porous chitosan scaffolds for tissue engineering. Biomaterials 20:1133-1142, 1999.

Mahmood TA, de Jong R, Riesle J, Langer R, van Blitterswijk CA: Adhesion-mediated signal transduction in human articular chondrocytes: the influence of biomaterial chemistry and tenascin-C. Exp Cell Res 301:179-188, 2004.

Mahmoudifar N, Doran PM: Effect of seeding and bioreactor culture conditions on the development of human tissue-engineered cartilage. Tissue Eng 12:1675-1685, 2006.

Malda J, Woodfield TB, van der Vloodt F, Wilson C, Martens DE, et al: The effect of PEGT/PBT scaffold architecture on the composition of tissue engineered cartilage. Biomaterials 26:63-72, 2005.

Mao JS, Cui YL, Wang XH, Sun Y, Yin YJ, et al: A preliminary study on chitosan and gelatin polyelectrolyte complex cytocompatibility by cell cycle and apoptosis analysis. Biomaterials 25:3973-3981, 2004.

Maroudas A, Schneiderman R: "Free" and "exchangeable" or "trapped" and "non-exchangeable" water in cartilage. J Orthop Res 5:133-138, 1987.

Marreco PR, da Luz Moreira P, Genari SC, Moraes AM: Effects of different sterilization methods on the morphology, mechanical properties, and cytotoxicity of chitosan membranes used as wound dressings. J Biomed Mater Res B Appl Biomater 71:268-277, 2004.

Mayne R: Cartilage collagens. What is their function, and are they involved in articular disease? Arthritis Rheum 32:241-246, 1989.

Mooney DJ, Langer R: Engineering biomaterials for tissue engineering: The 10-100 micron size scale, in Palsson B, Hubbell JA, plonsey R, et al (eds): Tissue Engineering(ed 1st). Boca Raton, Florida, USA, CRC, 2003, pp11-1-11-9.

Mooney DJ, Langer R, Ingber DE: Cytoskeletal filament assembly and the control of cell spreading and function by extracellular matrix. J Cell Sci 108 (Pt 6):2311-2320, 1995.

Mori T, Okumura M, Matsuura M, Ueno K, Tokura S, et al: Effects of chitin and its derivatives on the proliferation and cytokine production of fibroblasts in vitro. Biomaterials 18:947-951, 1997.

Moroni L, Licht R, de Boer J, de Wijn JR, van Blitterswijk CA: Fiber diameter and texture of electrospun PEOT/PBT scaffolds influence human mesenchymal stem cell proliferation and morphology, and the release of incorporated compounds. Biomaterials 27:4911-4922, 2006.

Moskowitz RW. Osteoarthritis: Diagnosis and medical/surgical management. 3rd ed. Philadelphia: Saunders, 2001.

Mukherjee DP, Smith DF, Rogers SH, Emmanual JE, Jadin KD, et al: Effect of 3D-microstructure of bioabsorbable PGA:TMC scaffolds on the growth of chondrogenic cells. J Biomed Mater Res B Appl Biomater 88:92-102, 2009.

Mwale F, Stachura D, Roughley P, Antoniou J: Limitations of using aggrecan and type X collagen as markers of chondrogenesis in mesenchymal stem cell differentiation. J Orthop Res 24:1791-1798, 2006.

Nettles DL, Elder SH, Gilbert JA: Potential use of chitosan as a cell scaffold material for cartilage tissue engineering. Tissue Eng 8:1009-1016, 2002.

Obradovic B, Martin I, Padera RF, Treppo S, Freed LE, et al: Integration of engineered cartilage. J Orthop Res 19:1089-1097, 2001.

Park GE, Pattison MA, Park K, Webster TJ: Accelerated chondrocyte functions on NaOH-treated PLGA scaffolds. Biomaterials 26:3075-3082, 2005.

Pei M, Solchaga LA, Seidel J, Zeng L, Vunjak-Novakovic G, et al: Bioreactors mediate the effectiveness of tissue engineering scaffolds. FASEB J 16:1691-1694, 2002.

Pelttari K, Winter A, Steck E, Goetzke K, Hennig T, et al: Premature induction of hypertrophy during in vitro chondrogenesis of human mesenchymal stem cells correlates with calcification and vascular invasion after ectopic transplantation in SCID mice. Arthritis Rheum 54:3254-3266, 2006.

Peniche C, Fernandez M, Rodriguez G, Parra J, Jimenez J, et al: Cell supports of chitosan/hyaluronic acid and chondroitin sulphate systems. Morphology and biological behaviour. J Mater Sci Mater Med 18:1719-1726, 2007.

Peterson L, Brittberg M, Kiviranta I, Akerlund EL, Lindahl A: Autologous chondrocyte transplantation. Biomechanics and long-term durability. Am J Sports Med 30:2-12, 2002.

Pham QP, Sharma U, Mikos AG: Electrospinning of polymeric nanofibers for tissue engineering applications: a review. Tissue Eng 12:1197-1211, 2006.

Philips MW: Clinical trial comparison of intra-articular sodium hyaluronan products in horses. J Equine Vet Sci 9:39-40, 1989.

Pieper JS, van der Kraan PM, Hafmans T, Kamp J, Buma P, et al: Crosslinked type II collagen matrices: preparation, characterization, and potential for cartilage engineering. Biomaterials 23:3183-3192, 2002.

Piermattei DL, Flo GL, DeCamp CE. Brinker, piermattei, and flo's handbook of small animal orthopedics and fracture repair. 4th ed. St. Louis, Mo.: Saunders/Elsevier, 2006.

Poole AR, Rosenberg LC, Reiner A, Ionescu M, Bogoch E, et al: Contents and distributions of the proteoglycans decorin and biglycan in normal and osteoarthritic human articular cartilage. J Orthop Res 14:681-689, 1996.

Qi WN, Scully SP: Effect of type II collagen in chondrocyte response to TGF-beta 1 regulation. Exp Cell Res 241:142-150, 1998.

Qi WN, Scully SP: Extracellular collagen modulates the regulation of chondrocytes by transforming growth factor-beta 1. J Orthop Res 15:483-490, 1997.

Radice M, Brun P, Cortivo R, Scapinelli R, Battaliard C, et al: Hyaluronan-based biopolymers as delivery vehicles for bone-marrow-derived mesenchymal progenitors. J Biomed Mater Res 50:101-109, 2000.

Raghunath J, Rollo J, Sales KM, Butler PE, Seifalian AM: Biomaterials and scaffold design: key to tissue-engineering cartilage. Biotechnol Appl Biochem 46:73-84, 2007.

Reid DL, Aydelotte MB, Mollenhauer J: Cell attachment, collagen binding, and receptor analysis on bovine articular chondrocytes. J Orthop Res 18:364-373, 2000.

Reno C, Marchuk L, Sciore P, Frank CB, Hart DA: Rapid isolation of total RNA from small samples of hypocellular, dense connective tissues. BioTechniques 22:1082-1086, 1997.

Rose RJ: The intra-articular use of sodium hyaluronate for the treatment of osteo-arthrosis in the horse. N Z Vet J 27:5-8, 1979.

Roughley PJ: The structure and function of cartilage proteoglycans. Eur Cell Mater 12:92-101, 2006.

Sasmazel HT, Gumusderelioglu M, Gurpinar A, Onur MA: Comparison of cellular proliferation on dense and porous PCL scaffolds. Biomed Mater Eng 18:119-128, 2008.

Schiffman JD, Schauer CL: One-step electrospinning of cross-linked chitosan fibers. Biomacromolecules 8:2665-2667, 2007.

Schneiderbauer MM, Dutton CM, Scully SP: Signaling "cross-talk" between TGF-beta1 and ECM signals in chondrocytic cells. Cell Signal 16:1133-1140, 2004.

Seda Tigli R, Karakecili A, Gumusderelioglu M: In vitro characterization of chitosan scaffolds: influence of composition and deacetylation degree. J Mater Sci Mater Med 18:1665-1674, 2007.

Seddighi MR, Griffon DJ, Schaeffer DJ, Fadl-Alla BA, Eurell JA: The effect of chondrocyte cryopreservation on cartilage engineering. Vet J 178:244-250, 2008.

Seitzinger AH, Traub-Dargatz JL, Kane AJ: A comparison of the economic costs of equine lameness, colic, and equine protozoal myeloencephalitis (EPM). Proc 9th Symp Int Soc Vet Epidemiol Econ 1048–1050, 2000.

Shoulders MD, Raines RT: Collagen structure and stability. Annu Rev Biochem 78:929-958, 2009.

Silva M, Shepherd EF, Jackson WO, Dorey FJ, Schmalzried TP: Average patient walking activity approaches 2 million cycles per year: pedometers under-record walking activity. J Arthroplasty 17:693-697, 2002.

Slavik GJ, Ragetly GR, Ganesh N, Griffon DJ, Cunningham BT: A Replica Molding Technique for Producing Fibrous Chitosan Scaffolds for Cartilage Engineering. J Mater Chem 17:4095-4101, 2007.

Steinert AF, Proffen B, Kunz M, Hendrich C, Ghivizzani SC, et al: Hypertrophy is induced during the in vitro chondrogenic differentiation of human mesenchymal stem cells by bone morphogenetic protein-2 and bone morphogenetic protein-4 gene transfer. Arthritis Res Ther 11:R148, 2009.

Stevens MM, George JH: Exploring and engineering the cell surface interface. Science 310:1135-1138, 2005.

Subramanian A, Lin HY: Crosslinked chitosan: its physical properties and the effects of matrix stiffness on chondrocyte cell morphology and proliferation. J Biomed Mater Res A 75:742-753, 2005.

Suh JK, Matthew HW: Application of chitosan-based polysaccharide biomaterials in cartilage tissue engineering: a review. Biomaterials 21:2589-2598, 2000.

Suphasiriroj W, Yotnuengnit P, Surarit R, Pichyangkura R: The fundamental parameters of chitosan in polymer scaffolds affecting osteoblasts (MC3T3-E1). J Mater Sci Mater Med 20:309-320, 2009.

Suzuki D, Takahashi M, Abe M, Sarukawa J, Tamura H, et al: Comparison of various mixtures of beta-chitin and chitosan as a scaffold for three-dimensional culture of rabbit chondrocytes. J Mater Sci Mater Med 19:1307-1315, 2008.

Takeuchi R, Saito T, Ishikawa H, Takigami H, Dezawa M, et al: Effects of vibration and hyaluronic acid on activation of three-dimensional cultured chondrocytes. Arthritis Rheum 54:1897-1905, 2006.

Tan H, Gong Y, Lao L, Mao Z, Gao C: Gelatin/chitosan/hyaluronan ternary complex scaffold containing basic fibroblast growth factor for cartilage tissue engineering. J Mater Sci Mater Med 18:1961-1968, 2007.

Taravel MN, Domard A: Collagen and its interactions with chitosan, III some biological and mechanical properties. Biomaterials 17:451-455, 1996.

Tew S, Redman S, Kwan A, Walker E, Khan I, et al: Differences in repair responses between immature and mature cartilage. Clin Orthop Relat Res (391 Suppl):S142-52, 2001.

Tigli RS, Gumusderelioglu M: Evaluation of RGD- or EGF-immobilized chitosan scaffolds for chondrogenic activity. Int J Biol Macromol 43:121-128, 2008.

Todhunter RJ, Johnston SA: Osteoarthritis, in Slatter D (ed): Textbook of Small Animal Surgery(ed 3rd Ed.). Philadelphia, PA, Saunders, 2003, pp2208-2245.

Tomihata K, Ikada Y: In vitro and in vivo degradation of films of chitin and its deacetylated derivatives. Biomaterials 18:567-575, 1997.

Tsai CL, Hsu Sh SH, Cheng WL: Effect of different solvents and crosslinkers on cytocompatibility of Type II collagen scaffolds for chondrocyte seeding. Artif Organs 26:18-26, 2002.

Tsai WB, Chen CH, Chen JF, Chang KY: The effects of types of degradable polymers on porcine chondrocyte adhesion, proliferation and gene expression. J Mater Sci Mater Med 17:337-343, 2006.

Tuzlakoglu K, Alves CM, Mano JF, Reis RL: Production and characterization of chitosan fibers and 3-D fiber mesh scaffolds for tissue engineering applications. Macromol Biosci 4:811-819, 2004.

van der Kraan PM, Buma P, van Kuppevelt T, van den Berg WB: Interaction of chondrocytes, extracellular matrix and growth factors: relevance for articular cartilage tissue engineering. Osteoarthritis Cartilage 10:631-637, 2002.

VandeVord PJ, Matthew HW, DeSilva SP, Mayton L, Wu B, et al: Evaluation of the biocompatibility of a chitosan scaffold in mice. J Biomed Mater Res 59:585-590, 2002.

Vunjak-Novakovic G: The fundamentals of tissue engineering: Scaffold and bioreactors., in Book G, Goode J (eds): Tissue Engineering of Cartilage and BoneChichester, West Sussex, John Wiley & Sons Publication, 2002, pp34-46.

Vunjak-Novakovic G, Obradovic B, Martin I, Bursac PM, Langer R, et al: Dynamic cell seeding of polymer scaffolds for cartilage tissue engineering. Biotechnol Prog 14:193-202, 1998.

Wallis WJ, Simkin PA, Nelp WB: Protein traffic in human synovial effusions. Arthritis Rheum 30:57-63, 1987.

Wang YC, Kao SH, Hsieh HJ: A chemical surface modification of chitosan by glycoconjugates to enhance the cell-biomaterial interaction. Biomacromolecules 4:224-231, 2003.

Wenling C, Duohui J, Jiamou L, Yandao G, Nanming Z, et al: Effects of the degree of deacetylation on the physicochemical properties and Schwann cell affinity of chitosan films. J Biomater Appl 20:157-177, 2005.

Wilke MM, Nydam DV, Nixon AJ: Enhanced early chondrogenesis in articular defects following arthroscopic mesenchymal stem cell implantation in an equine model. J Orthop Res 25:913-925, 2007.

Wise JK, Yarin AL, Megaridis CM, Cho M: Chondrogenic Differentiation of Human Mesenchymal Stem Cells on Oriented Nanofibrous Scaffolds: Engineering the Superficial Zone of Articular Cartilage. Tissue Eng Part A 15:913-921, 2008.

Wollenweber M, Domaschke H, Hanke T, Boxberger S, Schmack G, et al: Mimicked bioartificial matrix containing chondroitin sulphate on a textile scaffold of poly(3-hydroxybutyrate) alters the differentiation of adult human mesenchymal stem cells. Tissue Eng 12:345-359, 2006.

Woods A, Wang G, Beier F: Regulation of chondrocyte differentiation by the actin cytoskeleton and adhesive interactions. J Cell Physiol 213:1-8, 2007.

Yamane S, Iwasaki N, Kasahara Y, Harada K, Majima T, et al: Effect of pore size on in vitro cartilage formation using chitosan-based hyaluronic acid hybrid polymer fibers. J Biomed Mater Res A 81:586-593, 2006.

Yamane S, Iwasaki N, Majima T, Funakoshi T, Masuko T, et al: Feasibility of chitosan-based hyaluronic acid hybrid biomaterial for a novel scaffold in cartilage tissue engineering. Biomaterials 26:611-619, 2005.

Yen HJ, Tseng CS, Hsu SH, Tsai CL: Evaluation of chondrocyte growth in the highly porous scaffolds made by fused deposition manufacturing (FDM) filled with type II collagen. Biomed Microdevices 11:615-624, 2009.

Yoshida H, Faust A, Wilckens J, Kitagawa M, Fetto J, et al: Three-dimensional dynamic hip contact area and pressure distribution during activities of daily living. J Biomech 39:1996-2004, 2006.

Zaidel-Bar R, Cohen M, Addadi L, Geiger B: Hierarchical assembly of cell-matrix adhesion complexes. Biochem Soc Trans 32:416-420, 2004.

Zhu H, Ji J, Lin R, Gao C, Feng L, et al: Surface engineering of poly(D,L-lactic acid) by entrapment of chitosan-based derivatives for the promotion of chondrogenesis. J Biomed Mater Res 62:532-539, 2002.

Zimmerman E, Geiger B, Addadi L: Initial stages of cell-matrix adhesion can be mediated and modulated by cell-surface hyaluronan. Biophys J 82:1848-1857, 2002.

APPENDIX A: RAW DATA

Cartilage Tissue Engineering on Fibrous Chitosan Scaffolds Produced by a Replica Molding Technique

Scaffold number	ug DNA/ mg ww	ug DNA culture / mg ww	ug GAG per wet wt (mg)	GAG / DNA ratio per mg DW (or WW)	Collagen/DNA ratio per DW	Water content after (%)	increase in dry weight from d-1 to d21(%)
10	0.12	0.065	1.578	24.419	63.676		
10	0.04	0.039	2.048	51.923	164.751		
10	0.13	0.061	0.293	4.813	123.922	0.933	359.024
10	0.11	0.052	2.041	39.320	85.010	0.922	446.124
10		0.046	1.671	36.687	69.699	0.922	510.490
32	0.19	0.059	2.329	39.313	60.067	0.926	510.510
32	0.15	0.042	1.387	33.382	94.086		
32	0.2	0.048	0.829	17.267	279.234	0.942	315.951
32	0.18	0.044	0.545	12.248	123.972	0.926	455.939
32		0.054	1.877	34.515	61.744	0.926	383.183
32					38.786	0.926	287.770
56	0.15	0.052	1.805	34.759	81.099		
56	0.17	0.050	1.848	36.765	101.844		
56	0.18	0.048	1.942	40.429	223.270	0.931	339.608
56	0.15	0.029	0.994	34.104	103.396	0.937	384.358
56		0.058	1.937	33.185	28.712	0.931	429.767
56					126.455	0.931	411.151
0	0.45	0.825	16.251	19.708	9.345	0.935	326.998
0	0.53	0.716	11.549	16.133	12.524		
0	0.35	0.751	12.460	16.584	3.403		
0	0.56	0.680	14.167	20.845	7.656	0.946	396.491
0		0.747	17.629	23.595	8.568	0.935	297.485
0					3.713	0.935	237.907

		count 1	count 2	count 3	count 4	count 5
10um 16	**inner**	3	2	0	2	3
	outer	0	30	61	26	25
10um 22	**inner**	103	7	20	7	17
	outer	107	101	61	43	74
10um 2	**inner**	4	2	0	10	5
	outer	202	231	23	124	296
32um 19	**inner**	1	0	37	23	11
	outer	57	48	86	30	126
32um 1	**inner**	5	106	4	0	8
	outer	40	143	78	131	80
32um 2	**inner**	93	138	101	134	181
	outer	207	162	40	56	46
32um 16	**inner**	0	0	2	4	2
	outer	19	54	5		
56 um 1	**inner**	0	1	34	71	54
	outer	266	165	208	184	2
56um 19	**inner**	53	28	92	11	27
	outer	101	115	120	214	115
56um 2	**inner**	9	49	93	159	70
	outer	119	108	103		187
56um 16	**inner**	53	41	47	21	1
	outer	100	320	67	142	144
PGA 1	**inner**	110				
	outer	114	136	146	129	184
PGA 2	**inner**	26	98	63	99	71
	outer	218	242	212	109	229
PGA 19	**inner**	3	6	10	9	20
	outer	86	61	136	305	145
PGA 16	**inner**	78	14	64	61	78
	outer	64	55	82	49	80

APPENDIX B: RAW DATA

Effect of Chitosan Scaffold Microstructure on Mesenchymal Stem Cells Chondrogenesis

	seeding wet weight (g)	10 days wet weight (g)	21 days wet weight (g)	seeding dry weight (g)	10 days dry weight (g)	21 days dry weight (g)	water content 10 days (%)	water content 21 days (%)
sponge 1	0.161	0.158	0.132	0.0072	0.0067	0.0070	0.959	0.954
sponge 2	0.103	0.137	0.115	0.0052	0.0059	0.0068	0.954	0.955
sponge 3	0.112	0.120	0.136	0.0050	0.0071	0.0063	0.944	0.951
sponge 4	0.174	0.108	0.151	0.0057	0.0059	0.0047	0.951	0.956
sponge 5	0.157	0.164	0.152	0.0070	0.0069	0.0063	0.942	0.961
sponge 6	0.140	0.129	0.150			0.0069		0.944
sponge 7	0.108	0.127	0.130					
sponge 8	0.153	0.121	0.107					
sponge 9	0.168	0.120	0.161					
sponge 10	0.152		0.123					
fibrous 1	0.117	0.096	0.028	0.0058	0.0067	0.0070	0.938	0.950
fibrous 2	0.121	0.074	0.109	0.0053	0.0060	0.0056	0.941	0.957
fibrous 3	0.107	0.085	0.048	0.0040	0.0051	0.0065	0.939	0.947
fibrous 4	0.052	0.074	0.122	0.0034	0.0065	0.0051	0.946	0.938
fibrous 5	0.037	0.107	0.140	0.0030	0.0057	0.0063	0.942	0.936
fibrous 6	0.050	0.102	0.130			0.0041		0.947
fibrous 7	0.067	0.084	0.123					
fibrous 8	0.124	0.121	0.083					
fibrous 9	0.063	0.099	0.098					
fibrous 10	0.050		0.078					
fibrous 11	0.094							
fibrous 12	0.120							
fibrous 13	0.073							
fibrous 14	0.052							
fibrous 15	0.101							
fibrous 16	0.059							
fibrous 17	0.059							
fibrous 18	0.075							

	Seeding DNA (ug/mg)	10 days DNA (ug/mg)	21 days DNA (ug/mg)	10 days GAG (ug/mg)	21 days GAG	10 days GAG/DNA	21 days GAG/DNA
sponge 1	31.906	27.575	45.026	1.480	0.717	0.054	0.016
sponge 2	32.032	27.621	42.373	0.975	0.805	0.020	0.019
sponge 3	39.653	48.859	28.576	0.135	1.254	0.005	0.044
sponge 4	46.300	26.069		2.469		0.051	
sponge 5	32.953	48.859					
fibrous 1	48.138	29.565	39.256	0.957	2.416	0.032	0.055
fibrous 2	27.496	47.508	43.922	0.826	3.005	0.017	0.061
fibrous 3	26.842	48.859	47.059	4.625		0.095	
fibrous 4	30.969	48.763		2.047	2.494	0.042	
fibrous 5	31.346	48.859		2.113		0.043	

	surface area covered by ECM (%)	21 days Coll II mRNA	21 days Coll I mRNA	21 days Coll X mRNA
sponge 1	9.6	0.460212073	1.630204279	0.225121732
sponge 2	6.15	0.955087005	0.917037578	1.15704414
sponge 3	3.75	0.777566194	0.663600138	0.716370203
sponge 4	5.1	1.807134729	0.789158006	1.901463926
fibrous 1	40.05	2.241767789	2.7084454	1.134321093
fibrous 2	7.05	4.541767789	1.185698	3.123236563
fibrous 3	12.75			
fibrous 4	45.3			

APPENDIX C: RAW DATA

Modification of the Chemical Composition of Chitosan Scaffolds to Improve Mesenchymal Stem Cell Adhesion

sample	ug coll 2 per mg scaffold
chitosan	0.000
chitosan	0.000
chitosan-collagen	3.045
chitosan-collagen	3.594
chitosan-collagen	5.680
reacetylated chitosan	0.000
reacetylated chitosan	0.000
reacetylated chitosan - collagen 1	5.144
reacetylated chitosan - collagen 1	4.842
reacetylated chitosan - collagen 1	4.954
reacetylated chitosan - collagen 2	5.754
reacetylated chitosan - collagen 2	9.501
reacetylated chitosan - collagen 2	8.860

group	name	WW (g)	DW (mg	Dwpost (mg)	water content pre-seeding	water content	DNA	seeding efficiency	media DNA 24h	media DNA 72h	cell count	cell count 2h	cell count 4h	cell count 6h	cell count 18h	cell count 22h
chitosan	O1	0.0208	1.9	2.3	0.909	0.85E	3.294	0 6'7	4.883	14.149	1.6	0.2	0.2	0.6	0.2	C
chitosan	O2	0.023	2	2.2	0.913	0.904	2.038	0 382	5.445	18.332	0.4	0	1.4	0.4	0.8	0.2
chitosan	O3	0.021	2.2	2.5	0.895	0.881	2.270	0 425								
chitosan	O4	0 0369	1.9	3.5	0.947	0.91E	3.177	0 595								
chitosan	O5	0.0296	2	3.2	0.902	0.092	2.667	0 490								
chitosan	O6	0.0271	1.7	1.3	0.937	0.994	2.578	0 483								
chitosan	O7	0.032	1.8	3.5	0.944	0.891	2.183	0 409								
chitosan	O8	0.0279	1.8	3.1	0.935	0.839	2.702	0 506								
chitosan	O9	0.0368	1.9	3.2	0.948	0.91E	2.36'	0 442								
chitosan	O10	0.0265	1.8	2	0.932	0.92E	1.916	0 359								
chitosan-collagen	OC1	0.0211	1.9	1	0.910	0.95E	2.406	0 451	3.857	8.9'6	0.4	0	0	0	0	C
chitosan-collagen	OC2	0.0313	2	3.1	0.936	0.901	5.482	1 027	5.293	4.933	1.2	0	0.8	0.2	0.2	C
chitosan-collagen	OC3	0.0276	1.7	1.4	0.938	0.949	8.33'	1 560								
chitosan-collagen	OC4	0.0382	1.9	1.3	0.950	0.95E	3.975	0 744								
chitosan-collagen	OC5	0.027	1.9	2.5	0.930	0.907	3.71'	0 695								
chitosan-collagen	OC6	0.0238	2.2	3.3	0.908	0.851	2.873	0 538								
chitosan-collagen	OC7	0.0212	2.2	1.5	0.896	0.92E	3.213	0 602								
chitosan-collagen	OC8	0 0384	2.2	2.5	0.943	0 93E	4.834	0 905								
chitosan-collagen	OC9	0.0290	2.0	3.1	0.922	0.094	5.410	1 0'0								
chitosan-collagen	OC10	0.0382	2.2	3.2	0.942	0.91E	3.446	0 645								
reacetylated chitosan	I1	0.0251	2.2	2.5	0.912	0.90C	0.915	0 171	3.370	6.446	0	0	0	0	0	C
reacetylated chitosan	I2	0.0259	2.0	1.0	0.911	0.901	1.047	0 196	4.000	4.067	0	0	0	0	0.4	C
reacetylated chitosan	I3	0.0197	1.9	1.5	0.904	0.919	1.179	0 221								
reacetylated chitosan	I4	0.0417	2.8	3.2	0.940	0.92E	1.844	0 345								
reacetylated chitosan	I5	0.0349	2.1	5	0.940	0.857	2.783	0 521								
reacetylated chitosan	I6	0.0305	1.8	1.3	0.941	0.93E	1.124	0 2'0								
reacetylated chitosan	I7	0.0333	2.1	2.5	0.937	0.922	1.233	0 231								
reacetylated chitosan	I8	0.0329	2.2	2.3	0.933	0.93C	1.038	0 194								
reacetylated chitosan	I9	0.0274	2.2	2.2	0.920	0.92C	0.946	0 177								
reacetylated chitosan	I10	0.0311	2.2	3.2	0.929	0.897	1.524	0 285								
reacetylated chitosan - collagen 1	IC1	0.0306	2.2	3	0.928	0.90Z	1.419	0 266	4.693	6.736	0	0	0	0	0	C
reacetylated chitosan - collagen 1	IC2	0 0405	2.1	3.2	0.948	0 921	1.396	0 262	3.086	5.878	0	0.2	1	0	0.4	C
reacetylated chitosan - collagen 1	IC3	0.0273	1.9	2.3	0.930	0.90E	1.777	0 333								
reacetylated chitosan - collagen 1	IC4	0.0206	1.9	2.3	0.908	0.88E	1.286	0 241								
reacetylated chitosan - collagen 1	IC5	0.0308	2	2.5	0.935	0.919	1.24'	0 232								
reacetylated chitosan - collagen 1	IC6	0.0217	1.7	2	0.922	0.90C	1.174	0 220								
reacetylated chitosan - collagen 1	IC7	0.0243	1.9	2.5	0.922	0.897	1.206	0 226								
reacetylated chitosan - collagen 1	IC8	0.0222	1.9	2.3	0.914	0.89E	1.129	0 2'1								
reacetylated chitosan - collagen 1	IC9	0.0237	1.9	2.7	0.920	0.88E	1.350	0 253								
reacetylated chitosan - collagen 1	IC10	0.0303	2.3	2.3	0.924	0.90E	1.175	0 220								
reacetylated chitosan - collagen 2	2C1	0.0187	2	2.3	0.893	0.85C	1.777	0 333	4.819	8.104	0.4	0	0.2	0	0	C
reacetylated chitosan - collagen 2	2C2	0.0237	1.9	1.3	0.920	0.92C	0.866	0 162	4.223	9.584	0	1	1	0	0	0.2
reacetylated chitosan - collagen 2	2C3	0.0213	1.8	1.1	0.915	0.94E	1.123	0 2'0								
reacetylated chitosan - collagen 2	2C4	0.0312	1.8	2.3	0.942	0.92E	0.876	0 164								
reacetylated chitosan - collagen 2	2C5	0.0289	1.7	3.3	0.941	0.83E	1.723	0 323								
reacetylated chitosan - collagen 2	2C6	0 0271	1.8	1.5	0.934	0 941	1.015	0 190								
reacetylated chitosan - collagen 2	2C7	0.0182	2.1	2.3	0.885	0.84E	1.229	0 230								
reacetylated chitosan - collagen 2	2C8	0.0344	1.8	2.2	0.948	0.93E	1.369	0 256								
reacetylated chitosan - collagen 2	2C9	0.025	1.9	1.3	0.924	0.924	0.983	0 184								
reacetylated chitosan - collagen 2	2C10	0.0154	1.9	2.1	0.077	0.054	1.500	0 296								

APPENDIX D: RAW DATA

Effect of Type II collagen Coating of Chitosan Fibrous Scaffolds on Mesenchymal Stem Cell Adhesion and Chondrogenesis

sample	coll II content (ug/mg)
chitosan	0.000
chitosan	0.000
chitosan - collagen 2mg/ml	9.748
chitosan - collagen 2mg/ml	13.326
chitosan - collagen 2mg/ml	16.230
chitosan - collagen 4mg/ml	20.704
chitosan - collagen 4mg/ml	23.767
chitosan - collagen 4mg/ml	22.400
PGA	0.000
PGA	0.000

mRNA expression level	Coll I	Coll II	Coll X	Acan
chitosan	1.495	2.419	2.866	1.616
chitosan	1.576	1.088	3.366	0.278
chitosan	0.846	1.452	3.003	1.598
collagen coated chitosan	1.425	2.753	2.162	2.222
collagen coated chitosan		5.822	2.964	2.644
collagen coated chitosan	1.708	2.901	3.538	1.627
PGA	1.186	2.248	1.389	
PGA	1.065	0.238	1.136	1.655
PGA	1.514	1.158	1.206	1.231
PGA	0.235	0.356	0.269	0.115

	fiber size	WW (mg)	DW (mg)	DW increase (%)	water content (%)	seeding DNA (ug)	culture DNA (ug)	Cell yield	GAG content (ug)	cell gain (%)	GAG/ DNA	area covered by ECM (%)
chitosan 1	15	40.3	4.6		0.8859	10.4924		0.8078				33.2
chitosan 2	15	36	3.2		0.9111	7.09067		0.5459				64.2
chitosan 3	17	48.8	3.2		0.9344	5.44605		0.4193				30.4
chitosan 4	13	57.8	4.5		0.9221	8.2554		0.6356				28.2
chitosan 5	14	48.7	3.9		0.9199	6.06116		0.4666				30
chitosan 6	13	48										47.6
chitosan 7	12	60										
chitosan 8	18	59.2										
chitosan 9		67.3	4.2	0.46055	0.9376		9.2739	0.714	10.583	0.24	1.141	
chitosan 10		55.2	5.1	0.71449	0.9076		7.8432	0.6038	10.787	0.05	1.375	
chitosan 11		67.5	6.3	1.15292	0.9067		11.45	0.8815	14.585	0.53	1.274	
chitosan 12		56.9	5.5	0.79484	0.9033		9.7894	0.7537	14.409	0.31	1.472	
chitosan 13		79.3	6	0.95109	0.9243		11.165	0.8595	18.695	0.49	1.674	
chitosan 14		70.2										
Med chitosan 1						17.7655						
Med chitosan 2						18.3557						
Med chitosan 3						16.552						
chitosan - collagen 2mg/ml 1	15	31.1	7.8		0.7492	12.1588		0.9361				71
chitosan - collagen 2mg/ml 2	15	26.9	4		0.8513	9.03734		0.6958				71.6
chitosan - collagen 2mg/ml 3	17	31	3.8		0.8774	7.8252		0.6025				29.2
chitosan - collagen 2mg/ml 4	20	25.3	3.3		0.8696	7.47618		0.5756				28.6
chitosan - collagen 2mg/ml 5	15	32.4	3.2		0.9012	7.98547		0.6148				81.8
chitosan - collagen 2mg/ml 6	20	35.7										45.4
chitosan - collagen 2mg/ml 7	15	45										
chitosan - collagen 2mg/ml 8	20	32.5										
chitosan - collagen 2mg/ml 9		61.3	6.7	1.11893	0.8907		29.712	2.2875	17.57	2.34	0.591	
chitosan - collagen 2mg/ml 10		69.3	6.8	1.25947	0.9019		23.018	1.7721	15.761	1.59	0.685	
chitosan - collagen 2mg/ml 11		73.5	7.4	1.55322	0.8993		21.678	1.669	21.1	1.44	0.973	
chitosan - collagen 2mg/ml 12		48.4	5.2	0.82298	0.8926		15.37	1.1834	21.628	0.73	1.407	
chitosan - collagen 2mg/ml 13		48	5.5	0.93012	0.8854		14.069	1.0832	15.888	0.58	1.129	
chitosan - collagen 2mg/ml 14		25.9										
Medium chitosan - collagen 2mg/ml 1						18.5829						
Medium chitosan - collagen 2mg/ml 2						15.6767						
Medium chitosan - collagen 2mg/ml 3						15.6618						
chitosan - collagen 4mg/ml 1	16	27.1	2.8		0.8967	8.05813		0.6204				67.8
chitosan - collagen 4mg/ml 2	20	25.3	3.1		0.8775	9.07536		0.6987				43.2
chitosan - collagen 4mg/ml 3	14	27.9	3.9		0.8602	10.2044		0.7856				57.4
chitosan - collagen 4mg/ml 4	15	29.3	4.2		0.8567	15.3318		1.1804				63.4
chitosan - collagen 4mg/ml 5	14	44.2	4.1		0.9072	9.92959		0.7645				53.6
chitosan - collagen 4mg/ml 6	18	35.3										69
chitosan - collagen 4mg/ml 7	15	48.2										44.4
chitosan - collagen 4mg/ml 8		56.3										
chitosan - collagen 4mg/ml 9		47.5	6	1.40514	0.8737		16.373	1.2606	23.716	0.56	1.448	
chitosan - collagen 4mg/ml 10		41.6	5.6	0.96118	0.8654		17.591	1.3543	21.973	0.67	1.249	
chitosan - collagen 4mg/ml 11		50.8	5.4	1.03804	0.8937		16.981	1.3074	13.969	0.61	0.823	
chitosan - collagen 4mg/ml 12		63	6.5	1.23838	0.8968		22.998	1.7706	18.345	1.19	0.798	
chitosan - collagen 4mg/ml 13		68.7	6.6	1.31832	0.9039		24.025	1.8497	15.536	1.28	0.647	
chitosan - collagen 4mg/ml 14		31.3										
Medium chitosan - collagen 4mg/ml 1						16.5622						
Medium chitosan - collagen 4mg/ml 2						17.636						
Medium chitosan - collagen 4mg/ml 3						17.7833						
PGA 1	15	68	4.7		0.9309	6.30312		0.4853				27.2
PGA 2	15	46	3.1		0.9326	3.55062		0.2734				24.4
PGA 3	14	59	4.3		0.9271	5.64087		0.4343				58
PGA 4	15	65.6	4.4		0.9329	6.53301		0.503				25.8
PGA 5	14	49.2	3		0.939	3.86771		0.2978				57.4
PGA 6	14	51.2										32.8
PGA 7	15	47.6										
PGA 8	14	48.6										
PGA 9	13	37.2	2.9	3.8E-14	0.922		6.7001	0.5158	16.692	0.29	2.491	
PGA 10		37.5	3.2	0.08824	0.9147		5.1843	0.3991	11.436	0	2.206	
PGA 11		26.7	2.7	-0.05714	0.8989		5.8787	0.4526	14.004	0.14	2.382	
PGA 12		33.4	2.8	-0.02941	0.9162		5.0728	0.3906	11.04	-0.02	2.176	
PGA 13		29.8	3.2	0.13043	0.8926		6.9488	0.535	12.815	0.34	1.844	
PGA 14		38.8										
Medium PGA 1						19.3636						
Medium PGA 2						15.9938						
Medium PGA 3						18.5827						